UNIVERSITY OF LONDON THESIS

Degree PhD Year 2006 Name of Author O'DONOVAN
Peter John

Photochemical Reactions of DNA 6-TG and Their Biological Consequences

By

Peter John O'Donovan

A thesis submitted for the degree of Ph.D.

at

The University of London

July 2006

Cancer Research UK
London Research Institute
Clare Hall Laboratories
South Mimms
Herts EN6 3LD

and

Department of Biochemistry
University College London
WC1E 6BT

ProQuest LLC
789 East Eisenhower Parkway
P.O. Box 1346
Ann Arbor, MI 48106-1346

I, Peter John O'Donovan, confirm that the work presented in this thesis is my own. Where information has been derived from other sources, I confirm that this has been indicated in the thesis.

For my family and Cristina.

"*An Irishman's heart is nothing but his imagination*"

George Bernard Shaw

Abstract

6-Thioguanine (6-TG) incorporation into DNA is an inevitable consequence of treatment with the immunosuppressive drug Azathioprine (Aza). On administration, Aza is chemically cleaved to form 6-mercaptopurine which, after further metabolism, results in the accumulation of DNA 6-TG. Unlike the standard DNA bases, 6-TG absorbs strongly in the UVA region of the electromagnetic spectrum. I have shown that 6-TG and UVA interact in solution to form two major photoproducts. These have been identified as guanine-6-thioguanine (G-S-G) and guanine-6-sulfonate (G-6-SO_3). These photoproducts are formed via singlet oxygen generated by 6-TG acting as a Type II photosensitiser. G-6-SO_3 is also formed by UVA irradiation of the 6-TG deoxyribonucleoside as well as from 6-TG in both single- and double-stranded DNA.

A significant level of DNA 6-TG has been measured in a number of human cell lines following growth in medium containing 6-TG. This DNA 6-TG sensitises the cells to killing by low doses of UVA. Cytotoxicity is not influenced by mismatch repair or nucleotide excision repair status. Sub-lethal combinations of 6-TG and UVA are synergistically mutagenic. I show that the 6-TG/UVA mutation spectrum differs from spontaneous and UVA spectra, and contains a high number of G to C and A to C transversions. 6-TG/UVA treatment of cells generates measurable levels of potentially mutagenic reactive oxygen species, a significant fraction of which is produced in DNA itself.

6-TG/UVA inhibits replication in cells. In response, PCNA becomes mono-ubiquitinated, suggesting possible translesion synthesis at the photochemical DNA lesions. Strikingly, 6-TG/UVA also causes covalent crosslinking of PCNA at the replication fork. This may also reflect reactions of singlet oxygen.

DNA 6-TG has been quantified in skin biopsies from Aza treated patients. An investigation into the possible role of 6-TG/UVA-induced mutagenic DNA damage in the development of basal cell carcinoma in Aza patients has been initiated.

Acknowledgements

First and foremost I would like to thank my supervisor, Dr. Peter Karran, for his guidance, his ideas, and his support. Secondly I would like to thank my second supervisor Dr. Tomas Lindahl and my thesis committee member Dr. Dale Wigley for their support and guidance.

I would also like to thank lab members past and present; Judith Offman and Steve Durant for all their help when I started my PhD, Beatriz Montaner for her help and discussions, Fiona Bristow and Olivier Reelfs for helping to make the lab somewhere I have enjoyed to spend my time, Peter McPherson for all his help, and Ramin Sadri.

I need to thank my collaborators Dr. Yao-Zhong Xu and Dr. Xiaohong Zhang for their help with the photochemistry, for performing the mass spectrometry and NMR, and for synthesis of G-6-SO_3 markers for RP-HPLC. Dr. Catherine Harwood, Dr. Jane McGregor, Dr. Conal Perrett and Ms. Karin Purdie, who provided me with BCC samples and skin biopsies for DNA 6-TG quantification.

Special thanks are owed to CRUK LRI Central Cell Services, and the Oligonuleotide Synthesis Service. I would like to thank those in the DNA Sequencing and FACS laboratories in the CRUK LRI Equipment park.

My colleagues at Clare Hall, whom have made some part of even the worst days fun and enjoyable. You all know who you are, and you have been very important in getting through this PhD.

A sincere thanks to parents, my brother, and my family for supporting me in everything I have done in my PhD and in my life in general. Without them I would not be writing this thesis. And to Cristina, whom is a constant inspiration for everything I do, and whom is a part of everything worthwhile in my life.

Publications

O'Donovan, P., Perrett, C., *et al.* (2005) "Azathioprine and UVA Light Generate Mutagenic Oxidative DNA Damage". Science **309**(5742): 1871-4

Table of Contents

Abstract 4

Acknowledgements 5

Publications 6

Table of Contents 7

Table of Figures 12

Table of Tables 14

List Of Abbreviations 15

Introduction 18

1.1 DNA Damage *18*

1.1.1 Spontaneous DNA Damage 18

1.1.2 Ionising Radiation Induced DNA Damage 18

1.1.3 Alkylation of DNA 19

1.1.3.1 Clinical Uses of Alkylating Agents 21

1.1.4 Oxidative DNA Damage 21

1.1.4.1 ROS 21

1.1.4.2 ROS Induced DNA Damage 24

1.1.4.3 Indirect Base Damage after Oxidative Stress 25

1.1.4.4 Oxidatively Induced DNA Strand Breaks 27

1.1.4.5 Oxidative Protein Damage 27

1.1.5 UV Induced DNA Damage 27

1.1.5.1 UVC 28

1.1.5.2 UVB 28

1.1.5.3 UVA 30

1.2 Repair of DNA Damage *31*

1.2.1 Reversal of DNA Damage 31

1.2.2 Base Excision Repair 32

1.2.3 Nucleotide Excision Repair 36
1.2.4 Post-Replicative Mismatch Repair 39
1.2.4.1 Bacterial MMR 39
1.2.4.2 Mammalian MMR 39
1.2.5 Double Strand Break Repair 41
1.2.5.1 Homologous Recombination 41
1.2.5.2 Non-Homologous End Joining 43
1.2.5.3 Single Strand Annealing 47
1.3 Consequences of Defective DNA Repair 47
1.3.1 Defective Mismatch Repair 49
1.4 Avoidance and Tolerance of DNA Damage 52
1.4.1 Translesion Synthesis (TLS) 52
1.5 Skin Cancer 57
1.5.1 Cutaneous Malignant Melanoma 59
1.5.2 Non-Melanoma Skin Cancer 59
1.5.2.1 Squamous Cell Carcinoma 59
1.5.2.2 Basal Cell Carcinoma 60
1.5.3 UVR in Skin Cancer 64
1.6 Skin Cancer in Organ Transplant Recipients 65
1.6.1 NMSC in Organ Transplant Recipients 65
1.6.2 Melanoma in OTRs 66
1.6.3 Risk Factors in OTR Tumourogenesis 66
1.6.4 Effects of Immunusuppressants 67
1.6.4.1 Cyclosporin A and Prednisolone 67
1.6.4.2 Azathoiprine 67
1.7 Overview of Work Described in this Thesis 68
2 Materials and Methods 69
2.1 Chemicals and Reagents 69
2.2 UVA, UVC and IR Irradiation 71
2.2.1 UVA Irradiation 71
2.2.2 UVC Irradiation 71

2.2.3 IR Irradiation 71

2.3 HPLC Techniques *71*

2.3.1 HPLC System 71

2.3.2 RP-HPLC of DNA Bases 72

2.3.3 RP-HPLC of Deoxynucleosides 72

2.4 Molecular Biology Techniques *72*

2.4.1 Genomic DNA Preparation and Depurination 72

2.4.2 PCR and DNA Sequencing 72

2.4.3 Protein Extractions 73

2.4.4 Western Blotting 73

2.5 6-TG/ UVA Photochemistry *74*

2.5.1 6-TG Standard Curve for Quantification 74

2.5.2 Analysis of 6-TG/UVA Photoreactions 74

2.5.3 Digestion of Oligonucleotides 75

2.5.4 Oxidation of 6-TG by MMPP 75

2.6 Biological Assays *76*

2.6.1 Cell Culture and Maintenance 76

2.6.2 6-TG Dose Response 76

2.6.3 UVA Dose Response 76

2.6.4 6-TG/UVA Treatment of Cells 76

2.6.5 Quantification of DNA 6-TG 77

2.6.6 Hydroxyurea and 6-TG/UVA Treatment 77

2.6.7 *APRT* Mutation Frequency Assay 77

2.6.8 ROS Staining, FACS Analysis and Microscopy 78

2.7 Enzymatic Assays *78*

2.7.1 ^{32}P Labelling of Oligonucleotides 78

2.7.2 Annealing of Complementary Oligonucleotides 78

2.7.3 Cleavage Assays 79

2.7.3.1 Fpg 79

2.7.3.2 Aag 79

2.8 Analysis of PCNA State after 6-TG/UVA *79*

2.8.1 PCNA Mono-Ubiquitination 79

2.8.2 Immunoprecipitation of PCNA 79
2.8.3 Rapid Lysis and Analysis after UVA 80
2.8.4 Glutaraldehyde Crosslinking of PCNA 80

2.9 Quantification of 6-TG from Patient Samples 81

3 Results I : UVA Photochemistry of 6-Thioguanine 82

3.1 Introduction 82
3.1.1 Chemical Oxidation of 6-TG and 6-MP 82
3.1.2 UVA Photo-oxidation of 6-MP 84
3.1.3 Detection of 6-TG 85

3.2 Results 85
3.2.1 Detection and Quantification of 6-Thioguanine 85
3.2.2 UVA Photochemistry of 6-Thioguanine 86
3.2.3 Mechanisms of 6-TG/UVA Photoproduct Formation 92
3.2.4 UVA Photochemistry of 6-Thioguanine Deoxyriboside and 6-TG in DNA 93
3.2.5 Quantification of 6-TG by Fluorescence Detection of G-6-SO_3 99

3.3 Discussion 101

4 Results II – Biological Effect of 6-Thioguanine/UVA 104

4.1 Introduction 104
4.1.1 Modes of Action of Thiopurines and Azathioprine 106
4.1.2 Structural Effects of 6-TG 107
4.1.3 6-TG and 6-MP Sensitisation to UV and Ionising Radiation 107
4.1.4 Biological Effects of UVA Irradiation 108
4.1.5 Mutagenicity of UVA 108

4.2 Results 109
4.2.1 Quantification of 6-TG Incorporation in DNA 109
4.2.2 Quantification of 6-TG in Aza Treated Patients 110
4.2.3 6-TG Sensitises Cells to UVA 111
4.2.4 Synergistic Mutagenicity of 6-TG and UVA 114
4.2.5 6-TG/UVA Treatment Generates Reactive Oxygen Species 117
4.2.6 Potential Repair of 6-TG/UVA Photodamage 122

4.2.7 Effects of 6-TG/UVA on Replication 128

4.3 Discussion 134

4.3.1 6-TG Sensitises Cells to UVA 134

4.3.2 Synergistic Mutagenicity of 6-TG and UVA 135

4.3.3 Repair of 6-TG/UVA DNA Photodamage? 137

4.3.4 Effects of 6-TG/UVA on Replication 139

4.3.5 Azathioprine and UVA 141

5 Future Perspectives 144

6 References 146

7 Appendix 160

Table of Figures

Fig 1.1 Generation of Reactive Oxygen Species (ROS) **23**

Fig 1.2 Chemical Structures of Oxidised Thymidine, Deoxycytidine, and Deoxyadenosine **23**

Fig 1.3 Oxidation of Deoxyguanosine (A) and Oxo^{8}deoxyguanosine (B) **26**

Fig 1.4 UV Spectrum (A) and Sunlight/DNA Action Spectrum (B) **29**

Fig 1.5 Chemical Strucutres of UV Induced Cyclobutane Pyrimidine Dimers (A) and (6-4) Pyrimidine-Pyrimidone Photoproducts (B) **29**

Fig 1.6 Mechanisms of Base Excision Repair **34**

Fig 1.7 Nucleotide Excision Repair in Mammalian Cells **37**

Fig 1.8 Human DNA Mismatch Repair (MMR). **42**

Fig 1.9 Mammalian Homologous Recombination Repair of DNA DSB **45**

Fig 1.10 Mammalian Non-Homologous End Joining **46**

Fig 1.11 Translesion Synthesis in Eukaryotes **54**

Fig 1.12 PCNA Modifications Modulate DNA Damage Tolerance and Avoidance **54**

Fig 1.13 Recombinational Restart of Stalled Replication Forks **58**

Fig 1.14 Sonic Hedgehog Signalling Pathway **62**

Fig 3.1 Chemical Oxidation Products of 6-TG **83**

Fig 3.2 Quantification of 6-TG by C_{18} RP-HPLC Coupled to A_{342nm} Detection **87**

Fig 3.3 UVA Mediated 6-TG Destruction and Photoproduct Formation **89**

Fig 3.4 Fluorescence Spectrum and Acid Lability of P1 ..... **91**

Fig 3.5 Chemical Structures of G-6-SO_3 (A) and G-S-G (B) **92**

Fig 3.6 Kinetics of 6-TG/UVA Photoreactions **94**

Fig 3.7 6-TGdR/UVA Photochemical Reactions **95**

Fig 3.8 UVA Irradiation of 6-TG Containing Oligonucleotides **97**

Fig 3.9 6-TG/UVA Photoreactions in ssDNA **98**

Fig 3.10 DNA 6-TG Quantification by Conversion to G-6-SO_3 ..... **100**

Fig 3.11 Proposed Mechanism for 6-TG/UVA Photreactions **102**

Fig 4.1 Metabolism of 6-MP and 6-TG **105**

Fig 4.2 Incorporation of 6-TG into DNA in HCT 116 ..... **112**

Fig 4.3 6-TG Sensitises Cells to UVA **113**

Fig 4.4 6-TG and UVA are Synergistically Mutagenic **116**

Fig 4.5 UVA and DNA 6-TG Combine to Generate ROS **118**
Fig 4.6 Fluoresence Microscopy Analysis of 6-TG/UVA Induced ROS in HCT 116. **119**
Fig 4.7 DNA 6-TG Dependence of ROS Production in HCT 116 ..... **120**
Fig 4.8 6-TG/UVA Induced ROS Production in CHO D422 ..... **121**
Fig 4.9 NER and Excision of Lethal 6-TG/UVA Photodamage **125**
Fig 4.10 Fpg Activity on UVA Irradiated 6-TG Containing Oligonucleotides **126**
Fig 4.11 Aag Activity on UVA Irradiated 6-TG Containing Oligonucleotides **127**
Fig 4.12 PCNA Modification after 6-TG/UVA **129**
Fig 4.13 PCNA Modification: Mono-Ubiquitination **130**
Fig 4.14 PCNA*: Not Induced by Other Forms of DNA Damage **132**
Fig 4.15 Kinetics of PCNA* Formation and Crosslinking of PCNA **133**
Fig 7.1 Resolution of 6-TG from Adenine and Guanine by RP-HPLC Coupled to A_{342nm} Detection **161**
Fig 7.2 Anti-Oxidants Decrease the Rates of 6-TG/UVA Photoreactions **162**
Fig 7.3 Kinetics of 6-TGdR/UVA Photoreactions **163**
Fig 7.4 Digestion of Oligonucleotides and Conversion of Deoxyadenosine to Deoxyinosine **164**
Fig 7.5 6-TG/UVA Photoreactions in dsDNA **165**
Fig 7.6 6-TG Sensitises CHO D422 to UVA **166**
Fig 7.7 PCR Amplification of CHO D422 *APRT* Locus from 6-TG/UVA Induced *APRT* Mutants **167**
Fig 7.8 Visualisation of ROS in CHO D422 ..... **169**

Table of Tables

Table 1.1 Human DNA Glycosylases, their Functionality, and Substrates **33**
Table 1.2 Known Translesion Synthesis Polymerases **55**
Table 2.1 Oligonucleotides Used in this Thesis **69**
Table 2.2 Cell Lines Used in this Thesis **70**
Table 3.1 UVA Dependent Destruction of 6-TG **86**
Table 3.2 Relationship Between 6-TG Destruction and Photoproduct Formation **88**
Table 3.3 Spectral Properties of 6-TG/UVA Photoproducts **88**
Table 3.4 Digestion of Oligonucleotides to Deoxynucleosides **96**
Table 3.5 Percent A_{342nm} Peak Area Remaining after 50kJ/m^2 UVA Irradiation **102**
Table 4.1 Quantification of DNA-6-TG in Skin from Aza Treated Patients **110**
Table 4.2 Spontaneous, UVA and 6-TG + UVA Mutation Spectra **115**
Table 7.1 6-TG/UVA Mutation Spectrum at the CHO D422 *APRT* Locus **168**
Table 7.2 PCNA Interacting Proteins **170**

List Of Abbreviations

1meA	1-methyladenine
3-meA	3-methyladenine
3-meC	3-methylcytosine
(6-4)PP	(6-4) pyrimidines-pyrimidone
6-MP	6-mercaptopurine
6-TdGTP	6-thiodeoxyguanosine 5-triphosphate
6-TG	6-thioguanine
7-meG	7-methylguanine
A	adenine
A_{260nm}	absorbance at 260nm
A_{342nm}	absorbance at 342nm
ADP	adenosine 5-diphosphate
AdR	deoxyadenosine
AK	actinic keratosis
AML	acute myeloid leukaemia
AOA	ataxia ocular apraxia
AP	apurinc / apyrimidinic
APE1	AP endonuclease 1
Aph	aphidicolin
APRT	adenosyl phosphoribosyl transferase
AT	ataxia telangiectasia
ATLD	AT-like disorder
ATP	adenosine 5-triphosphate
Aza	Azathioprine
BCC	basal cell carcinoma
BER	base excision repair
BSA	bovine serum albumin
C	cytosine
CdR	deoxycytidine
Clb	chlorambucil
CMM	cutaneous malignant melanoma
CPD	cyclobutanepyrimidine dimer
CSA/B	Cockaynes syndrome protein A / B
CTX	cyclophosphamide
DMS	dimethyl sulfate
DNA	deoxyribonucleic acid
DNA-PK	DNA-dependent protein kinase
dNTP	deoxynucleosides 5-triphosphate
dRP	deoxyribosephosphate
DSB	double strand break
dsDNA	double stranded DNA
ECL	electro chemiluminescence
EDTA	ethylenediaminetetraacetic acid
EMS	ethyl methane sulfonate
FA	Fanconi anaemia
FapyG	2,6-diamino-4-hydroxy-5-formamidopyrimidine
FCS	fetal calf serum

FEN1	flap endonuclease 1
Fpg	FapyG glycosylase
G	guanine
G-6-SO_3	guanine-6-sulfonate
GA	glutaraldehyde
GdR	deoxyguanosine
GG-NER	global genome NER
Gh	guanidinohydantoin
G-S-G	guanine-6-thioguanine
GSH	glutathione
hABH	human AlkB homologue
HD	Hodgkin's disease
HNE	4-hydroxynonenal
HNPCC	hereditary non-polyposis colon cancer
HO-Pdg	hydroxypropanodeoxyguanosine
HPLC	high performance liquid chromatography
HPRT	hypoxanthine phosphoribosyl transferase
HR	homologous recombination
HU	hydroxyurea
IDL	insertion-deletion loop
IP	immunoprecipitation
IR	ionising radiation
Iz	imidazole
LET	linear energy transfer
LOH	loss of heterozygosity
MAP	Myh-associated polyposis
MDA	malodialdehyde
MED	minimal erythema dose
MEF	mouse embryonic fibroblast
MGMT	O^6-methylguanine-DNA-methyltransferase
MLH	MutL homologue
MMPP	magnesium monoperoxypthalate
MMR	DNA mismatch repair
MMS	methylmethane sulfonate
MNNG	*N*-methyl-*N*'-nitro-*N*-nitrosoguanidine
MNU	*N*-methyl-*N*-nitrosurea
MRN	Mre11/RAD50/Nbs1 complex
MS	mass spectrometry
MSH	MutS homologue
MSI	microsatellite instability
NAC	N-acetylcystine
NBS	Nijmegen break syndrome
NER	nucleotide excision
NHEJ	non-homologous end joining
NHL	non-Hodgkin's lymphoma
NMR	nuclear magnetic resonance
NMSC	non-melanoma skin cancer
$^1O_2$	singlet oxygen
O^6-meG	O^6-methylguanine
OGG1	oxo^{8}G DNA glycosylase

OTR	organ transplant recipient
Oxo^8G	8-oxo-7-hydro-deoxyguanosine
PAGE	polyacrylamide gel electrophoresis
PARP	poly(ADP-ribose) polymerase
PBS	phosphate buffered saline
PCNA	proliferating cell nuclear antigen
$PCNA^{Ubq}$	mono-ubiquitinated PCNA
PCR	polymerase chain reaction
PNK	ploynucleotide kinase
PNPK	polynucleotide kinase phosphatase
Polβ	DNA polymerase β
Polδ	DNA polymerase δ
Polε	DNA polymerase ε
RFC	replication factor C
RNA	ribonucleic acid
RNA PolII	RNA polymerase II
ROS	reactive oxygen species
RPA	replication protein A
RP-HPLC	reversed phase HPLC
RTR	renal transplant recipient
SAM	S-adenosyl methionine
SCAN	spinocerebellar ataxia with axonal neuropathy
SCC	squamous cell carcinoma
SCID	severe combined immunodeficiency
SDS	sodium dodecyl sulfate
SDSA	synthesis dependent strand annealing
Shh	sonic hedgehog
S_N1	unimolecular nucleophilic substitution
S_N2	bimolecular nucleophilic substitution
SMO	smoothened
Sp	spiroiminodihydantoin
SSA	single strand annealing
SSB	single strand break
ssDNA	single stranded DNA
SUMO	small Ubq-like modifier
T	thymine
$T_{1/2}$	half life
TBE	Tris borate EDTA
TCR	transcription coupled repair
TdR	deoxythymidine
TE	Tris-EDTA
TFIIH	transcription factor II H
TLS	translesion synthesis
TPMT	thiopurine methyltransferase
TTD	trichothiodystrophy
Ubq	Ubiquitin
UVR	ultraviolet radiation
XP	xeroderma pigmentosum
Z	Oxalozone

Introduction

1.1 DNA Damage

1.1.1 Spontaneous DNA Damage

Spontaneous DNA damage occurs primarily by deamination, oxidation and loss of bases (Kow 2002). DNA cytosine is the most easily deaminated base. This generates uracil and it has been estimated that this promutagenic reaction results in the formation of 60 to 500 uracils per day per genome (Krokan et al. 2002). The double helix provides significant protection and in double stranded DNA (dsDNA), the rate of deamination is just 0.5% of that in single stranded DNA (ssDNA) (Lindahl 1993). Methylcytosine, which constitutes around 5% of total DNA cytosine, is deaminated to thymine, also a potentially mutagenic change. Purine deamination occurs at less than 2% of the rate of pyrimidines. Adenine and guanine form hypoxanthine and xanthine, respectively. Loss of bases from DNA through cleavage of the N-glycosyl bond between base and deoxyribose, to leave an abasic (AP) site, affects purines more extensively than pyrmidines. Adenine and guanine are lost at a rate of 2,000 to 10,000 per day whereas the rate for pyrimidines is less than 5% of this (Barnes et al. 2004).

1.1.2 Ionising Radiation Induced DNA Damage

Ionising radiation (IR) can induce a variety of DNA damage. The damage induced is dependent on the type of ionizing radiation. When an energetic particle passes through matter, it loses energy by interacting with electrons in that material. The specific energy loss in such a reaction is described by the linear energy transfer value (LET). α-particles, a high LET source, transfer a large amount of energy in interacting with an electron, and are highly effective at inducing DNA damage. Low LET sources, such as γ-ray and X-rays, are less effective (Ward 2000). IR induced damage can be direct or indirect. Direct damage occurs after interaction of the radiation with DNA itself. This is believed to be responsible for approximately 35% of IR induced DNA damage. The remaining 65% is due to indirect effects (Ward 1994).

The primary effectors of indirect IR damage are reactive oxygen species (ROS). These are formed by the radiolysis of water and the hydroxyl radical (•OH) is believed

to be the major product. However, singlet oxygen ($^1O_2$), superoxide ($\bullet O_2^-$) and hydrogen peroxide (H_2O_2) may also be formed. DNA damage induced by ROS will be discussed in greater detail in a later section of this thesis.

The lethal effects of IR have been mostly attributed to the induction of DNA strand breaks. The majority of breaks affect only a single strand, but a number of double strand breaks (DSB) are also induced. IR induced DNA strand breaks tend to have damaged termini which differ from the canonical substrate for DNA ligases (3'-OH, 5'-phosphate) and so prevent repair by direct ligation. SSB formation occurs via •OH oxidation of deoxyribose residues, and the number of SSBs is dependent on induced •OH concentration (Milligan 1995). The mechanisms leading to DSB formation are less clear. It is proposed that they arise after the reaction of two •OH radicals with two closely opposed bases on opposite strands, but they may also arise from a single event.

Ionising radiation is a major tool in the treatment of a variety of tumours. Radiotherapy is used to treat tumours directly (early stage oral and cervical cancers, squamous and basal cell carcinomas), but it is more commonly used in conjunction with surgery and/or chemotherapy, where it can increase the efficacy of such treatments.

1.1.3 Alkylation of DNA

Alkylating agents damage DNA by the transfer of alkyl groups. This has been extensively reviewed (Sedgwick et al. 2002; Middleton et al. 2003; Drablos et al. 2004). The relative yield of each lesion is dependent on the nature of the agent, its reaction mechanism, and the secondary structure of the DNA. Alkylating agents may be divided into two classes depending on their reaction mechanism. S_N1 agents act via unimolecular nucleophilic substitution, and can modify nitrogen and oxygen atoms in DNA bases and the sugar-phosphate backbone. Examples of S_N1 agents include N-methyl-N-nitrosurea (MNU) and N-methyl-N'-nitro-N-nitrosoguanidine (MNNG). S_N2 agents, which act through a bimolecular nucleophilic substitution mechanism, almost exclusively alkylate nitrogen atoms. S_N2 agents include methyl methanesulphonate (MMS) and dimethylsulphate (DMS). In general, O-alkylations tend to be highly mutagenic and toxic, whereas N-alkylations, although cytotoxic, are less mutagenic

Alkylating agents can be further divided into monofunctional and bifunctional agents. Monofunctional agents contain a single reactive group, while bifunctional agents contain two. The presence of two reactive groups allows the modification of two sites in DNA. Examples of monofunctional agents include MMS, MNU and MNNG. In double stranded DNA, monofunctional alkylating agents mainly result in 7-methylguanine (7-meG), 3-methyladenine (3-meA) and O^6-methylguanine (O^6-meG). In single stranded DNA, 1-methyladenine (1-meA) and 3-methylcytosine (3-meC) are the predominant lesions. Ethylating agents, such as ethyl methanesulphonate (EMS), generally react with the same DNA nitrogen and oxygen groups as their methylating counterparts to produce the corresponding ethylated bases

Clinically, the most commonly used monofunctional alkylating agents are the tetrazines Temozolomide, Procarbazine, and Dacarbazine, which are metabolised to reactive intermediates that decompose to produce a methyl diazonium ion, which is the active alkylating species.

Bifunctional alkylating agents produce far more complex lesions than monofunctional agents. They can form intra- or inter-strand crosslinks. This class of alkylating agents includes the bifunctional nitrosureas, of which the chloroethylnitrosureas are clinically the most commonly used. These cause interstrand crosslinks predominantly between the N^1 position of guanine and the N^3 position of the complementary cytosine. If the second reaction is with an active group of a protein, DNA guanine-protein crosslinks are formed.

The nitrogen mustards represent another class of bifunctional alkylating agents. These are frequently used in cancer therapy, and include cyclophosphamide (CTX), melphalan, and chlorambucil (Clb). CTX and Clb are also used as immunosuppressants. The mechanism of action of nitrogen mustards is complex, and involves activation by cytochrome P450 in the liver, followed by uptake into target cells before the final alkylating form, phosphoramide mustard, is produced. It is proposed that the chloroethyl groups of phosphoramide mustard can cyclise to form a chloroethyl azidinium moiety, leading to formation of chloroethylazidridine, which may be the primary alklyating species.

1.1.3.1 Clinical Uses of Alkylating Agents

Therapeutic alkylating drugs are primarily methylating agents or chloroethylating agents. The methylating agents procarbazine and dacarbazine are commonly used for the treatment of Hodgkin's disease (HD) and non-Hodgkin's lymphoma (NHL) (Yung et al. 2000). Temozolomide is used in the treatment of high grade gliomas, and exhibits a greater anti-tumour activity when combined with procarbazine (Newlands et al. 2003). Among the chloroethylating agents, carmustine is used to treat HD, NHL, brain tumours and multiple myelomas. Lomustine is used against HD and brain tumours, while fotemustine is also used in the treatment of brain tumours. The nitrogen mustards are used against a wide range of cancers.

1.1.4 Oxidative DNA Damage

Aerobic organisms have an absolute requirement for oxygen. The oxidative metabolism by which energy is produced is responsible for producing DNA damaging reactive oxygen species (ROS). ROS production by metabolic processes is counteracted by various anti-oxidant defences. These include low oxygen tension (3 to 4%), compartmentalisation of oxidative metabolism to the mitochondrion in eukaryotes, sequestration of transition metals which take part in ROS generation, the production of intracellular thiol containing compounds to scavenge oxygen radicals, and many more. When the balance between ROS and anti-oxidant defences is disturbed in favour of excess production, this leads to a condition known as oxidative stress. In addition to ROS, oxidation can also occur by a process called one electron oxidation, in which the substrate itself becomes a radical as a result of direct energy transfer from a highly energetic particle, for example direct IR induced damage.

1.1.4.1 ROS

ROS describes a wide range of radical and non-radical oxygen species. These include the free radicals •OH, superoxide ($\bullet O_2^-$), peroxyl radicals ($\bullet RO_2$), alkoxyl radicals (•RO) and nitric oxide (•NO). Non-radical ROS include $^1O_2$, peroxynitrite ($ONOO^-$), and H_2O_2. Extensive knowledge of the generation and chemistry of these species has been obtained (Halliwell et al. 1998).

•OH is extremely reactive. The reactivity of •OH is so great that it does not diffuse more than one or two molecular diameters before it reacts with and oxidises a cellular component (Marnett 2000). •OH can be formed by a number of mechanisms. The primary mechanism involves the Fenton reaction (Fig 1.1 Reaction 1) (Henle et al. 1997). UV-induced homolytic fission of H_2O_2 also leads to •OH production (Fig 1.1 Reaction 2). Ionising radiation produces •OH by the homolytic fission of H_2O (Fig 1.1 Reaction 3). •OH can undergo three types of reaction; hydrogen abstraction, addition and electron transfer.

Superoxide radicals can be produced by leakage from the electron transport chain in mitochondria. They can also be generated enzymatically by xanthine oxidase. $•O_2^-$ itself reacts very poorly with DNA and other non-radical compounds. Dismutation results in the production of H_2O_2 (Fig 1.1 Reaction 4). This can then take part in Fenton type reactions to produce •OH.

Peroxyl radicals ($•RO_2$) are formed by reaction of •OH with an organic compound leading to formation of a carbon-centred radical, •R, which reacts with O_2 to form a peroxyl radical. Decompostion of organic peroxides, ROOH, can also lead to peroxyl radical formation, in addition to alkoxyl radicals (•RO). •NO is synthesised intracellularly by the nitric oxide synthase family of enzymes, and acts as a signalling molecule, and a neurotransmitter. •NO is unreactive with non-radicals but can produce •OH and peroxynitrite ($ONOO^-$) (Fig 1.1 Reaction 5 and 6).

Singlet oxygen, while not a radical, is an important form of reactive oxygen. It is generated from peroxyl radicals, hypochlorous acid, and also through type II photosensitisation reactions (Fig 1.1 Reaction 7). $^1O_2$ reacts via chemical reaction, or energy transfer. With regard to DNA damage, $^1O_2$ reacts almost exclusively with guanine residues.

(1) $Fe^{2+} + H_2O_2 + H^+ \longrightarrow Fe^{3+} + H_2O + \bullet OH$

(2) $H_2O_2 \xrightarrow{UV} 2\ \bullet OH$

(3) $H_2O \xrightarrow{IR} \bullet OH + \bullet H$

(4) $2\ \bullet O_2^- + 2H^+ \longrightarrow H_2O_2 + O_2$

(5) $NO^- + \bullet NO \longrightarrow \bullet ONNO^- \xrightarrow{H^+} N_2O + \bullet OH$

(6) $\bullet O_2^- + \bullet NO \longrightarrow ONOO^-$

(7) $H_2O_2 + OCl^- \longrightarrow {}^1O_2 + H_2O + Cl^-$

Fig 1.1 Generation of Reactive Oxygen Species (ROS). (Adapted from Halliwell and Gutteridge 1999, Henle and Linn 1997)

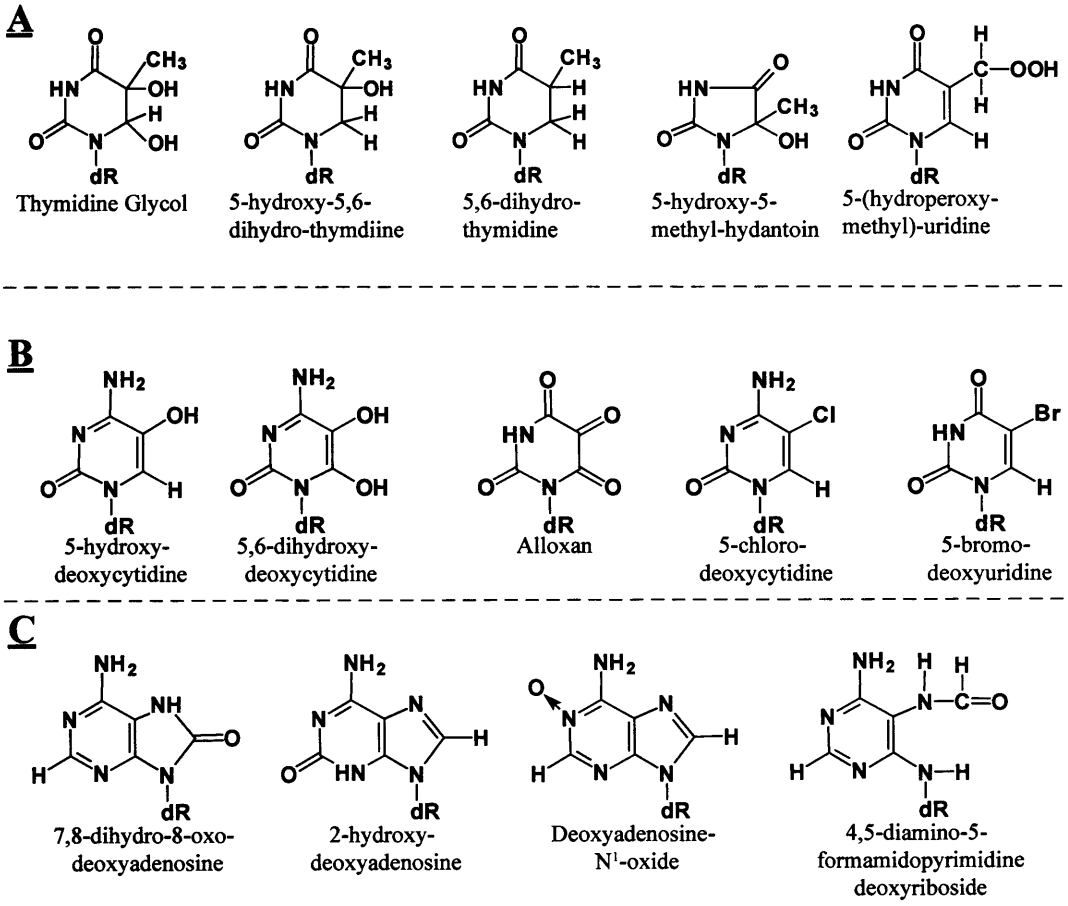

Fig 1.2 Chemical Structures of Oxidised Thymidine (A), Deoxycytidine (B) and Deoxyadenosine (C). A selection of the most frequently formed products are shown (Adapted from Bjelland and Seeberg 2003).

1.1.4.2 ROS Induced DNA Damage

The variety of DNA lesions induced by ROS have been reviewed in great detail (Bjelland et al. 2003; Cadet et al. 2003). Here I will present a brief overview of oxidised DNA deoxynucleosides.

Thymidine can be attacked by ROS at two positions, the 5,6-double bond or the 5-methyl group. Deoxycytidine only offers the 5,6 double bond. Many of its oxidation products are deoxycytidine versions of thymidine products and many can be deaminated to generate their deoxyuridine counterparts. Oxidation of pyrimidines can also lead to the generation of ring opened products such as formylamine, and urea. Approximately 5% of DNA deoxycytidine exists as 5-methyldeoxycytidine, and this allows 5-methyl oxidation to occur. As of the writing of this thesis, eight forms of oxidised deoxyadenosine have been identified, many of which are analogues of oxidised deoxyguanosine, discussed in greater detail below (Fig 1.2).

Currently, fifteen forms of oxidised deoxyguanosine are known (Fig 1.3). Deoxyguanosine has the lowest oxidation potential of all the DNA deoxynucleosides, and so is the most prone to oxidation. 8-oxo-7,8-dihydrodeoxyguanosine (which exists in equilibrium between 8-oxo-7-hydro- and 8-hydroxy-7,8-dihydro-deoxyguanosine) (oxo^8dG) is the best characterised oxidation product. Long range electron transfer (over distances greater than 200Å) through DNA specifically oxidises deoxyguanosine to oxo^8dG, with no oxidation of other DNA nucleosides (Yavin et al. 2005). Oxo^8dG can also be formed by a number of oxidising agents. Reaction with $^1O_2$ leads to 4,8-endoperoxide formation, which can be rearranged into 8-hydroperoxy-2'-deoxyguanosine, and this can be readily reduced to oxo^8dG. Endoperoxides can also lead to the formation of spiroiminodihydantoins (Sp). Exposure to γ-radiation, high intensity UVA, and type I photosensitisers can lead to the formation of a 2'-deoxyguanosine radical cation. This too produces oxo^8dG, but also results in the formation of 2,6-diamino-4-hydroxy-5-formamidopyrimidine (FapyG), a ring opened purine product. Both of these are produced via an oxo^8guanosyl radical. FapyG is a major product of exposure to a wide range of other oxidising agents, but is not formed by $^1O_2$ (Douki et al. 1999).

Oxo^{8}dG itself is far more easily oxidised than deoxyguanosine. Cyanuric acid deoxyriboside is a major product of both $ONOO^-$ and $^1O_2$ oxidation of oxo^{8}dG. The same is true for oxaluric acid deoxyriboside. The other $^1O_2$ oxidation products of oxo^{8}dG are guanidinohydantoin (Gh) and Sp deoxyribosides. One electron oxidation of oxo^{8}dG also leads to the production of Gh.

•OH generates an oxalozone (Z) derivative and its labile precursor, an imidazole (Iz). These are also minor products of one electron oxidation. 8-nitrodeoxyguanosine can be generated from $ONOO^-$, •NO or NO_2^-, and can be deaminated to 8-nitroxanthine deoxyriboside. 5-guanidino-4-nitroimidazole deoxyriboside is formed by $ONOO^-$, while free radical induced crosslinking can generate 5',8-cyclo-2'-deoxyguanosine.

In addition to single deoxynucleoside damage, ROS also causes tandem deoxynucleoside damage in DNA. This can occur by one electron oxidation or via hydroxyl radicals. Interestingly, a single •OH hit may be sufficient for the formation of tandem lesions. Tandem lesions include thymine-guanine([5-methyl]-8) deoxyriboside and formylamine-oxo^{8}dG.

1.1.4.3 Indirect Base Damage after Oxidative Stress

ROS produced when cells are under oxidative stress are capable of reacting with many cellular components, including lipids. Lipids are particularly susceptible to oxidation, and this leads to the formation of various aldehyde products. Of these, malodialdehyde (MDA) and 4-hydroxynonenal (HNE) are major products. MDA reacts with guanine, adenine and cytosine to form DNA adducts (Marnett 2000). The epoxide of HNE can react to form an etheno-adenine adduct. Hydroxypropanodeoxyguanosines (HO-PdGs) are formed by acrolein and crotonaldehyde, two other lipid peroxidation products.

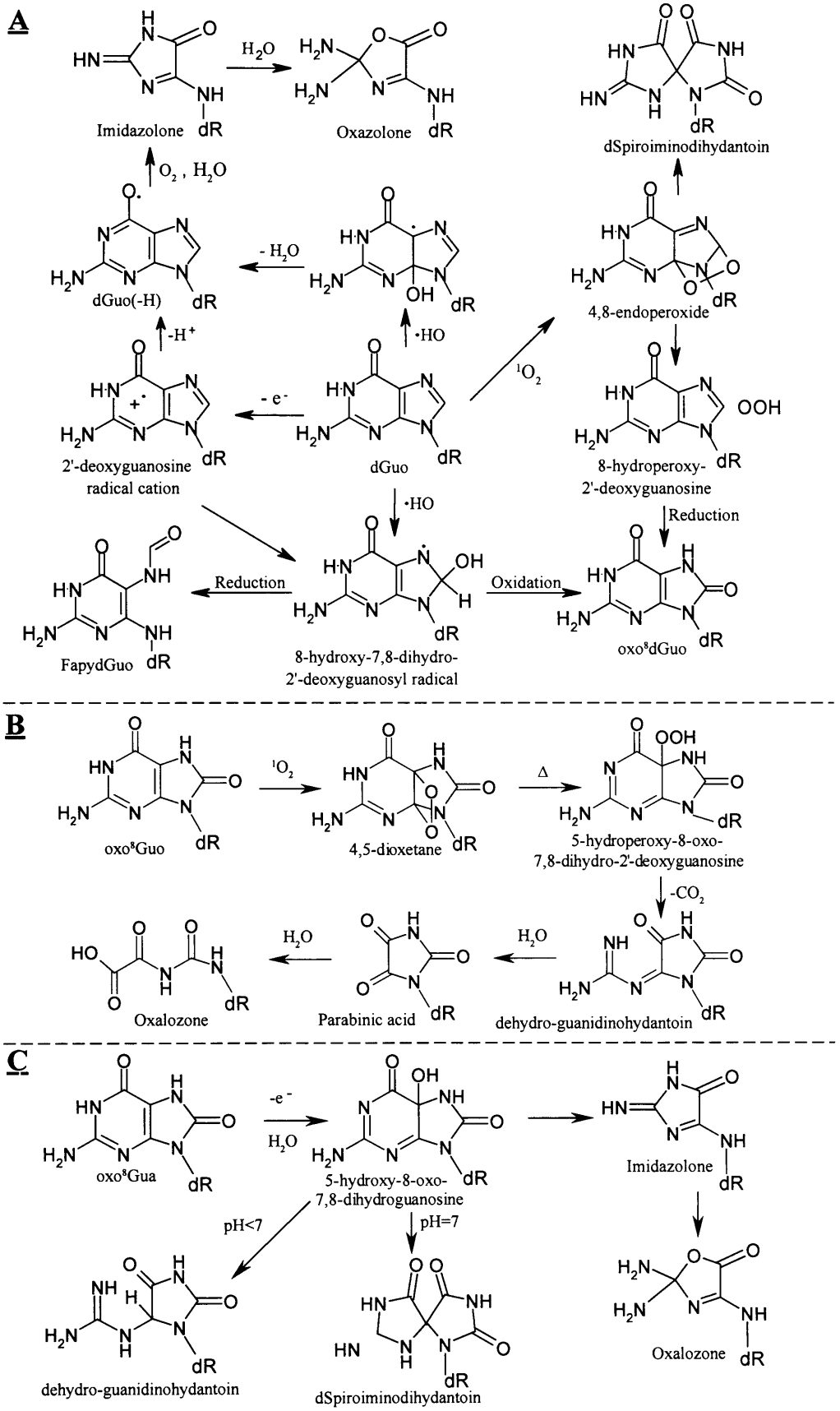

Fig 1.3 Oxidation of Deoxyguanosine (A) and Oxo⁸deoxyguanosine (B and C). (Adapted from Cadet et al. 2003, Bjelland and Seeberg 2003)

1.1.4.4 Oxidatively Induced DNA Strand Breaks

Treatment of cells with IR, H_2O_2 or other oxidising agents leads to the formation of single and double strand breaks (SSB and DSB respectively). The deoxyribose moieties are targeted by approximately 20% of DNA-attacking •OH radicals. This can result in deoxyribose ring fragmentation. Alternatively, ring saturation of bases may lead to destabilisation of the N-glycosyl bond, resulting in an increased rate of depurination and formation of AP sites (Sonntag 1987). The mechanism(s) of DSB formation is not yet fully understood. It may be due to localised attack by more than one radical, formation of two SSB sites within ten base pairs of each other, or transfer of a radical to the opposing strand after SSB formation. Additionally, if oxidised bases are not repaired before attempts are made to replicate them, then replication fork stalling may lead to the generation of DSBs.

1.1.4.5 Oxidative Protein Damage

Proteins turnover rapidly and protein oxidation is not considered to have acute effects. Protein crosslinking by ROS has been implicated in photoaging (Wulf et al. 2004). In this instance, collagen fibres appear to become oxidatively crosslinked after UV exposure. The oxygen dependence of this cross linking has been demonstrated by the protective effect of anti-oxidants. Polyphenols from green tea and extra virgin olive oil have been shown to protect from photoaging (Ichihashi et al. 2003), as indeed has topical application of Vitamin A and E solution, and emulsions containing ubiquinone (Coenzyme Q10) (Tournas et al. 2006). Chronic oxidative damage to proteins of the skin may therefore be important.

1.1.5 UV Induced DNA Damage

Ultraviolet radiation consists of electromagnetic radiation of wavelengths between 100 and 400nm. UV is split into 3 regions, UVA (320 to 400nm), UVB (280 to 320nm) and UVC (100 to 280 nm) (Fig 1.4A). UVB is further divided into shortwave (280 to 295nm) and longwave (295 to 320). UVC is the most genotoxic of these as the absorption maximum of DNA lies within this region, at 260nm (Fig 1.4B). Biologically

UVC is unimportant since it is absorbed by stratospheric ozone. Shortwave UVB is also filtered by the ozone layer. Incident solar radiation to which we are exposed contains only UVA and longwave UVB. UVA accounts for more than 90% of UV exposure on the earth's surface.

1.1.5.1 UVC

UVC irradiation of DNA leads primarily to the formation of pyrimidine dimers. The major dimeric products are cyclobutanepyrimidine dimers (CPDs) (Fig 1.5A). Of these, TT dimers are the most common, while CC dimers are least common (Cadet et al. 2005). CPD formation is heavily sequence dependent.

The (6-4) pyrimidine-pyrimidone photoproducts comprise the second major class of dimeric photoproducts (Fig 1.5B). These also cause a distortion of the DNA double helix structure, but to a greater extent than CPDs (Sinha et al. 2002). Adenine dimers, cytosine photohydrate, thymine glycol as well as DNA-protein crosslinks and DNA strand breaks are also formed, albeit as minor products.

1.1.5.2 UVB

The DNA damage spectrum of UVB is very similar to that of UVC. The same photoproducts, in the same relative ratios, are formed. The overall levels of photoproducts are lower at equivalent doses, however. This reflects the weaker UVB absorption by DNA. UVB also causes oxidative stress in exposed cells, as observed by induction of ROS and oxo^{8}G. It has been proposed that this is due to H_2O_2 production leading to generation of •OH. However, reaction of O_2 with excited state bases can generate $^1O_2$, which can also produce oxo^{8}G. One electron oxidation of guanine is another possibility.

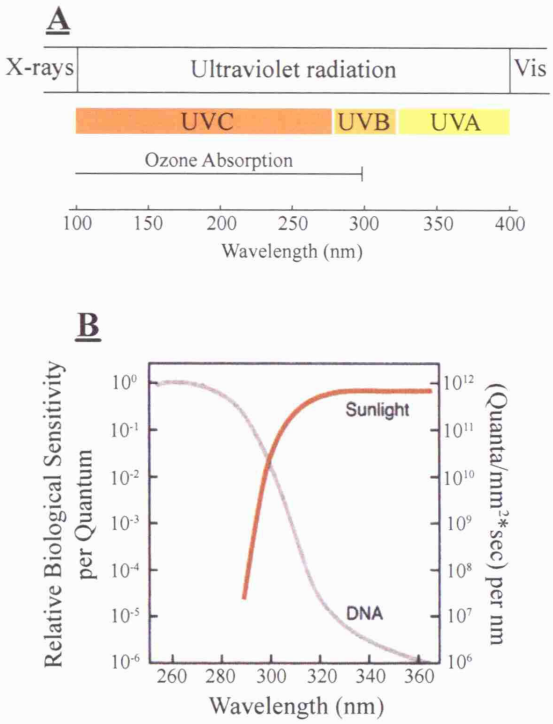

Fig 1.4 UV Spectrum (A) and Sunlight/DNA Action Spectrum (B). (Adapted from Friedberg et al. 2006)

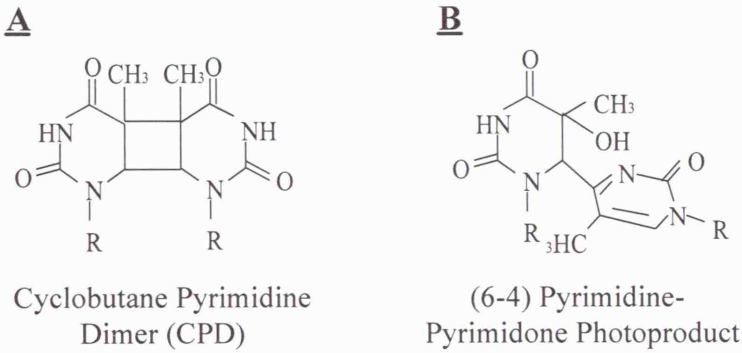

Fig 1.5 Chemical Structures of UV Induced Cyclobutane Pyrimidine Dimers (A) and (6-4) Pyrimidine-Pyrimidone Photoproducts (B). (Adapted from Ichihashi et al. 2003)

1.1.5.3 UVA

DNA is a very weak chromophore for UVA (Fig 1.4B). UVA is absorbed almost 10^5 fold less efficiently than UVC, and 10^3 times less than UVB. Other cellular chromophores may absorb UVA and act as UVA photosensitisers. Photosensitisation involves the excitation of a photosensitiser by absorption of photons of specific wavelengths (MacRobert et al. 1989). This generates a transient excited triplet state photosensitiser. The return of this species to its ground state can involve the transfer of energy directly to a cellular component forming either a free radical or a charged ionic species. This is a Type I photosensitisation reaction. A Type II reaction involves transfer of energy from the excited photosensitiser to O_2, generating singlet oxygen.

UVA exposure causes oxidative DNA damage. The spectrum of oxidative damage differs from γ-radiation, indicating that •OH is not the primary oxidising species. The major oxidative lesion has been determined to be oxo^{8}G, although it is produced at very low levels compared to those measured after an equivalent dose of UVB. At shorter wavelengths (<340nm), oxidative lesion formation may occur via one electron oxidation after direct absorption of UVA photons by DNA, while at longer wavelengths (>400nm), oxidation occurs via photosensitisation reactions, and the formation of $^1O_2$ (Kielbassa et al. 2000). At these longer wavelengths, the spectrum of DNA lesions closely resembles that formed by $^1O_2$ oxidation. DNA oxo^{8}G is mutagenic, and in *Saccharomyces cerevisiae,* it has been demonstrated that UVA is highly mutagenic in cells lacking the ability to repair this lesion (Kozmin et al. 2005). While cellular UVA chromophores have not yet been identified, it is thought that porphyrins such as haemoglobin precursors may represent the major UVA photosensitiser source. Thiol containing compounds may provide alternative UVA chromophores.

In addition to generating ROS through endogenous photosensitisers, UVA leads to an increase in free iron (Fe^{2+}) (Reelfs et al. 2004). This may place the cells under further oxidative stress by promotion of Fenton type reactions, as described earlier. UVA induced necrosis has been linked to the intracellular levels of free Fe^{2+} (Zhong et al. 2004). UVA also results in increased production of •NO (Paunel et al. 2005), itself an oxygen radical which can generate •OH and $ONOO^-$.

While UVA induced oxidation of DNA bases clearly has a biological significance, the primary UVA induced lesions are bipyrimidine photoproducts (Rochette et al. 2003). CPDs are formed at a frequency three fold higher than oxo^{8}G, and represent the major class of UVA photoproducts. These are almost exclusively TT dimers, and the ratio of thymine to cytosine containing dimers is far greater than with UVB. Interestingly, the level of UVA induced CPDs is almost 10^5 fold lower than for UVC, suggesting that their formation is a result of direct UVA photon absorption since UVA energy absorption by DNA is almost 10^5 fold lower than for UVC. The other main class of UVB and UVC induced dimers, (6-4)PPs, are not detected after UVA, nor are their Dewar valence isomers (Douki et al. 2003).

In addition to base damage, UVA induced oxidation can lead to DNA protein crosslinks and DNA strand breaks (Ichihashi et al. 2003). SSB formation has been proposed to occur via UVA excitation of the guanine radical cation, leading to the generation of a deoxyribose radical, and subsequent strand breakage (Adhikary et al. 2005).

1.2 Repair of DNA Damage

In order to cope with this wide spectrum of DNA damage and still maintain genome integrity, cells have developed an impressive array of DNA repair mechanisms. These mechanisms shall be discussed in the coming pages.

1.2.1 Reversal of DNA Damage

In some cases, DNA damage can be directly reversed without the need to excise bases or cut the DNA phosphodiester backbone. Photolyase enzymes can reverse UV induced CPDs and (6-4)PPs (Todo 1999). CPD photolyases, on exposure to blue light, can cleave CPDs into their monomer bases. CPD photolyases have been found in bacteria, and a number of eukaryotes, including yeast, plants and vertebrates (including goldfish). This class of enzyme appears to be absent in humans. (6-4)PP photolyases are found more widely than CPD photolyases, and reverse (6-4)PPs. As with CPD photolyases, this family of enzymes also appears to be absent in humans.

The alkyltransferases can directly repair a number of alkylated bases. DNA O^6-meG is repaired by O^6-methylguanine-DNA-methyltransferase (MGMT) (Pegg 2000; Margison et al. 2002; Drablos et al. 2004). MGMT transfers the methyl group from the O^6 of O^6-meG onto a cysteine residue in its active site. This deactivates the enzyme which is then degraded by the proteosome. A number of other alkyl groups, including ethyl, n-propyl and n-butyl, can also be removed from the guanine O^6 position, albeit more slowly.

The *E. coli* AlkB protein is part of the adaptive response to alkylation damage. It functions as a dioxygenase, which releases the methyl group from 1-meA and 3-meC by oxidative demethylation (Falnes et al. 2002; Trewick et al. 2002). The released methyl group is oxidised to formaldehyde. To date, eight human homologues of AlkB have been identified, hABH1-8 (Drablos et al. 2004). hABH2 and hABH3 act on 1-meA and 3-meC (Duncan et al. 2002). hABH3, like AlkB, also demethylates RNA, *in vitro*. The biological significance of these activities has been demonstrated using methylated DNA and RNA bacteriophages, *in vivo* (Aas et al. 2003). The functions of hABH4-8 are currently unknown.

1.2.2 Base Excision Repair

Base excision repair (BER) is the primary repair mechanism for the removal of oxidised, alkylated, deaminated, and hydroxylated bases (Lindahl et al. 1999; Hoeijmakers 2001; Lindahl 2001). Described very simply, BER consists of (a) removal of damaged base by cleavage of the sugar-base bond, (b) AP site incision, (c) excision of sugar-phosphate residue, (d) repair DNA synthesis, and (e) ligation of the DNA backbone (Fig 1.6). Each of these steps is described in more detail in the following paragraphs.

The first step in BER is removal of the damaged base. This is performed by a member of a group of enzymes known as DNA glycosylases. The DNA glycosylases scan the minor groove of DNA by facilitated diffusion. On recognition of a damaged base, the glycosylase kinks the DNA backbone and flips the base out into a recognition pocket in which cleavage of the N-glycosyl bond is catalysed (Parikh et al. 1998).

Eleven DNA glycosylases have been identified in humans to date (Table 1.1). These can be classified as monofunctional or bifunctional (Seeberg et al. 2000). Monofunctional glycosylases only cleave the base from the DNA backbone. Glycosylases that excise alkylated bases, or uracil, are monofunctional. Bifunctional glycosylases excise oxidised bases, and have an intrinsic AP lyase activity which cleaves the DNA backbone immediately 3' of the AP site generated by base removal. A general feature of DNA glycosylases is that after excision of the base, they remain tightly clamped to the AP site which they have just created. The glycosylase is displaced by the next enzyme to be recruited to the site of damage, an AP endonuclease.

Glycosylase	Functionality	Substrates Include...
UNG	mono-	Uracil (U)
SMUG1	mono-	U, 5-OHme-U
MBD4	mono-	U or T opposite G (at CpG)
TDG	mono-	U, T, ethenoC opposite G
OGG1	bi-	Oxo^{8}G, FaPy-G
MYH	bi-	A opposite oxo^{8}G, 2-OH-A opposite G
NTH1	bi-	Ring saturated and fragmented pyrimidines
AAG	mono-	3-me-purines, hypoxanthine, ethenoadenine
NEIL1	bi-	As for NTH1, FaPy-A, oxo^{8}G, thymine glycol
NEIL2	bi-	Oxidised and fragmented pyrimidines
NEIL3	bi-	Fragmented pyrimidines

Table 1.1 Human DNA Glycosylases, their Functionality, and Substrates (Adapted from Friedberg et al. 2006)

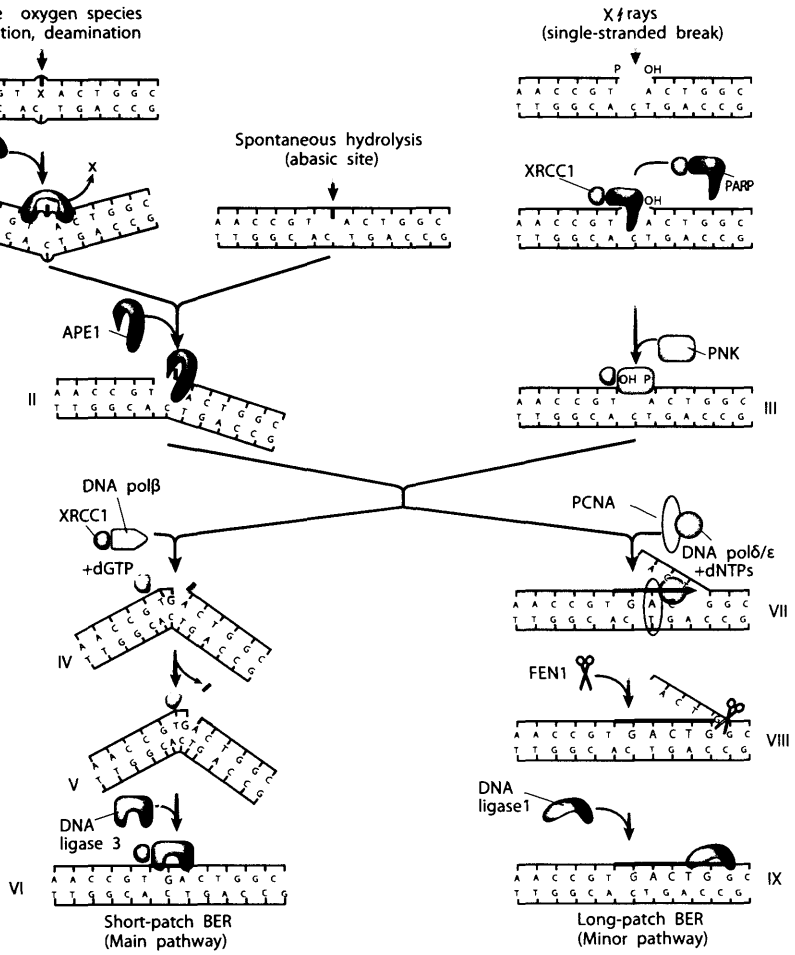

Fig 1.6 Mechanisms of Base Excision Repair. Damaged bases are excised by a DNA glycosylase. APE1 cleaves the abasic site. In short patch repair, DNA Polβ removes the abasic dRP, and performs DNA repair synthesis across the gap. The nick in the DNA backbone is ligated by DNA Ligase III. In long patch repair, DNA Polβ fails to excise the abasic dRP. Synthesis by DNA Polβ, δ or ε leads to displacement of the damaged strand. The displaced strand is cleaved by FEN1, and the backbone ligated by DNA ligase I. These pathways can also function for spontaneous AP sites, and single strand breaks. (Adapted from Hoeijmakers 2001)

AP incision is required after base removal by both classes of glycosylase. In humans APE1 is the primary AP endonuclease. APE1 recognises the 5' phosphate of an AP site, flips out the deoxyribose, and cleaves the sugar-phosphate bond. The cleaved AP site bears 3'-OH and 5'-phosphate termini. AP endonuclease processing is also necessary if the backbone has been cleaved by the AP lyase activity of a DNA glycosylase. In this case, APE1 removes the lyase product from the 3' end to generate a 3'-OH group. In addition to this function, APE1 is needed for the recruitment of DNA Polβ, required for the next step of the BER process.

Before repair DNA synthesis can be performed, the abasic dRP must be removed. Removal can occur via two distinct mechanisms. DNA Polβ, in addition to its polymerase domain, has an N-terminal deoxyribophosphatase domain. This excises the dRP, leaving a single nucleotide gap, which Polβ fills in. This is known as short patch BER. Polβ interacts with the XRCC1 subunit of the XRCC1-DNA Ligase III heterodimer. After insertion of the nucleotide by Polβ, Ligase III closes the nick, thereby completing repair.

If the 3' terminal dRP has a complex structure that is resistant to Polβ cleavage, then Polβ, Polδ or Polε can synthesise a repair patch with displacement of the damaged strand. This typically involves incorporation of between 2 and 8 nucleotides, and is known as long patch BER. After synthesis is complete, the flap endonuclease FEN1 cleaves the displaced strand in a reaction stimulated by PCNA, and DNA Ligase I ligates the nick.

In addition to the above, other factors may also be involved in BER. The bifunctional DNA glycosylases NEIL1 and NEIL2 cleave both 3' and 5' of the damaged base, creating termini bearing a 3' and 5' phosphate. In order for repair DNA synthesis to take place, the 3'-phosphate must be removed. This reaction is carried out by polynucleotide kinase phosphatase (PNPK) (Wiederhold et al. 2004). PNPK activity generates a 3'-OH terminus and allows the gap to be filled via short patch BER.

Poly(ADP-ribose) polymerase (PARP) is involved in SSB repair, although exactly how is not clear. It is also involved in BER. Indeed, the later steps of DNA nick repair require the proteins involved in the later stages of BER (Fig 1.6). PARP binds very strongly to dRP residues. A number of functions have been proposed for PARP. These include protection of the AP site to allow repair and provision of a scaffold for subsequent protein-protein interactions (Leppard et al. 2003), initiation of long patch repair if short patch repair is ineffective (Prasad et al. 2001), and acting as a specific source of ATP for the DNA ligation reactions (Oei et al. 2000).

In addition to the removal of damaged bases, BER can also repair AP sites formed through spontaneous base loss by hydrolysis, and also oxidised abasic sites formed through reaction of ROS with deoxyribose residues in the DNA backbone (Sung et al. 2006).

1.2.3 Nucleotide Excision Repair

Nucleotide excision repair (NER) is perhaps the most versatile of DNA repair mechanisms (Lindahl et al. 1999; Hoeijmakers 2001; Mitchell et al. 2003; Lombard et al. 2005). NER is activated by a wide variety of lesions that share a common ability to distort the DNA double helix. These include UV photoproducts, many bulky chemical adducts, and some oxidative lesions. In general, the greater the helix distortion by a lesion, the more efficient is its recognition by NER, although distortion alone is not sufficient to ensure repair. NER can be divided into two pathways, which can be discriminated by their distinct mechanisms of lesion recognition.

Global genome repair (GG-NER) involves lesion recognition by the XPC-HR23B complex or the XPE-DDB1 complex. These are ATP-independent DNA binding factors that recognise the distorted double helix. As the name suggests, GG-NER occurs throughout the genome and it is adversely affected by DNA packing in nucleosomes (Lombard et al. 2005).

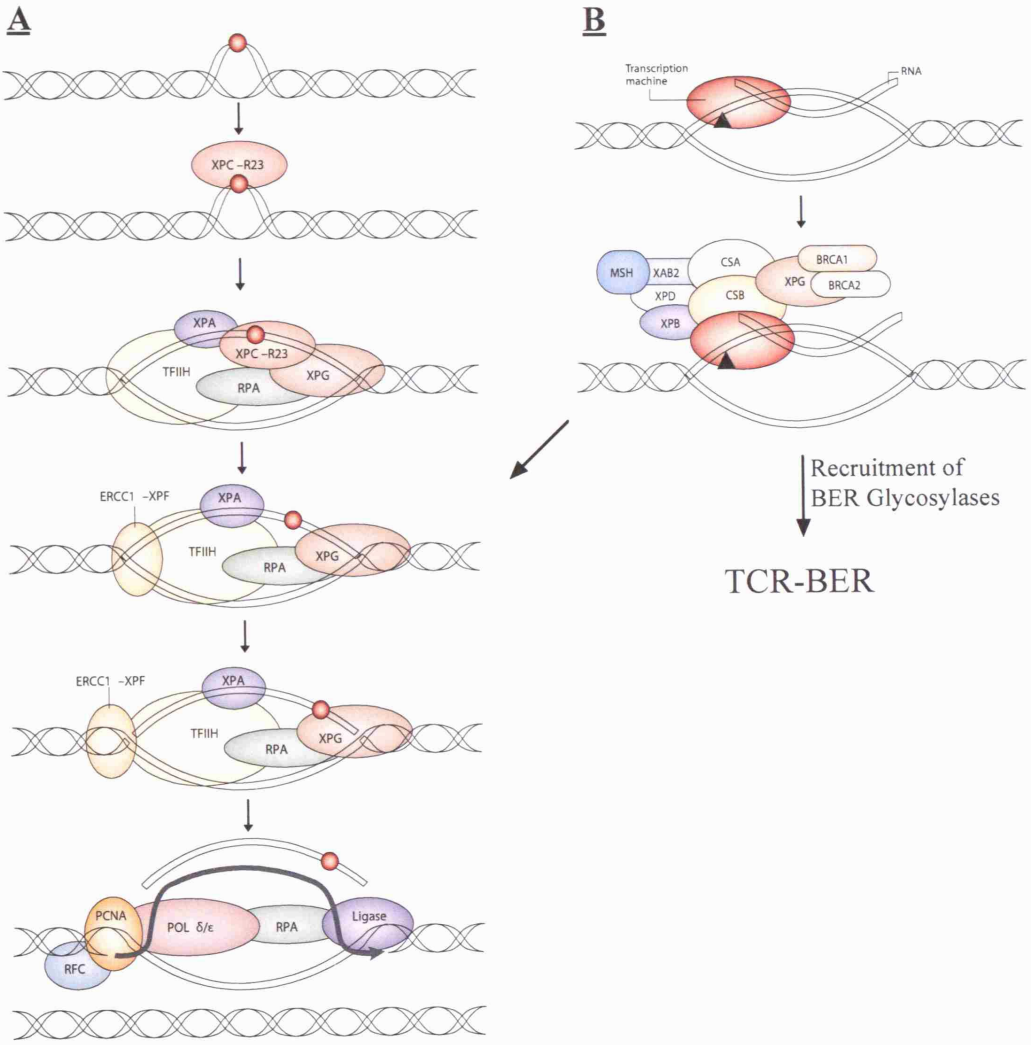

Fig 1.7 Nucleotide Excision Repair in Mammalian Cells. **A** Global genome repair (GG-NER) involves lesion recognition by XPC-HR23B, leading to TFIIH recruitment, followed by local DNA unwinding, and incision 3' and 5' of the lesion by XPF-ERCC1 and XPG, respectively. Oligonucleotide containing damaged bases is released and the gap filled by DNA Polδ or ε and sealed by DNA ligase. **B** Transcription coupled repair is initiated by stalling of RNA PolII at a lesion. CSB and other factors are recruited. RNA PolII is displaced from the site of damage, and the GG-NER factors recruited for strand excision and resynthesis. TCR may also lead to the repair of oxidative lesions by a form of TCR-BER. (Adapted from Friedberg 2001).

Transcription coupled repair (TCR) is initiated by stalling of RNA PolII at a damaged base (Svejstrup 2002). Inhibition of RNA PolII by α-amanitin abolishes TCR. TCR occurs only in actively transcribed regions of the genome, and repairs lesions 5 to 10 fold faster than GG-NER. After RNA PolII stalling, the CSA/CSB proteins are involved in its displacement from the damage site. The mechanism of this displacement is not clear, and may involve remodelling of the RNA PolII DNA interface, displacement of PolII from the DNA, DNA translocation, or degradation of PolII by the proteosome (Svejstrup 2003).

After recognition of the damaged base, the TFIIH complex is recruited to the site of damage. TFIIH is a 10 subunit complex, which contains the XPB and XPD helicases. These helicases cause local unwinding of about 30 base pairs around the lesion. XPA, RPA and XPG are all recruited to the TFIIH bound site to form the preincision complex. The ssDNA in the undamaged strand of the unwound DNA bubble is coated with and stabilised by RPA. XPA is proposed to be involved in the final confirmation of the location of the lesion, and is an essential factor for NER.

XPC-HR23B leaves the preincision complex, and ERCC1-XPF is recruited. ERCC1-XPF is an endonuclease which cleaves 5' of the lesion. XPG cleaves 3' of the lesion. The sites of cleaveage of these endonucleases are at the ssDNA/dsDNA boundary of the bubble structure. A 24 to 32 base oligonucleotide containing the lesion is released, and the gap is filled by the DNA Polδ or Polε holoenzyme. The backbone is finally sealed by a DNA ligase, probably LIG I (summarised in Fig 1.7).

TCR may also function to repair oxidative lesions, most notably oxo^{8}G (Pastoriza Gallego et al. 2003). It is proposed that this involves CSB as well as BRCA1 and BRCA2. The glycosylase NEIL1 may be involved in excision of the oxidised guanine as it is known to have activity in DNA bubble structures.

1.2.4 Post-Replicative Mismatch Repair

Mismatch repair (MMR) is a key mechanism for maintaining genome integrity. Replicative DNA polymerases contain an intrinsic editing function which reduces the error rate of replication from 1 in 100 to 1 in 10^7. MMR is responsible for repairing base-base mismatches and insertion deletion loops (IDLs) (which occur due to polymerase slipping during replication of short repeated sequences) (Kunkel et al. 2005; Jiricny 2006). MMR has also been shown to be involved in the removal of oxo^{8}dG incorporated into DNA from the dNTP pool (Colussi et al. 2002). In addition to its repair function, MMR may also be involved in inducing an arrest in the G_2 phase of the cell cycle in human cells. This is possibly a function related to the involvement of certain MMR proteins in DSB repair and meiotic recombination (Hawn et al. 1995).

1.2.4.1 Bacterial MMR

In *E. coli*, recognition of a base-base mismatch is carried out by the MutS homodimer. After binding to the mismatch, the MutL homodimer is recruited. The ATP-dependent activity of this ternary complex leads to the activation of the endonuclease activity of MutH. MutH is responsible for incision of the DNA backbone of the strand containing the incorrect base. Discrimination, between the parental and daughter DNA strands, occurs via MutH recognition of hemimethylated GATC sites. These sites are usually methylated, but methylation of the daughter DNA strand occurs approximately two minutes after their replication. This means that the parent strand sites are methylated, but not the error-containing daughter strand. The UvrD helicase unwinds the DNA to allow exonucleolytic degradation of the mismatched strand. Degradation is halted within 150 base pairs beyond the mismatch, the gap is filled by DNA PolIII, and the nick ligated by DNA ligase.

1.2.4.2 Mammalian MMR

Six human homologues of *E. coli* MutS have thus far been identified. Of these, three are known to be involved in post-replicative MMR (MSH2, MSH3 and MSH6). MSH1 is found in mitochondria, while MSH4 and MSH5 appear to have a role in meiotic recombination. In addition to its role in MMR, MSH2 has been shown to be involved in DSB repair (Villemure et al. 2003). MSH2 and MSH6 form the MutSα

heterodimer, which carries out the recognition of base-base mismatches and one and two base IDLs. MutSβ, a heterodimer of MSH2 and MSH3, is involved in the recognition of larger IDLs, and shows some overlap with substrates recognised by MutSα. Four MutL homologues have been identified in humans; MLH1, MLH3, PMS1, PMS2. These also function as heterodimers. The most important in post-replicative MMR is the dimer of MLH1 and PMS2, MutLα. MutLβ (MLH1 and PMS1) may acts as a backup to MutLα. MutLγ (MLH1 and MLH3), may also function in MMR, and it is known to function in meiotic recombination.

After MutSα binds to the mismatch, it forms a stable ternary complex with MutLα in an ATP-dependent manner. ATP causes MutSα to dissociate from mismatched linear duplex DNAs. Three models have been proposed to account for this and to explain MutSα function. In the first, it is proposed that MutSα actively translocates on DNA in an ATP dependent fashion (Blackwell et al. 1998). The second suggests that MutSα binds a mismatch in an ADP bound state. Exchange of ADP for ATP causes a conformational change in the protein which releases it from the mismatch, and allows it to slide along the DNA and interact with downstream repair factors (Gradia et al. 1999). The final model proposes that DNA bending on MutSα binding provides the verification of a mismatch, and also allows strand discrimination (Wang et al. 2004).

It seems probable that nicks in DNA are the sites for initiation of exonucleolytic digestion to remove the mismatched section. How this is initiated is still not clear. The currently favoured model could be correct for either of the MutSα sliding or translocation models. MutSα, perhaps together with MutLα, moves along the DNA in either direction. When a nick is encountered at a replication fork 5' to the mismatch, replication factor C (RFC) could be displaced from the replication fork, and EXO1 loaded. This could not take place 3' of the mismatch. Instead, a complex containing MutSα, MutLα, EXO1, PCNA and RFC may assemble at the 3' terminus of the nick, and mediate degradation towards the mismatch. In both cases ssDNA is stabilised by RPA binding, DNA is resynthesised by Polδ, and the nick ligated by LIG1. Alternatively, a physical coupling of MMR to replication has been proposed. A simplified version of human MMR is depicted in Fig 1.8.

PCNA and RFC are both implicated in MMR. PCNA, in addition to its function in the resynthesis step, has also been shown to have another function(s) early in MMR. PCNA interacts with MSH2 and MLH1, and MutSα and MutLα (Clark et al. 2000). It increases the mismatch binding specificity of MutSα, and it also interacts with EXO1.

1.2.5 Double Strand Break Repair

DNA double strand breaks (DSB) are among the most potentially cytotoxic lesions, since both strands of DNA are damaged. DSBs can be repaired by several mechanisms which fall into two major mechanistic classes; homologous recombination (HR), and non-homologous end joining (NHEJ).

1.2.5.1 Homologous Recombination

HR (Karran 2000; West 2003; Friedberg et al. 2006) involves the use of homologous sequences to repair a DSB without any loss of genetic information. HR is the primary mode of DSB repair during the S and G_2 phases of the cell cycle, since this is when a sister chromatid is present and available for use. The stages in HR are outlined in Fig 1.9.

The early steps of resection to form 3' overhangs, and strand invasion are mediated by the RAD51 family of recombinases. The first step involves resection of the break site by a 5' to 3' exonuclease. The human endonuclease responsible for this is still unknown. Mre11 has been proposed to fulfil this function (D'Amours et al. 2002), although this is unlikely because it has only 3' to 5' exonuclease activity, no known helicase function, and deletion mutants in yeast show only a minor impairment of HR.

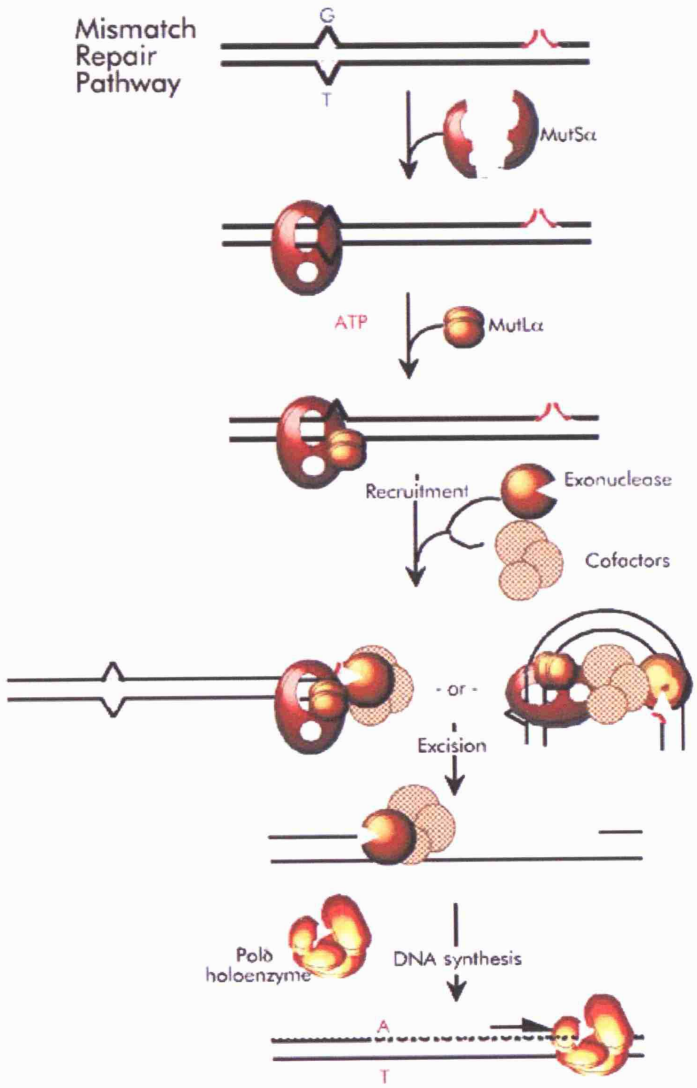

Fig 1.8 Human DNA Mismatch Repair (MMR). MutSα recognises DNA base mismatches after replication. MutLα is recruited. MutSα/MutLα may lead to nick recognition by formation of a sliding clamp or active translocation of DNA in an ATP dependent manner (left). DNA bending may also be responsible for nick site recognition (right). After recruitment of endonucleases and other cofactors to the nick, excision of the mismatch occurs, followed by resynthesis of DNA and ligation to close to the nick. (Adapted from Wang 2004)

The resulting 3' overhangs are coated by replication protein A (RPA), which may have a number of roles in HR. RPA serves to recruit RAD52 to the ssDNA at the DSB ends. RAD52 in turn recruits RAD51, which is required for the strand invasion step. RPA has also been shown to be involved in stabilising the displaced strand after invasion (Eggler et al. 2002). RAD51 functions as a long polymer of hundreds of monomers, which is wrapped around the invading ssDNA end. Invasion is ATP dependent and requires RAD54 (Van Komen et al. 2002), a SWI/SNF DNA remodelling factor.

The next stage in the process is unclear. The second free 3' overhang may also invade the homologous duplex. Alternatively, it may simply anneal to the strand displaced by the invasion of the first 3' end. It has also been proposed that the first 3' end to invade can acts as a primer for DNA synthesis and after sufficient synthesis has been achieved, can simply anneal to the other side of the DSB. This process is known as synthesis-dependent strand annealing (SDSA).

After DNA synthesis, the interlinked DNA molecules are connected via a double Holliday junction. In order to separate the two sister chromatids, the Holliday junctions must be resolved (Liu et al. 2004). This occurs by symmetrical cutting of the structure. In bacteria, RuvA, B and C are responsible for this. In yeast, only mitochondrial resolvases have been identified. In mammalian cells, no resolvase has yet been identified. Recently, Mus81 was suspected to have this activity. This has since been shown to be an endonuclease which has a strong preference for forked substrates, such as stalled or collapsed replication forks, over Holliday junction structures (Ciccia et al. 2003). Although there may be some *in vivo* activity of Mus81 on Holliday junctions, the major activity isolated so far can be separated from Mus81 containing protein fractions.

1.2.5.2 Non-Homologous End Joining

NHEJ (Hefferin et al. 2005; Lobrich et al. 2005) is the predominant method of DSB repair in G_1. It is, in principle, a simple mechanism whereby two ends of a DSB are religated to each other. In practice, DSBs are rarely formed with the undamaged, "clean" ends needed for this. For example, IR and ROS induced DSBs frequently have

phosphoglycolates at their termini. A basic schematic of NHEJ as it is currently understood is shown in Fig 1.10.

After DSB formation, the first proteins to bind to the free DNA ends are Ku70 and Ku80. These bind as a dimer, and may help to protect the DNA ends from further damage. On binding, Ku70/80 undergoes a conformational change so that a positively charged "tunnel" is formed through which DNA is passed. The Ku70/80 dimer recruits the catalytic subunit of the DNA dependent protein kinase, DNA-PK. DNA-PKcs can be autophosphorylated when activated by ssDNA binding. DNA-PKcs is also involved in actually bridging the DSB gap by forming protein-protein interactions between the two molecules of DNA-PKcs on either side of the break. DNA-PKcs is also responsible for the recruitment of the ligase LIGIV/XRCC4 complex. LIGIV is responsible for the final ligation of the DNA ends, while XRCC4 recruits phosphonucleotide kinase (PNK). PNK has both a 5'kinase and a 3' phosphatase activity, and so could be involved in processing the DSB ends to prepare them for ligation. DNA-PKcs also recruits Artemis (Jeggo et al. 2005), which is involved in V(D)J recombination in generation of the antibody repertoire. Artemis is phosphorylated by DNA-PKcs, and this activates its 3' to 5' ssDNA exonuclease activity. When bound to DNA-PKcs, Artemis also has a 3' and 5' overhang endonuclease activity.

After bridging and processing is completed, gap filling takes place involving DNA Polμ and Polλ. These polymerases have been shown to interact with the Ku70/80 dimer. LIGIV finally ligates the backbone and repair is completed.

There is evidence that the MRN complex (Mre11/RAD50/Nbs1) may be involved in an alternate NHEJ pathway. Recently, a new NHEJ factor has been identified, Cernunnos-XLF (Ahnesorg et al. 2006; Buck et al. 2006), although its role is not yet understood.

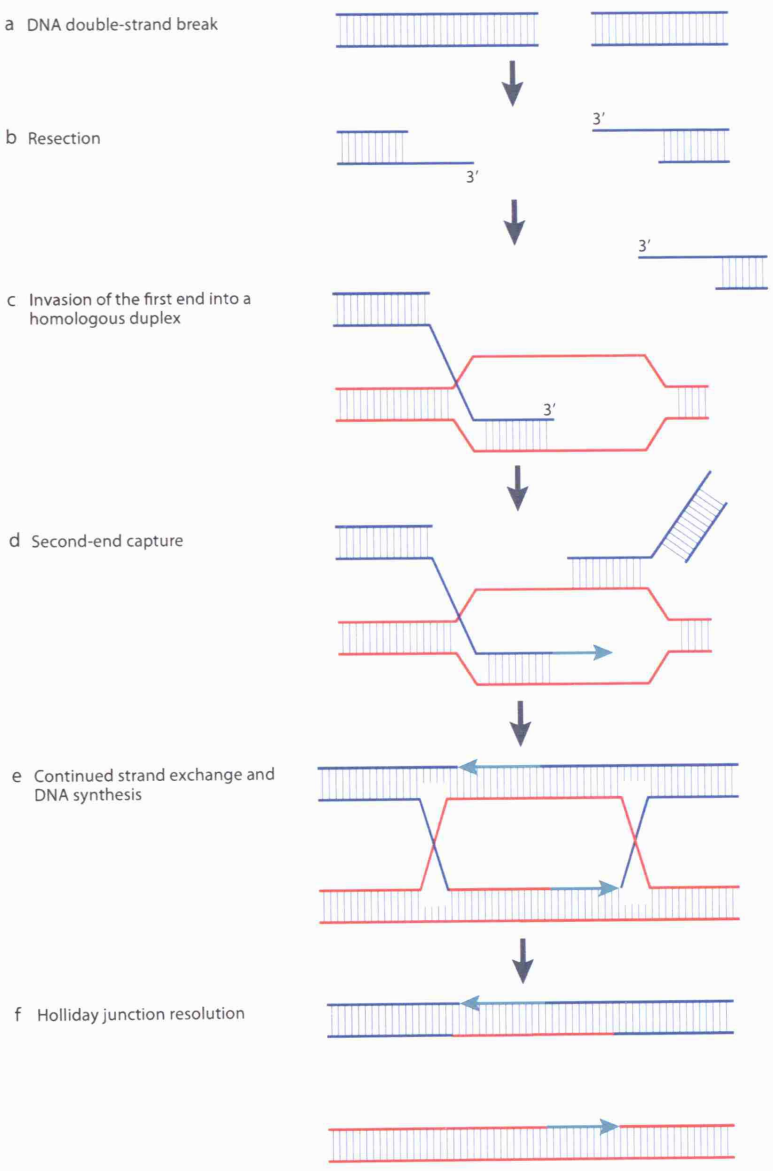

Fig 1.9 Mammalian Homologous Recombination Repair of DNA DSB. The mechanism can be divided into six distinct steps. a, DSB formation. b, Resection to form 3' overhangs. c, Invasion of one 3' overhang, and strand displacement. d, Second end capture. e, Continued strand exchange and DNA synthesis. f, Holliday junction resolution. (Adapted from West 2003).

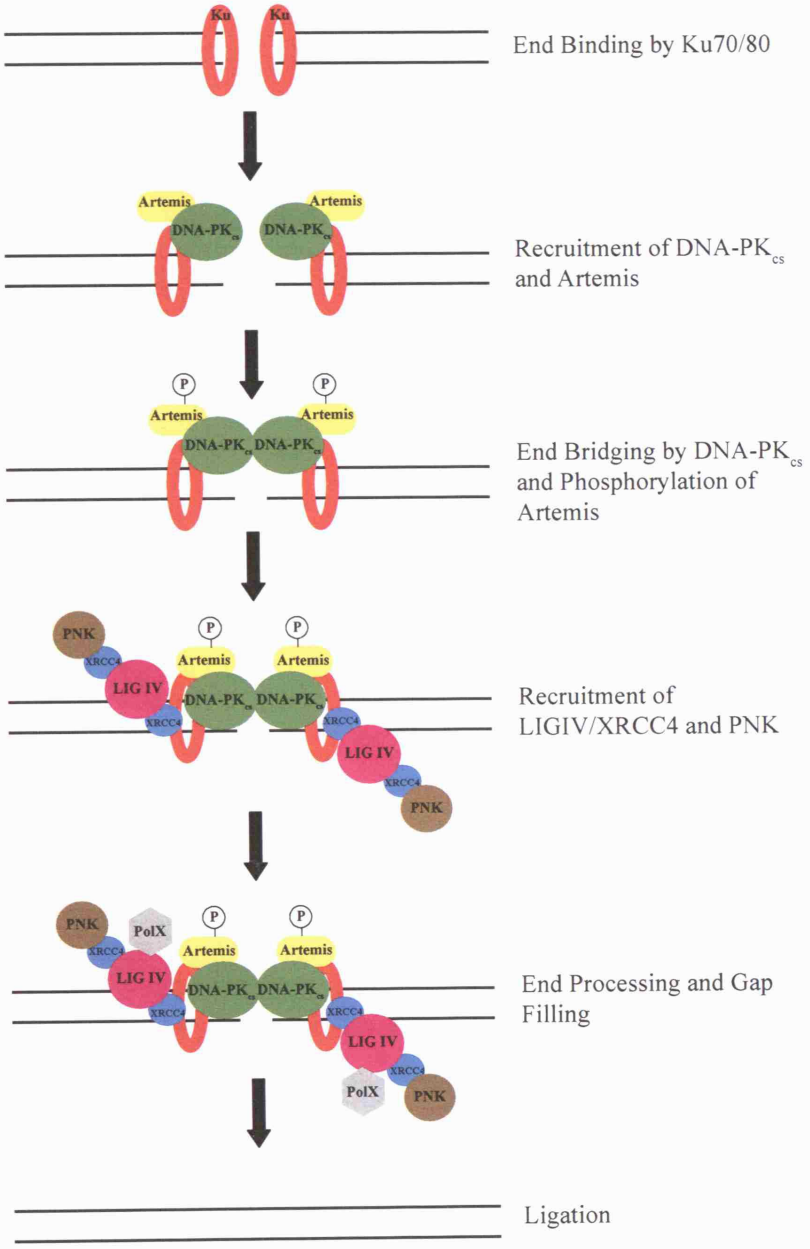

Fig 1.10 Mammalian Non-Homologous End Joining. The Ku70/80 heterodimer is the first protein to bind to DNA DSB ends. DNA-PK$_{cs}$ is recruited along with Artemis. DNA-PK$_{cs}$ bridges the gap between ends, and phosphorylates Artemis, which is required for the exonuclease activity of Artemis. DNA Ligase IV/XRCC4 complex is recruited, along with PNK. Ends are processed and gap filling performed by one of the X family of DNA polymerases (Polμ and Polλ). LIG IV ligates the nicks in the DNA backbone to complete repair. (Adapted from Hefferin 2005)

1.2.5.3 Single Strand Annealing

Single strand annealing (SSA) (Pastink et al. 2001) can be viewed as a subpathway of HR. SSA relies on the existence of regions of homology either side of the DSB. After resection of the 5' strands, the resulting 3' overhangs can anneal at the sites of homology. The non-homologous ends must be removed, leading to a loss of genetic information. Ligation of the DNA backbones seals the break. The process is believed to involve the MRN complex, as well as XPF/ERCC1, and in yeast, Msh2 and Msh3 appear to be involved.

1.3 Consequences of Defective DNA Repair

Failure of DNA repair can have extremely deleterious effects on the cell and organism. Such failures lead to loss of, or damage to, genetic information.

MGMT, involved in the direct reversal of guanine methylation after exposure to S_N1 type methylating agents, has been shown to be subject to transcriptional silencing in some colon tumours (Esteller 2002).

Until recently, no inherited syndromes had been attributed to defective BER. Single nucleotide polymorphisms in the MYH DNA glycosylase, however, have been linked to an increased susceptibility to colorectal cancers in a condition now termed MYH-associated polyposis (MAP) (Al-Tassan et al. 2002; Sampson et al. 2005). Mouse knockouts for APE1, XRCC1 and Polβ are embryonic lethal, suggesting BER is important during development (Lindahl 2001). By contrast, most DNA glycosylase knockout mice show very mild phenotypes. This may be due to the overlapping functions of many of the known glycosylases. TDP1 is a glycosylase which cleaves a bond between the 3' end of DNA and a Tyrosine amino acid. While not directly involved in BER, it is associated with LIGIII, which is responsible for the final ligation step in BER (Wood et al. 2005). Mutations in TDP1 are responsible for the neurological disorder spinocerebellar ataxia with axonal neuropathy (SCAN). The Aprataxin protein interacts directly with, and stabilises the BER factor XRCC1. Aprataxin removes AMP

from adenylated DNA Ligase, allowing its activation. Aprataxin mutations underlie ataxia ocular apraxia (AOA).

A number of inherited syndromes are associated with defective NER (Friedberg et al. 2006). Of these, xeroderma pigmentosum (XP) is the most studied, and common. Currently, eight complementation groups of XP have been identified (A to G, and V). Seven of these (A to G) contain defects in genes encoding products involved in NER. The clinical hallmark of XP is an extreme chronic hypersensitivity to UV radiation. This is due to the role of NER in the removal and repair of UV induced DNA damage. XP patients show a greatly increased incidence of skin cancer. Cockaynes Syndrome (CS) is another NER defective syndrome. CS cells show normal global genome repair, but lack the ability to perform TCR. The underlying mutations occur in the CSA and CSB genes. CS patients show growth and developmental defects, neurological disorders, premature aging, and UV sensitivity, although no predisposition towards skin cancer is evident. XP/CS complex displays clinical features which are intermediate between XP and CS. Trichothiodystrophy (TTD) patients can be placed in XP-D or XP-B complementation groups. Although patients are UV sensitive, there is no proneness to cancer. Clinical features include brittle hair and nails, ichthyosis, and physical and mental retardation. These features not observed in XP may be due to the dual role of XP-B and XP-D in transcription initiation as part of TFIIH (Hoeijmakers 2001; Laine et al. 2006).

Defects in HR are also associated with cancer predisposition. Mutations in the BRCA1 and BRCA2 genes predispose to breast and ovarian cancers. On a cellular level, this is characterised by genomic instability, which is seen as chromosome rearrangements. Individuals heterozygous for BRCA1/2 mutations are predisposed to cancer, and loss of the second allele is common in tumours from such individuals. BRCA1/2 interact with RAD51 and can act as chromatin remodelling and transcription factors. Fanconi Anaemia (FA) is an autosomal and X-linked recessive syndrome, with at least 12 complementation groups (Kennedy et al. 2005). The genes responsible for 11 of these have been cloned, and 10 are involved in a common pathway. The FANCD2 product is BRCA1, and so is implicated in DSB repair. FANCM is the human orthologue of the bacterial helicase-associated endonuclease for forked structured DNA (Hef), which is involved in the processing of stalled replication forks into DSBs. FA is

characterised by a hypersensitivity to DNA crosslinking agents, and clinically, patients exhibit bone marrow failure, acute leukaemia, and solid tumours.

Artemis is involved in NHEJ, and V(D)J recombination. Artemis mutations have been shown to lead to a severe combined immunodeficiency (SCID) (Moshous et al. 2001). Deficiencies in LIGIV also lead to immunodeficiency, in addition to developmental and growth problems, and a marked radiosensitivity (O'Driscoll et al. 2001). Nijmegen Breakage Syndrome (NBS) is characterised by mutations in NBS1 (Varon et al. 1998), part of the MRN complex. Clinically, the symptoms are similar to those found in LIGIV mutants, although NBS cells show defects in DNA damage response signalling pathways, and hence defective cell cycle checkpoint activation. ATM and ATR are involved in signalling DSBs, and subsequent activation of cell cycle checkpoints, which leads to an arrest of the cell cycle to allow repair to occur. ATM deficiency leads to the condition known as ataxia telangiectasia (AT) (McKinnon 2004). ATR deficiency leads to Seckel Syndrome (O'Driscoll et al. 2004). Both AT and Seckel syndrome have clinically similar symptoms. MRE11 is involved in the DNA damage response as part of the MRN complex, and mutations in MRE11 are responsible for AT-Like Disorder (ATLD).

1.3.1 Defective Mismatch Repair

MMR is involved in the repair of replication errors introduced by the replicative DNA polymerases. Defects in MMR lead to increases in point mutations and frameshifts (Harfe et al. 2000; Jiricny et al. 2003; Peltomaki 2003; Jiricny 2006). The spectrum of mutations depends on the component of MMR which is deficient. Microsatellites are extensive regions of multiply repeated elements of up to six nucleotides long. In transcribed regions of the genome only mono-, di-, or tri-nucleotide repeats are usually found. These repeat regions are particularly prone to slippage during replication. In MMR deficient cells, these errors remain uncorrected and generate frameshifts, which can result in truncated proteins. This is known as microsatellite instability (MSI), and is a hallmark of MMR deficient cells and tumours. Because of the redundancy inherent in the MMR system, it is proposed that more than one MMR gene must be mutated to acquire a strong mutator phenotype (Malkhosyan et al. 1996). This is supported by the finding that most MSI tumours have more than one MMR gene mutated. Hereditary Non-Polyposis Colorectal Cancer (HNPCC) is an inherited cancer

predisposing condition. HNPCC tumours exhibit MSI due to defective MMR. In those HNPCC families in which the underlying mutations have been determined, mutations in hMLH1 make up 50% of cases, hMSH2 40% and others 10%. It has been proposed that EXO1 and Polδ mutations may be involved in HNPCC, but this is unlikely since lethal effects on replication would probably result. MSI has also been found in between 10 and 25% of sporadic colorectal and other tumours, primarily due to silencing of the hMlh1 promoter by cytosine methylation.

In addition to inducing MSI, MMR defects also render cells resistant to a number of cytotoxic agents. In *E.coli dam* mutants, which are hypersensitive to methylating agents, inactivation of MMR led to restoration of the wild type level of methylation resistance (Karran et al. 1982). Repair of DNA O^6-meG by MGMT was mentioned earlier in this chapter. Cells lacking MGMT are hypersensitive to methylating agents as O^6-meG is the primary cytotoxic DNA lesion produced by agents such as MNU and MNNG. Tolerance to these drugs can be achieved by inactivating MMR. It has been proposed that this toxicity is due to replication across unrepaired O^6-meG (Karran et al. 1994). Although either C or T can be incorporated opposite O^6-meG, neither of these forms a correct base pair. Both base pairs are recognised by the MMR system, but since MMR removes the daughter DNA strand, the O^6-meG lesion remains. During repair, O^6-meG:C and O^6-meG:T mismatches are formed again. Continued processing leads to futile repair cycles, with the eventual formation of DSBs, and subsequent cell death. Inactivation of MMR would, of course, avoid this, and hence confer resistance to this type of methylating agent.

An alternative model has been proposed whereby the MMR components act as sensors of DNA damage, and can signal to downstream effectors (Fishel 2001). Activation of MMR is associated with activation of DNA damage response signalling pathways involving the ATR protein, leading to arrest of the cell cycle in G_2, and subsequent apoptosis. It has been shown recently that ATR activation after treatment with MNNG is dependent on MutSα and occurs primarily during S-phase (Yoshioka et al. 2006). *In vitro* analyses showed that ATR localises to O^6-meG:T mismatches, and that activation of ATRs kinase activity is dependent on the presence of these

mismatches. Taken together, these data add credence to the idea that MMR recognition is involved in the DNA damage response in addition to repair.

Methylating agents are not the only drugs against which MMR deficiency can afford resistance. 6-Thioguanine (6-TG) can be incorporated into DNA after treatment with 6-TG itself, or 6-mercaptopurine (6-MP) and its prodrug Azathioprine. 6-TG is used as an anti-leukaemic agent, as is 6-MP. The primary use of Azathioprine in the clinic is as an immunosuppressant after organ transplant and in the treatment of autoimmune diseases. MMR deficiency leads to resistance to 6-TG induced cytotoxicity (Aquilina et al. 1990). Once incorporated into DNA, 6-TG is methylated by chemical reaction with the methyl donor S-adenosyl methionine (SAM) (Swann et al. 1996). Unlike O^6-meG, 6-meTG is a very poor substrate for MGMT, and so persists in DNA. Upon replication, C and T are inserted opposite 6-meTG at similar rates. As with O^6-meG, neither of these can form correct base pairs with 6-meTG, and are both recognised by the MMR system. It is proposed that the toxicity of 6-meTG occurs in a similar manner to that proposed for O^6-meG.

MMR deficiency has been implicated in development of secondary acute myeloid leukaemia/myelodysplastic syndrome (AML/MDS) after treatment with alkylating agents, and after immunosuppression with thiopurines (Karran et al. 2003; Offman et al. 2004). Therapy-related AML now accounts for at least 10% of all AML cases. MSI is considerably more frequent in secondary AML (50%) than in *de novo* AML cases (≤5%) (Casorelli et al. 2003). It has been proposed that selection of drug tolerant MMR deficient leukocyte precursors contributes to this incidence and this is supported by evidence suggesting that secondary AML is associated with chemotherapy rather than radiotherapy treatment of the primary cancer.

There is also evidence suggesting that MMR may contribute to the activity of the chemotherapeutic drug cisplatin (Fink et al.; Branch et al. 2000). A minor increase in cisplatin sensitivity of approximately 2-fold was observed in MMR deficient cells, and this could be relieved by correction of the MMR defect (Lin et al. 1999). Although when MSH2 deficient mouse embryonic fibroblasts were analysed there was no significant difference is sensitivity compared to wild type cells (Claij et al. 2004). *In vitro* studies have shown that a wide variety of lesions, including oxo^{8}G, UV

photoproducts and benz(a)pyrene adducts can acts as substrates for MMR recognition proteins, but whether these findings have any biological significance remains to be established.

1.4 Avoidance and Tolerance of DNA Damage

In this chapter, I have already introduced known mechanisms of DNA repair, and have described the enormous variety of damage against which they protect. What happens if the lesions cannot be repaired? Or at least, what happens if they are not repaired before the DNA is replicated? If a DNA lesion is encountered by a replicative DNA polymerase, and the polymerase cannot replicate it, then the replication fork can become stalled or strand synthesis may become uncoupled with synthesis of one strand continuing while the other is blocked. Stalled replication forks can be highly toxic. There are two types of mechanism which may be used to restart replication at these sites, and to recouple DNA synthesis of both strands; translesion synthesis (TLS) and recombinational repair.

1.4.1 Translesion Synthesis (TLS)

TLS involves the use of specialised polymerases that are able to replicate through a DNA lesion (Lehmann 2002; Friedberg et al. 2005; Lehmann 2005). In *E. coli*, there are three known TLS polymerases, while in mammalian cells ten have thus far been identified (Table 1.2). A common feature of these TLS polymerases is that they have a larger and "looser" active site than the replicative polymerases. This allows them to accommodate often quite bulky lesions in their active sites, facilitating incorporation of a nucleotide opposite the damage. Another feature of these polymerases is their low fidelity compared to the replicative polymerases (error rates as high as 1 in 20 nucleotides) when replicating undamaged DNA. This is partly explained by their "loose" active site, and also by the fact that TLS polymerases lack an exonucleolytic proofreading function common in their replicative counterparts. Most TLS polymerases belong to the Y-family of DNA polymerases.

Human Polη is responsible for TLS of UV induced CPDs. Polη accurately inserts dAMP opposite both T residues of a TT dimer, and performs this with the same efficiency as it replicates an undamaged template. The fidelity of CPD replication is

increased by Polη extending the insertion more efficiently if AA is incorporated opposite the TT dimer. I previously stated that seven of the eight known XP complementation groups are due to NER defects. The final complementation group, XPV is due to mutations in the gene encoding Polη. In addition to CPDs, Polη can perform TLS of oxo^{8}G, O^6-meG and other lesions, although not (6-4)PPs. In the absence of Polη, an increase in double strand breaks at CPD stalled replication forks has been noted, indicative of replication fork collapse (Limoli et al. 2002).

Polι, another low fidelity TLS DNA polymerase can initiate bypass of a number of lesions. Although it catalyses insertion, Polι is unable to perform subsequent extension. Polκ can bypass lesions caused by polycyclic hydrocarbons. Rev1 is classed as a Y-family DNA polymerase like Polη, Polι and Polκ, but is strictly not a DNA polymerase but a dCMP transferase. Polζ is a B-family polymerase. Polζ is relatively poor at inserting a nucleotide opposite a lesion, but can efficiently extend after insertion. It has been proposed that Polζ may act together with other TLS polymerases that are efficient at insertion but not extension, such as Polι.

For TLS to occur, switching from a replicative polymerase to a TLS polymerase must occur at the site of damage. How this happens is not yet fully understood. The *E. coli* orthologue of the replication processivity factor PCNA is the heterodimeric β-clamp. Like PCNA, this forms a ring structure through which the replicating DNA passes, and which clamps DNA polymerases to DNA. The β-clamp has been shown to be capable of binding a replicative and a TLS polymerase at the same time, with one polymerase bound to each subunit (Lehmann 2006). This has substantiated the "tool belt" model for PCNA involvement in polymerase switching, where up to three polymerases could be bound to PCNA at any given time, ready to be engaged when needed.

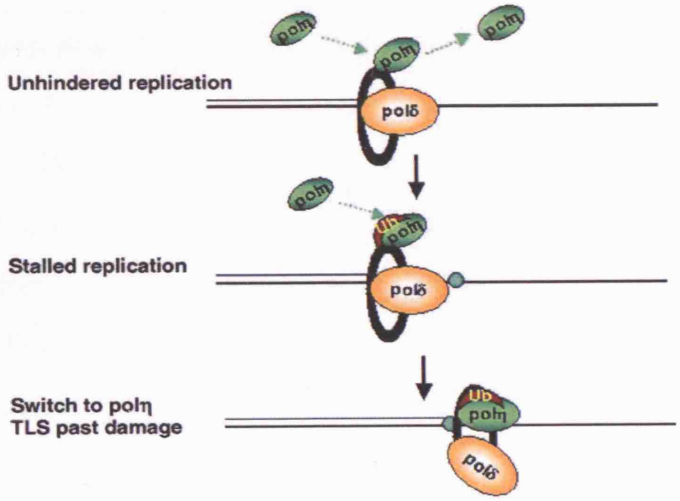

Fig 1.11 Translesion Synthesis in Eukaryotes. During normal DNA replication, the TLS polymerase Polη is loosely associated with PCNA. When the replication fork is stalled by DNA damage, PCNA becomes mono-ubiquitinated by the RAD6/RAD18 pathway. This increases the affinity of PCNA for Polη, which now binds more strongly. Polδ is displaced, allowing TLS by Polη. (Adapted from Lehmann 2006)

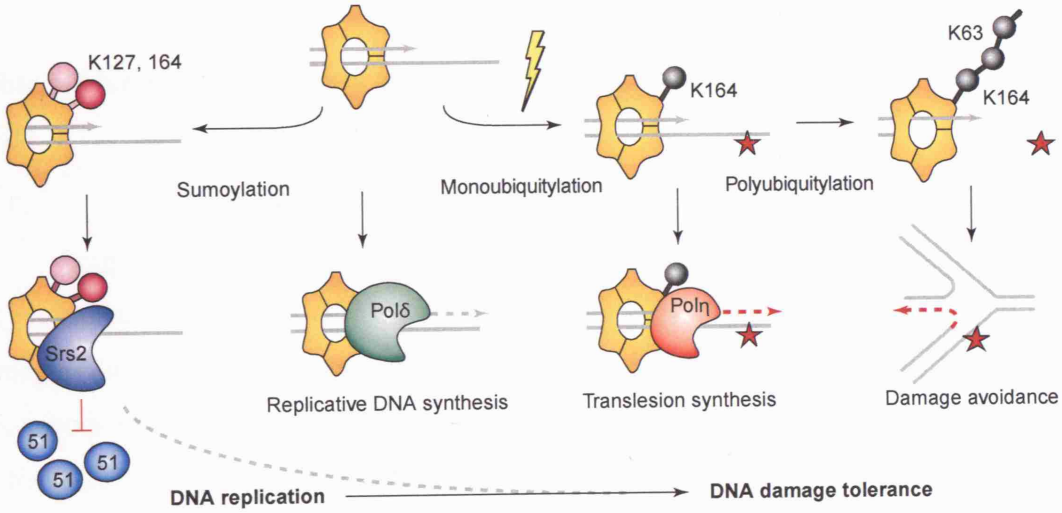

Fig 1.12 PCNA Modifications Modulate DNA Damage Tolerance and Avoidance. In yeast, mono-ubiquitination of PCNA on K164 promotes polymerase switching of Polδ for a TLS polymerase. Poly-ubiquitination of PCNA on K164 by K63 ubiquitin chains appears to direct restart of a stalled fork through recombinational mechanisms. Sumoylation of PCNA during normal replication appears to inhibit recombinational repair when forks are stalled, thus promoting TLS. Adapted from (Ulrich 2005)

Polymerase	Organism	Family
Pol II	E. coli	B
Pol IV	E. coli	Y
Pol V	E. coli	Y
Rev1	Yeast / Human	Y
Polζ	Yeast / Human	B
Polη	Yeast / Human	Y
Polκ	Human	Y
Polι	Human	Y
Polλ	Human	X
Polμ	Human	X
Polβ	Human	X
Polθ	Human	A
Polν	Human	A

Table 1.2 Known Translesion Synthesis Polymerases (Adapted from Friedberg et al. 2005)

Support for this model comes from work demonstrating that the Y-family polymerases can bind to PCNA, albeit weakly. After replication fork stalling DNA damage (induced by UV and HU, but not by IR), PCNA becomes ubiquitinated. In yeast, both mono- and poly-ubiquitination is observed, both via the K164 residue of the PCNA monomer. Mono-ubiquitination induces TLS, while poly-ubiquitination leads to damage avoidance, which will be discussed later. Interestingly, unlike poly-ubiquitination which leads to degradation of proteins by the 26S proteasome, poly-ubiquitinated PCNA after DNA damage contains ubiquitin chains linked by the K63 residue of Ubq (for proteasome degradation, K48 linked chains are formed). In mammalian cells, only PCNA mono-ubiquitination has been observed after DNA damage.

Y-family polymerases have a much greater binding affinity for K164 mono-ubiquitinated PCNA than for unmodified PCNA (Kannouche et al. 2004; Ulrich 2004). This is mediated through the recently identified UBM and UBZ domains of the polymerases (Bienko et al. 2005). One current model involves the transient association of Y-family polymerases with PCNA until the replication fork is stalled at a DNA lesion. This results in PCNA monoubiquitination leading to stabilisation of Y-family polymerase-PCNA binding (Fig 1.11). The actual mechanism for polymerase handover from replicative to TLS is not yet known.

In addition to PCNA ubiquitination, sumoylation of PCNA is also involved in TLS regulation (Ulrich 2005; Ulrich et al. 2005) (Fig 1.12). In yeast, this is proposed to affect TLS as a result of recruitment of the anti-recombinogenic helicase Srs2. This blocks recombinational repair by preventing formation of RAD51 filaments. If TLS is prevented by deletion of RAD18 (which together with RAD6 is responsible for PCNA ubiquitination), then Srs2 mediated prevention of recombination at the replication fork causes cell death. However, if the PCNA SUMO ligase Siz1 is deleted and Rad18 is deleted, then repair and fork restart occurs by homologous recombination.

Another feature of TLS polymerases is that they are not highly processive. Usually, only one to eight nucleotides are incorporated before they dissociate from the DNA. Because of this, the final step in TLS involves a second polymerase switching event with the replicative polymerase becoming re-engaged.

If TLS is compromised or the lesion cannot be bypassed, the stalled replication machinery may be removed to allow recombinational repair to take place (McGlynn et al. 2002) (Fig 1.13). After a fork has stalled, unwinding may occur, leading to the generation of a Holliday junction. This structure is known as a "chicken foot". It has recently been demonstrated that, *in vitro*, the Bloom helicase (Blm) can facilitate this unwinding (Ralf et al. 2006). A number of mechanisms for resolution of the "chicken foot" structure to allow fork restart have been proposed. Firstly, the dsDNA ends formed may invade the homologous sequences from which they were originally replicated. The lesion would be effectively bypassed by branch migration of the double Holliday junction. A Holliday junction resolvase (such as RuvABC in *E. coli*) could then act on this structure leading to the generation of a replication fork from which

replication could be restarted past the lesion. Secondly, the "chicken foot" structure may be cleaved by a Holliday junction resolvase, forming two distinct DNA duplexes, which could reform a replication fork by HR.

Both of these models posit cleavage of the replication fork. Non-cleavage models have also been proposed. Blockage of leading strand synthesis can cause an uncoupling of synthesis of the strands and the lagging strand may continue to be replicated for a time. On fork unwinding this leads to single strand overhang of the lagging strand. This may be digested by an exonuclease until there is no remaining overhang, and replication can be restarted. This mechanism is dependent on repair of the stall inducing lesion by DNA repair mechanisms in the extra time afforded by the exonucleoytic digestion. The alternative model involves template switching. In this model, the lagging strand overhang is used as a template for DNA synthesis by the DNA repair polymerases. Once this has been replicated, the "chicken foot" structure can be isomerised to reform the replication fork, but with replication restarting beyond the lesion. It should be mentioned here that while these mechanisms for damage avoidance would provide elegant solutions to the problem of stalled replication forks, most of these activities have not be observed either *in vitro* or *in vivo*.

1.5 Skin Cancer

Skin cancer is the most prevalent form of cancer. In the USA, over one million new cases are diagnosed every year (de Gruijl 1999), while in Britain the figure is almost 60,000. This is believed to be an underestimate, since most cancer registries do not record non-melanoma skin cancers (NMSC). The statistics for skin cancer incidence are most readily available for the USA, and so I refer mostly to these. Skin cancers can be divided into three groups; cutaneous malignant melanoma (CMM), squamous cell carcinoma (SCC), and basal cell carcinoma (BCC).

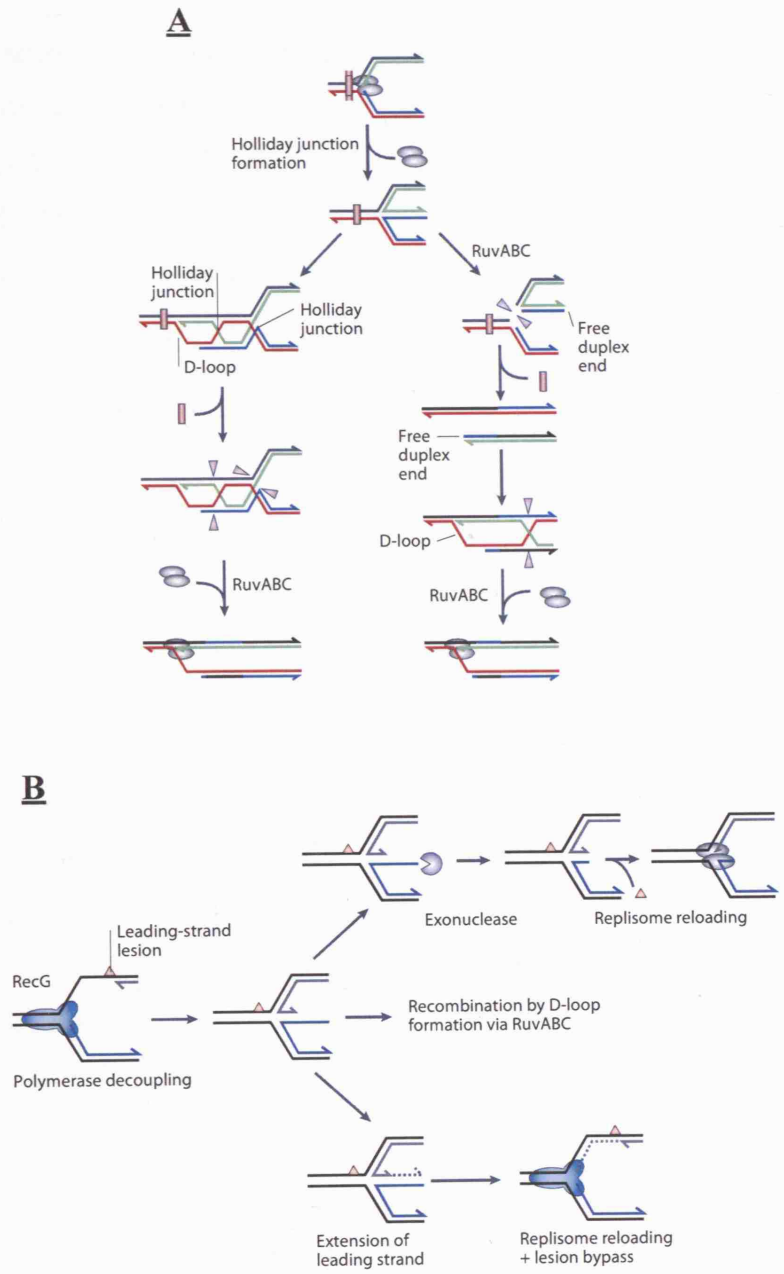

Fig 1.13 Recombinational Restart of Stalled Replication Forks. Holliday junctions may be formed by unwinding of replicated DNA at a stalled replication fork. These may be resolved by mechanisms involving cleavage of Holliday junctions by a Holliday junction resolvase (**A**). Alternatively, fork restart may occur via non-cleavage pathways involving exonuclease digestion or template switching (**B**). In each case, the lesion can be efficiently bypassed. (Adapted from McGlynn 2002)

1.5.1 Cutaneous Malignant Melanoma

CMM accounts for approximately 54,000 cases of skin cancer in USA every year. The incidence of CMM in North Western Europe is approximately 1 in 10^4 per year (de Gruijl 1999). It is by far the most aggressive skin cancer, with a very poor prognosis, and is responsible for two to three deaths per 10^5 people per year in North Western Europe. CMM is highly refractory to standard chemotherapeutic agents and radiotherapy (Sosman et al. 2006). Loss of regulation of cellular signalling pathways is commonly observed, with most CMM cases exhibiting defective Ras, or other MAPK signalling, or mutations at the CDKN2A locus (Haluska et al. 2006). Chemokine and growth factor receptors are also affected. These discoveries have provided potential therapeutic targets. While CMM is largely resistant to most therapeutic agents, combination of treatments has offered some success. An example of this is use of the anti-angiogenic drug bevacizurab in conjunction with standard chemotherapy.

1.5.2 Non-Melanoma Skin Cancer

NMSC includes BCC and SCC. In the general population, BCC accounts for 80% of NMSC, with SCC responsible for the remaining 20% (Alam et al. 2001). BCC is believed to arise *de novo* (not through earlier pre-malignant stages), while SCC is proposed to develop through a multistage process from actinic keratosis. In general, NMSC has an excellent prognosis. BCC is non-invasive and metastasis is extremely rare. SCC is more invasive and there is a small but significant risk of metastasis. Metastasis is associated with a very poor prognosis (less than 20% survival at ten years).

1.5.2.1 Squamous Cell Carcinoma

In the USA, the relative lifetime risk of SCC is of the order of 9-14% for males, and 4-9% for females (Alam et al. 2001). While exact incidence numbers are not available, there appears to be an upward trend in the number of cases over the past ten years. There are a large number of risk factors for SCC including UVR and various chemical carcinogens. SCC is more likely to occur in chronically damaged or injured

skin. The most invasive tumours are usually those found on the head and neck, and have the potential to recur at the primary tumour site. Patients that present with only a primary cutaneous SCC have an excellent prognosis.

The multistage model for SCC development arose when it was discovered that actinic keratosis (AK) is effectively a pre-SCC lesion which shares many similarities of morphology and growth with SCC. The presence of AK imparts a much higher risk of developing SCC, as does carcinoma *in situ* (CIS/ Bowens disease). Keratoacanthoma (KA) is morphologically very similar to SCC, and there is some debate as to whether KA may be a specific type of SCC, an aborted malignancy, or a genetically incomplete SCC (Boukamp 2005). The majority of SCC have mutations in the *P53* gene, although these are also present in large patches of normal skin, and may simply act as accessory mutations which are permissive for SCC development (Alam et al. 2001). SMAD4 is involved in TGFβ signalling, and plays a major role in skin development and homeostasis. Inactivation of *SMAD4* may be associated with development of SCC (Qiao et al. 2006). A number of studies suggest that various signalling pathways utilising the transcription factor NF-κB may also be involved in SCC development (Dajee et al. 2003; Lind et al. 2004; Loercher et al. 2004). The *PTCH* gene is known to play a major role in BCC development, and mutations in *PTCH* in SCC have also been found (Ping et al. 2001).

1.5.2.2 Basal Cell Carcinoma

BCC is the most common malignancy in Caucasians, and has been recently reviewed in detail (Rubin et al. 2005; Crowson 2006). While it rarely metastasises, aggressive BCC can invade and cause severe local tissue damage. Individuals with fair skin, red hair and who freckle easily are far more likely to develop BCC than other groups. Sunlight is an acknowledged risk factor, and unlike SCC, BCC is associated more with intense, intermittent, childhood exposure to UVR than with continuous, cumulative exposure. IR and arsenic are also acknowledged BCC risk factors (Crowson 2006).

Nevoid basal cell carcinoma syndrome (NBCCS) is an autosomal dominant inherited genetic condition, which occurs in approximately one in every 56,000 people

(Quinn et al. 2003). Around 33% of cases are due to new germline mutations, with no family history. The hallmark of this condition is an extremely high incidence of BCC. Some cases report more than 500 BCCs during the patient's lifetime. NBCCS represents 0.5% of total BCC cases. In addition to BCC, NBCCS individuals are prone to other malignancies such as rhabdomyosarcoma and medulloblastoma. Sufferers also show multiple developmental abnormalities. The gene responsible for NBCCS was mapped to chromosome 9q22-31, and subsequently identified as the *PTCH* gene (Hahn et al. 1996). Loss of heterozygosity (LOH) is found in the majority of cases, with the second allele being inactivated through a somatic event. The majority (>80%) of these mutations result in the production of truncated forms of the PTCH protein.

PTCH is also implicated in sporadic BCC where it is mutated in 40 to 60% of cases, and there is LOH in more than 70% of these (Gailani et al. 1996). It is also proposed to be involved in XP-BCC, sporadic medulloblastoma, sporadic meningioma, breast cancers and primitive neuroectodermal tumours (PNETs) (Raffel et al. 1997)Xie, Johnson, et al. 1997;(Wolter et al. 1997). *PTCH* is the human homologue of Drosophila *ptch* that is involved in segment polarity during development. PTCH is the receptor for the hedgehog (Hh) family of signalling peptides (Wicking et al. 1999; Bale et al. 2001). Three Hh homologues exist in vertebrates; sonic (Shh), desert (Dhh) and Indian (Ihh). Shh is the most widely expressed of these peptides and is itself implicated in carcinogenesis (digestive tract tumours, pancreatic tumours, and XP-BCC) (Bodak et al. 1999; Berman et al. 2003; Thayer et al. 2003; Couve-Privat et al. 2004). PTCH is a transmembrane protein and acts as a repressor of another membrane bound protein smoothened (SMO). On binding of Shh to PTCH, the repression of SMO is relieved, allowing activation of the GLI1 transcription factor (Fig 1.14). There are three known members of the GLI family. Target genes of GLI include *PTCH* itself, *WNT*, *TGFβ* and *HIP*.

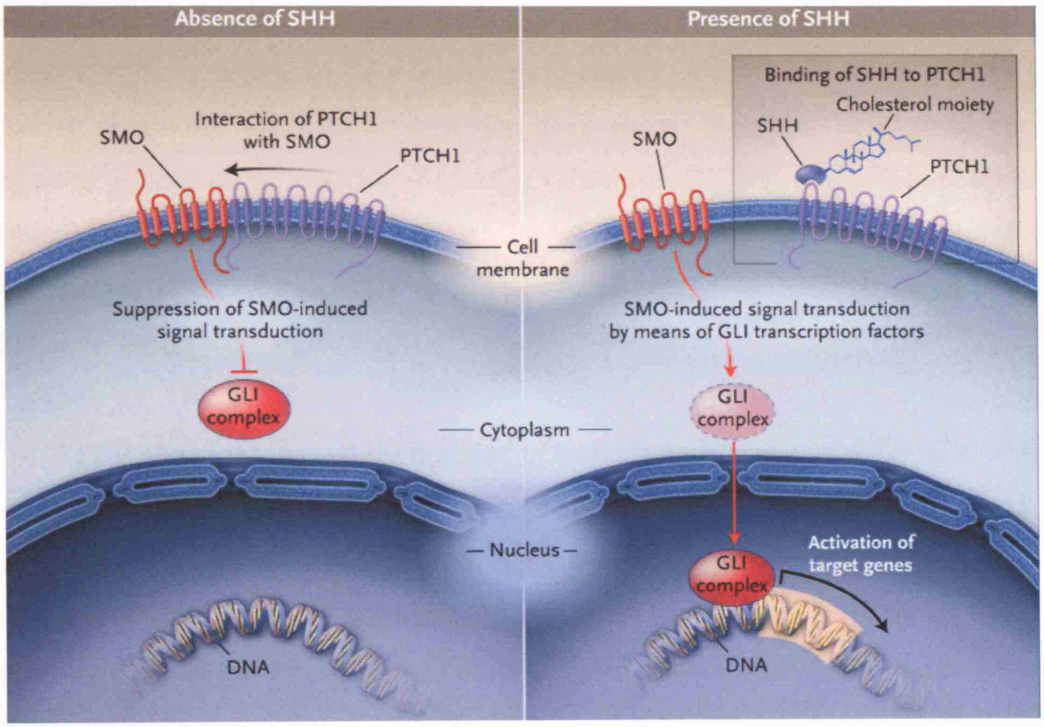

Fig 1.14 Sonic Hedgehog Signalling Pathway. In the absence of sonic hedgehog (Shh) PTCH represses SMO, preventing activation of the transcription factor GLI1. Binding of Shh to PTCH relieves the repression of SMO resulting in activation of GLI1 and subsequent activation of Gli1 regulated genes. (Adapted from Rubin 2005)

PTCH2 is a PTCH homologue with 57% identity to the *PTCH* sequence (Zaphiropoulos et al. 1999). PTCH2 has also been found up-regulated in BCC cells, and it is proposed to be up-regulated as a target of GLI1. Mutations in *SMO* have been observed in 10 to 20% of sporadic BCCs. Mutations in *SMO* can lead to constitutive pathway activation by either enhancing SMO activity or by abolishing its repression by PTCH. The importance of SMO in this pathway has been demonstrated by BCC prevention and regression in mice using cyclopamine, which in an antagonist to SMO (Athar et al. 2004). GLI1 was first identified as an oncogene in glioblastoma. In addition to glioblastoma, over expression of GLI1 and GLI2 in mice also causes BCC-like tumours (Regl et al. 2002; Cui et al. 2004). In human BCC, these have both been found up-regulated. GLI activity is negatively regulated by PKCα, which is down-regulated in BCC (Neill et al. 2003).

P53 is the most frequently mutated gene in cancer known to date. 50% of BCCs have mutations in this gene (Ling et al. 2001; Kim et al. 2002). In these instances, the mutations appear to be mostly UVB induced C to T transitions at dipyrimidine sites, and there is no detectable LOH. Interestingly, the same mutations are found in patches of morphologically normal sun exposed skin of these individuals. The widespread nature of this phenomenon suggests that these are pre-existing mutations, and while they may facilitate BCC development, they are not the rate limiting step. The protein 14-3-3σ is involved in activation of the G_2 to M checkpoint and in the regulation of passage from G_1 to S phase. Inactivation of *14-3-3σ* in murine cells leads to immortalisation. In 75% of breast cancers, the *14-3-3σ* gene is epigenetically silenced by CpG methylation. Protein levels are unaffected in SCC, but in BCCs they may be down-regulated by as much as 70% (Lodygin et al. 2003). Notch1 has also been implicated in BCC development since tumours are formed at high incidence in $Notch^{-/-}$ mice (Nicolas et al. 2003).

BCC can be treated either surgically or non-surgically. Non-surgical treatments include radiotherapy and photodynamic therapy. It has been shown recently that small molecule inhibitors of the Shh signalling pathway can suppress proliferation and induce apoptosis in murine BCC models (Williams et al. 2003). BCC tumourogenesis was

decreased substantially by immunisation with a HIP (Hedgehog interacting protein) polypeptide (Vogt et al. 2004).

1.5.3 UVR in Skin Cancer

UVR is one of the major risk factors for skin cancer (Ehrhart et al. 2003). The highest incidence of skin cancer is in climates with high levels of sunshine, and tumours are primarily located on sun exposed skin. Most of the studies involving UVR in the aetiology of skin cancer involve UVB, since these are the most directly genotoxic of the wavelengths that constitute sunlight. In XP patients, 60% of mutations in oncogenes or tumour suppressors from skin cancers are CC to TT changes, a UVB signature mutation, compared to 10 to 15% in sporadic tumours (Daya-Grosjean et al. 2000). In *SMO* from XP patients, CC to TT changes are responsible for almost 90% of mutations (Couve-Privat et al. 2002). The same has been found for *P53* in these patients (D'Errico et al. 2000). In sporadic tumours, approximately 40% of mutations in these genes are single C to T changes at dipyrimidine sites, another hallmark of UVB.

In addition to UVR induced mutations that arise due to direct absorption of photons, there is also a contribution from reactive oxygen species (Ikehata et al. 2004). These are known to be produced by UVA irradiation. In a study in which mice were exposed to natural sunlight and carcinogenesis monitored, the majority of mutations in a LacZ transgene were C to T transitions at dipyrimidine sites (90%). What are believed to be ROS induced mutations (C:G to A:T) accounted for almost 7%. Whether this is due to UVB or UVA induced ROS is not clear.. Mutations believed to arise from direct absorption of UVA by DNA have also been found in sporadic SCCs. UVR dose could to be an important determinant of tumour type. At higher UV exposure, tumours may be more invasive and more prone to metastasis (Ramos et al. 2004). With regard to CMM, there is some debate as to which UV band is primarily responsible. In mice it has been observed that UVB is responsible for CMM carcinogenesis, with little or no involvement of UVA (De Fabo et al. 2004). This is in direct opposition to data from fish suggesting that UVA is the primary waveband responsible from melanoma in this model system (Setlow et al. 1989). UVR penetration through the skin is dependent on wavelength. UVA is absorbed far less efficiently, and so penetrates through the epidermis to the lower levels of the dermis. On the other hand, UVB does not

significantly penetrate beyond the epidermis as it is efficiently absorbed by the DNA of epidermal cells. This leads to a differential mutation spectra from UVR in different parts of the skin, and this has been observed with UVR mutations in *P53* from skin malignancies (Agar et al. 2004), although the distinction between UVA and UVB induced mutations in this system is ambiguous.

The effects of UVR on carcinogenesis are not simply confined to mutation induction. UVB is known to induce local immunosuppression in exposed skin, which is a risk factor for NMSC development (discussed later in this chapter) (Allanson et al. 2005). It has recently been shown that UVB causes a rapid decease in PTCH mRNA levels, leading to abrogation of the Shh signalling pathway (Brellier et al. 2004) and a possible involvement in carcinogenesis.

1.6 Skin Cancer in Organ Transplant Recipients

Solid organ transplants began in 1933 with a renal allograft, and since then the numbers and success rates of organ transplant have steadily increased. Worldwide, more than one million transplants have been performed. The increased success of these procedures is a result of better surgical techniques, and also improved immunosuppression of the host, which prevents graft rejection.

1.6.1 NMSC in Organ Transplant Recipients

The incidence of NMSC is greatly increased in organ transplant recipients (OTRs). This has been the subject of extensive review (Euvrard et al. 1997; Stockfleth et al. 2001; Euvrard et al. 2003). BCC incidence is increased about 10-fold, and SCC between 65- and 250-fold, compared to the non-OTR population. This has the effect of altering the BCC:SCC ratio and SCC are more common in OTRs. Over time, the risk for BCC increases linearly, while that of SCC increases exponentially. Individuals usually develop multiple tumours, and cases with more than 100 SCCs have been recorded. The increased NMSC incidence is geographically related to sunlight exposure, and increases as latitude decreases. An Australian study of renal transplant recipients (RTRs) in Queensland observed a cumulative incidence for NMSC of 7%, 12 months post-transplantation, and this increased to over 70% after 20 years (Bouwes Bavinck et

al. 1996). In a Dutch cohort, the 1 year incidence was 0.2%, rising to 40% after 20 years. More recently, a study from the Oxford Transplant Centre in the U.K., involving data from a number of Northern European countries, suggests the incidence after 20 years may be as high as 61% (Bordea et al. 2004). The latency between transplantation and NMSC development is also affected by latitude, with a mean lag of seven to eight years in the Dutch study, and less than three years in Australia.

The level of immunosuppression also plays a role in the aetiology of NMSC in OTRs. Studies have shown that triple immunosuppressive therapy, using three immunosuppressants, increased the incidence of NMSC more than double therapy with any two of the three agents. Heart and lung transplants often require a higher level of immunosuppression than renal transplants, and the incidence of NMSC is higher in these cohorts (Veness et al. 1999). There is a lower incidence of NMSC in patients treated with a low dose immunosuppressive regimen compared to those on a higher dose regimen (Fortina et al. 2004). In general, SCC in OTRs is more aggressive than in the general population (Lindelof et al. 2006) with over 13% recurring locally, and 5-8%metastasising.

1.6.2 Melanoma in OTRs

In addition to NMSC, OTRs show an increased incidence of CMM; 1.6- to 3.4-fold in Europe, 2- to 4-fold in Australia. CMM accounts for around 6% of skin cancers in adult OTRs, and almost 15% in children (Euvrard et al. 2003).

1.6.3 Risk Factors in OTR Tumourogenesis

The primary risk factor, UV exposure from sunlight, has already been discussed. Genetic factors may also play a role. TPMT levels have been potentially linked to cancer incidence. Factors such as HLA-subtypes, used for tissue typing and matching of donor and recipient, and glutathione S-transferases may be involved (Aractingi et al. 2003; Fryer et al. 2005). Oncogenic viral infections may also be implicated in NMSC development (Harwood et al. 1999). SCCs in OTRs are frequently associated with warts, and evidence of HPV infection has been found in some SCCs from these patients,

suggesting an important role for immunosuppression *per se* in the aetiology of these tumours.

1.6.4 Effects of Immunusuppressants

Commonly used immunosuppressants include Azathioprine (Aza), Cyclosporin A and prednisolone. Aza and prednisolone were used together until the mid-1980s when the standard regimens changed to Cyclosporin A in conjunction with Aza or prednisolone, or both. These are now being phased out in favour of a newer generation of agents including tacrolimus, sirolimus and mycophenolate mofetil. It is important to remember that chronic immunosuppression *per se* –via loss of immunosurveillance and protection against oncogenic viral infections - contributes to the development of skin cancers in OTRs. The immunosuppressive drugs may also contribute through direct carcinogenic effects. For example, Aza and Cyclosporin A are designated human carcinogens by the IARC, Lyon.

1.6.4.1 Cyclosporin A and Prednisolone

Cyclosporin A functions as an immunosuppressant by inhibiting T-cell signal transduction pathways. It is an acknowledged carcinogen in itself. In addition to inhibition of T-cell signalling, Cyclosporin A has been implicated in a local down regulation of DNA repair and apoptosis in skin (Herman et al. 2001), although the available data are not conclusive.

Prednisolone is known to block the transcription of a number of cytokines, TNF-α and interferon-γ, all of which are involved in the immune response. It can also inhibit the migration of monocytes. One study has observed an increase in NMSC in non-OTRs treated with prednisolone (Karagas et al. 2001).

1.6.4.2 Azathoiprine

The mechanisms by which Aza leads to immunosuppression involve its cleavage to 6-MP and subsequent generation of 6-TdGTP, and are described in detail in Chapter 4. The association of Aza treatment with NMSC has been proposed previously (Taylor et al. 1992). Aza is carcinogenic in mice when exposed to UV (Reeve et al. 1985).

Another study reported a correlation between cellular levels of 6-TdGTP and SCC in OTRs (Lennard et al. 1985).

1.7 Overview of Work Described in this Thesis

The work described in this thesis was undertaken to examine the possibility that Azathioprine, 6-MP, or 6-TG (as sources of 6-TdGTP and DNA 6-TG) might contribute to NMSC development in OTRs. I report experiments on the UVA photochemistry of 6-TG and DNA 6-TG (Chapter 3). Chapter 4 describes some of the biological effects of 6-TG/UVA and identifies possible underlying mechanisms by which 6-TG sensitises cells to UVA. Finally, preliminary studies on skin samples from patients treated with Aza are reported. An ongoing investigation of a possible synergistic role for Aza and UVA in NMSC in OTRs is also described.

2 Materials and Methods

2.1 Chemicals and Reagents

Unless stated, all chemicals were obtained from Sigma-Alridch. Standard solutions of 0.5M EDTA, 1M Tris-HCl, Tris-EDTA (TE), 1M $MgCl_2$, 5M NaCl, Phosphate Buffered Saline (PBS), and Tris Borate EDTA (TBE) were prepared by Cancer Research UK London Research Institute (LRI) Central Services. All other stock solutions were made according to standard methods (Sambrook et al. 2001). HPLC grade H_2O, methanol, acetonitrile and phosphoric acid were purchased from BDH. Glacial acetic acid was obtained from Fisher Scientific. CM-H_2DCFDA was supplied by Molecular Probes, and Aphidicolin by CalBiochem.

Oligonucleotides containing 6-TG, G and oxo^{8}G, and primers for PCR and sequencing of CHO D422 *APRT* were synthesized by the CRUK LRI Oligonucleotide Synthesis Service. Inosine containing oligonucleotides were purchased from Oligos Etc. Oligonucleotide sequences are shown in Table 2.1.

Name	Sequence (5' to 3')	Source
TOP-G	CTAATCTTAAT(**G**)TAACAC	CRUK
TOP-TG	CTAATCTTAAT(**6-TG**)TAACAC	CRUK
TOP-Oxo^{8}G	CTAATCTTAAT(**oxo^{8}G**)TAACAC	CRUK
TOP-I	CTAATCTTAAT(**I**)TAACAC	Oligos Etc.
BOT	GTGTTACATTAAGATTAG	CRUK
APRT 1f	TGTTCCCGGACTGGTATGAC	CRUK
APRT 2r	GGTTGAAGAAAGAAGGGATGG	CRUK
APRT 3f	CTTACACCTCAGCCCTAACA	CRUK
*APRT*5r	CTGGTGGCTCACAAAGGTCA	CRUK

Table 2.1 Oligonucleotides Used in this Thesis

E. coli Fpg and Endo IV, and mouse Aag were purchased from Trevigen. Nuclease P1 was purchased from USBiological, and Acid Phosphatase from Sigma.

Anti-PCNA antibody (PC10) and anti-ubiquitin antibody (P4D1) obtained from Santa Cruz Biotechnology.

For cell culture work, Dulbeccos MEM (E4) medium and Giemsa stain were prepared by CRUK LRI Central Cell Services. Foetal Calf Serum (FCS) was purchased from Gibco/Invitrogen, and sterile plasticware from Corning, Becton Dickinson, Millipore and Nunc.

BCC and blood samples were generously provided by Dr. Catherine Harwood, Dr. Jane McGregor, and Ms. Karin Purdie. Skin biopsies for 6-TG quantification were kindly provided by Dr. Conal Perrett.

All human and hamster cell lines used in this work were obtained from the CRUK LRI Central Cell Services, whom also performed long term maintenance of these lines. MEF cells lines F1.2 and F11.1 were kind gifts of Dr. Deborah Barnes. Cell lines used in this work are shown in Table 2.2.

Cell Line	Organism	Origin	DNA Repair Status
HCT116	Human	Colon Carcinoma	MMR Deficient
A2780-SCA5	Human	Ovarian Carcinoma	Proficient
XP12RO	Human	XPA Fibroblasts	NER Deficient
MRC5-VA	Human	Fibroblasts	Proficient
CHO D422	Hamster	Ovary	Proficient
F1.2	Mouse	Embryo	$OGG1^{-/-}$
F11.1	Mouse	Embryo	Proficient

Table 2.2 Cell Lines Used in this Thesis

All molecular biology kits were obtained from QIAGEN, unless otherwise stated. dNTPs were purchased from Amersham Pharmacia, BigDye Terminator v3.0 Cycle Sequencing Kit from Applied Biosystems. All PCR and sequencing reactions were performed on a Peltier Thermal Cycler PTC-200.

2.2 UVA, UVC and IR Irradiation

2.2.1 UVA Irradiation

UVA irradiation was performed using a UVH 253 lamp (UVLight Technologies) fitted with a black filter glass with a low range cut off at 320nm, and high range cut off at 400nm. A dose rate of 0.1kJ/m^2/s was used as standard irradiation conditions, as measured using a UVA Light Meter dosimeter (UVLight Technologies).

2.2.2 UVC Irradiation

UVC irradiation was performed using the built in germicidal UVC lamps in a HeraSafe tissue culture hood (Heraeus). The dose rate for irradiation was 1.0J/m^2/s.

2.2.3 IR Irradiation

A caesium 137 γ-radiation source was used in conjunction with an IBL 437C irradiator (CIS Bio International). A dose rate of approximately 2.3Gy/min was delivered.

2.3 HPLC Techniques

2.3.1 HPLC System

The HPLC system used consisted of a Waters 1525 Binary HPLC Pump, a Waters 717plus Autosampler, a Waters 2487 Dual-Wavelength Absorbance Detector and a Waters 2475 Multi-Wavelength Fluorescence Detector. A Waters Symmetry C_{18} Reversed Phase Column was used for separation (5μm particle size, 4.6mm internal diameter, and 150mm in length) in line with a Waters Symmetry C_{18} guard column. Columns were stored as per manufacturers instructions. Samples were injected from either Waters 1.0ml clear glass vials or Waters 8x40mm Total Recovery Glass vials. Waters Breeze v3.20 software was used for HPLC system control, trace analysis, and peak integration.

2.3.2 RP-HPLC of DNA Bases

Mobile phase used was 0.01M NaH_2PO_4 (pH 2.7), 2.4% acetonitrile (A). Column wash was performed using HPLC grade methanol (B). The program was as follows: 0 – 15 minutes, 100% A; 15 – 25 minutes, linear gradient from 100% A to 20% A and 80% B; 25 to 35 minutes, linear gradient from 20% A and 80% B to 100% A. Flow rate was either 0.5ml/min or 1ml/min. Column eluate was monitored by A_{342nm}, A_{260nm}, and fluorescence detection.

2.3.3 RP-HPLC of Deoxynucleosides

The HPLC program was the same as for DNA bases. The mobile phase (A) used was 0.01M KH_2PO_4 (pH 6.7). Eluate was monitored as for DNA bases.

2.4 Molecular Biology Techniques

2.4.1 Genomic DNA Preparation and Depurination

Genomic DNA extracts from cultured cells and tissue samples (BCC, skin and blood) were prepared using the QIAGEN DNeasy Tissue Kit, as per the manufacturers instructions. DNA was quantified in QIAGEN elution buffer, using a Genequant spectrophotometer (Amersham Pharmacia Biotech) or a NanoDrop spectrophotometer (NanoDrop Technologies).

Depurination of DNA was performed by resuspending an ethanol precipitated DNA pellet in 0.1N HCl, and incubating at 70°C for 30 minutes. Samples were neutralised by addition of NaOH or a large excess of Tris-HCl, pH 7.5.

2.4.2 PCR and DNA Sequencing

All PCRs were performed using the QIAGEN HotStar Taq polymerase, and included buffers, as per manufactures instructions. Prior to sequencing, PCR reactions were visualised by ethidium bromide staining after agarose gel electrophoresis. The remaining aliquots of PCR reactions were purified using the QIAGEN QIAquick PCR Purification Kit. Sequencing was carried out with the BigDye Terminator v3.0 Cycle

Sequencing Kit as instructed by the manufacturer. Excess sequencing reagents were removed with the QIAGEN DyeEx 2.0 Spin Kit. Electrophoresis was performed by the CRUK LRI Equipment Park using either an ABI Prism 377 or ABI Prism 3100 sequencer. Sequences were analysed using Sequencher v4.5 software (Genecodes).

2.4.3 Protein Extractions

Total protein extracts were prepared from approximately 10^6 cells. Cells were spun down and the pellet resuspended in Whole Lysis Buffer (1% NP40, 10mM NaF, 1mM Na_3VO_4, 1mM $Na_4P_2O_7$, 1 EDTA free Protease Inhibitor Cocktail Tablet (Roche)). Suspensions were incubated for 1 hour at 4°C, and centrifuged for 30 minutes at 13,000rpm. Supernatant was removed and contains cellular proteins.

Chromatin and soluble bound protein fractions were also prepared. Cell pellets were resuspended in 500µl Soluble Lysis Buffer (10mM Tris-HCl, pH7.5, 2.5mM $MgCl_2$, 0.5% NP40, 1 Protease Inhibitor Tablet), incubated for 8 minutes on ice, and centrifuged for 5 minutes at 735g. Supernatant contains the soluble protein fraction. The remaining pellet was resuspended in 200µl of Chromatin Lysis Buffer (20mM Na_2HPO_4, 0.5M NaCl, 1mM EDTA, 0.75% Triton X-100, 10% Glycerol, 5mM $MgCl_2$, 1 Protease Inhibitor Tablet), incubated on ice for 20 minutes, and centrifuged at 12,000g for 5 minutes. Supernatant contains chromatin bound protein fraction.

All protein extracts were quantified using the Bradford method for protein quantification.

2.4.4 Western Blotting

Around 100µg of total protein was loaded onto an 8% SDS PAGE gel along with 10µl of Prestained Low Range Markers (Biorad). Separated proteins were transferred to a PVDF membrane (Immobilon-P, Millipore) overnight at 20V using a Biorad wet transfer apparatus. Membranes were washed, and blocked for one hour with 5% (w/v) non-fat powdered milk (anti-PCNA), or 5% BSA (anti-ubiquitin), in PBS-T (PBS + 0.1% Tween) at room temperature. Membranes were washed three times with PBS-T. Antibody was prepared as a 1 in 2000 dilution in 5% milk, or BSA, in PBS-T.

Membranes were incubated for 3 hours at room temperature with primary antibody, followed by three washes with PBS-T. Immunoreactive proteins were detected using HRP-conjugated secondary antibody (1 in 1000 dilution of anti-mouse (Biorad) in 5% milk ,or BSA). Membranes were washed three times, and antibody complexes detected using ECL substrate (Amersham Pharmacia), and visualised on Hyperfilm MR (Amersham Pharmacia).

For reprobing membranes, bound antibodies were removed by incubation with Stripping Buffer (100mM β-mercaptoethanol, 2% SDS, 62.5mM Tris-HCl, pH 6.7) for 30 minutes at 50°C. The membranes were washed three times for 10 minutes in PBS-T, followed by blocking and probing as described above.

2.5 6-TG/ UVA Photochemistry

2.5.1 6-TG Standard Curve for Quantification

20µl of 6-TG (in 0.1N KOH) was added to 20µl of DNA extracted from CHO D422 (~250ng/ml). 360µl of 0.1N HCl was added to this solution, and incubated at 70°C for 30 minutes. 340µl of 0.1N NaOH was added, and 20µl of the solution was analysed by RP-HPLC. Peak area was plotted against moles of 6-TG injected, and a standard curve plotted.

2.5.2 Analysis of 6-TG/UVA Photoreactions

A solution of 6-TG in 0.1N KOH was UVA irradiated, and analysed by RP-HPLC. For investigation of rates of reaction, 200µl 6-TG solution was UVA irradiated at a dose rate of 0.1kJ/m^2/s. Every 60 seconds, 10µl samples were taken, diluted to 20µl in dH_2O, and 10µl injected for analysis by RP-HPLC. For determining the effects of anti-oxidants, 5mM solutions of NAC and GSH in PBS were prepared, and 100µl was added to 100µl 6-TG solution before irradiation. Analysis of 6-TGdR was performed in the same manner, but 0.1mM 6-TGdR was prepared in dH_2O.

For purification of P1 and P2, fractions of eluate from RP-HPLC were collected every 60 seconds. Fractions were measured for fluorescence and A_{342nm}, indicating the

presence of P1 and P2 respectively. Maximum absorbance wavelengths were determined using a UV/Vis spectrophotometer (Ultraspec 1100pro, Amersham Pharmacia). Fluorescence excitation and emission maxima were measure using a scanning spectrofluorimeter (RF-1501, Shimadzu). In both cases, quartz cuvettes were used.

Authentic G-6-SO_3 was prepared according to published methods (Rackwitz et al. 1974; Erdmann et al. 1990; Pike et al. 2001). Briefly, 1mg/ml 6-TG in 0.1N NaOH was diluted in 0.2M $NaHCO_3$ to a volume of 300µl. To this, 10µl of 0.25% $KMnO_4$ was added, and incubated for 10 minutes at room temperature. The reaction was stopped by addition of 10µl of 30% H_2O_2. Samples were spun at 13,000 rpm for 5 minutes. Supernatant contains G-6-SO_3.

2.5.3 Digestion of Oligonucleotides

Oligonucleotide solutions were prepared at 0.1mM. To 4µl of oligonucleotide solution, 2µl of 300mM NaAcetate (pH5.4), 4µl of 25mM $ZnCl_2$, 8µl of dH_2O, and 2 µl of Nuclease P1 (1U/µl in 30mM NaAcetate (pH5.4)) were added, and the reaction mix incubated for 1 hour at 37°C. 4µl of 1mM $MgCl_2$, and 4µl of Acid Phosphatase (0.5U/µl in 50mM NaAcetate (pH4.5), 1mM $MgCl_2$) were added and the solution incubated for a further 1 hour at 37°C. Samples were diluted to a final volume of 100µl with dH_2O, and 90µl injected for analysis by RP-HPLC. For double stranded oligonucleotides, samples were heated to 80°C for 5 minutes prior to digestion.

2.5.4 Oxidation of 6-TG by MMPP

Magnesium monoperoxypthalate (MMPP – Sigma-Aldrich) stock solution was prepared in dH_2O to a concentration of 10mM. 10µl was added to 40µl of depurinated and neutralised DNA from 6-TG treated cells (or 30µl non 6-TG containing DNA and 10µl of 6-TG stock solution in dH_2O) and 50µl of dH_20. Samples were incubated for 20 minutes at room temperature. 90µl was injected for RP-HPLC analysis.

2.6 Biological Assays

2.6.1 Cell Culture and Maintenance

All cell lines utilised were maintained in Dulbeccos MEM (E4) medium, supplemented with 10% FCS, at 37°C in a humidified atmosphere containing 10% CO_2. Cultures were passaged 3 times a week by detaching the cells with 5ml of 0.25% Trypsin in 0.1% Versene for 3 to 5 minutes at 37°C. 1ml of this suspension was diluted in 25ml of fresh E4 medium in a clean, sterile 75cm^2 flask. Cell numbers were determined by haemocytometer counting. Long term maintenance of cultures was performed by CRUK LRI Central Cell Services according to their protocols.

2.6.2 6-TG Dose Response

Cells were plated out at 500 cells/well in 6-well plates. Each well contained 5ml E4 medium with 10% FCS. Cells were allowed to attach for 3 to 4 hours, and 6-TG (in 0.1N KOH) added to each well. The maximum volume of 6-TG added was 100µl. Cultures were allowed to grow for 7 to 10 days, Giemsa stained, and colonies counted. Survival was determined as number of colonies relative to untreated controls.

2.6.3 UVA Dose Response

Cells were plated out as described above. Once cells had attached, wells were washed twice with sterile PBS, and UVA irradiated under 1ml PBS at a dose rate of 0.1kJ/m^2/s. Wells were washed once with PBS and fresh E4 medium with 10% FCS added. After 7 to 10 days growth, colonies were Giemsa stained and counted, and survival calculated.

2.6.4 6-TG/UVA Treatment of Cells

Cells were cultured in the presence of 6-TG for 48 hours. Cells were plated out and UVA irradiated as above. Colonies were stained, counted and survival determined after 7 to 10 days.

2.6.5 Quantification of DNA 6-TG

Cells were grown for 48 hours in the desired concentration of 6-TG. Cells were harvested and DNA extracts prepared as described. DNA was depurinated, and 6-TG quantified as described previously. % substitution of guanine by 6-TG was determined by quantification of injected DNA using the A_{260nm} peak of adenine and guanine as observed after RP-HPLC.

2.6.6 Hydroxyurea and 6-TG/UVA Treatment

Cells were plated out and allowed to attach. HU was added to plates to a final concentration of 1mM. 30 minutes after addition of HU, 6-TG was added to plates to a concentration of 5μM. Cultures were maintained overnight, and irradiated with UVA as above. Survival was determined by clonogenic assay as described. These cells were also analysed by FACS and microscopy, performed as described below.

2.6.7 *APRT* Mutation Frequency Assay

CHO D422 cells were treated with 6-TG/UVA (0.1μM/1.0kJ/m^2). Post UVA, cultures were maintained in E4 with 10% FCS for 7 days. Cells were plated out at a density of 1x10^6 cells per 10cm dish in E4 with FCS containing 4mM 8-azaadenine. Cultures were maintained for 10 to 12 days. A single colony from each original culture was picked, expanded over 2 to 3 weeks in medium containing 8-azaadenine, harvested and DNA extracted. The remaining colonies in each plate were Giemsa stained, and mutation frequency calculated relative to untreated controls.

The *APRT* gene was amplified by PCR from the DNA extracts, as described previously. Amplified products were sequenced and a mutation spectrum was determined by comparison with unmutated *APRT* sequences. This spectrum was compared to previously published spontaneous and UVA spectra. Statistical differences were determined using paired Students t-test, with $p<0.05$ being classed as significant.

2.6.8 ROS Staining, FACS Analysis and Microscopy

Cells were treated with 6-TG for 48 hours. For FACS analysis, cells were plated out in 10cm dishes ($7.5x10^5$ cells), and for microscopy on coverslips, and allowed to attach overnight. Cells were washed twice with PBS and incubated with 5μM CM-H_2DCFDA (50μg dissolved in 43.3μl methanol, then diluted in 18ml PBS) for 20 minutes at 37°C. Cells were washed twice with PBS, and UVA irradiated with 1 or 3kJ/m^2. For visualisation by microscopy, cell nuclei were stained with DAPI (5 minutes at 37°C in 300nm DAPI in PBS). Coverslips were placed on microscope slides and examined for green and blue fluorescence by microscopy (Zeiss Axioplan fitted with Hamamatsu C4747-95 digital camera, images were acquired using OpenLab v2.2.5 (Improvision)). For FACS analysis, cells were gently scraped into suspension in PBS without DAPI staining. FACS analysis was performed on a Beckton Dickinson FACScan using the FL1 channel for green fluorescence. Data acquisition and analysis was performed using CellQeust v3.3 software.

2.7 Enzymatic Assays

2.7.1 ^{32}P Labelling of Oligonucleotides

Oligonucleotides were diluted to a concentration of 0.5pmoles/μl. 4μl of oligonucleotide solution was added to 1μl of T4 kinase buffer, 1μl of T4 PNK (New England Biolabs) and 4.5μl γ-ATP (Amersham Pharmacia). This was incubated at 37°C for 40 minutes, and then labelled oligonucleotide separated from residual γ-ATP and ADP in a G50 spin column (Amersham Pharmacia). Labelled oligonucleotides were stored at 4°C.

2.7.2 Annealing of Complementary Oligonucleotides

Equimolar amounts of the complementary oligonucleotides were mixed. An appropriate volume of 10X Annealing Buffer (0.1M Tris-HCl, pH7.5, 0.1M $MgCl_2$) was added. The solution was heated to 80°C for 5 minutes followed by incubation for 1 hour at room temperature.

2.7.3 Cleavage Assays

2.7.3.1 Fpg

^{32}P labelled TOP-G, TOP-TG and TOP-Oxo^{8}G were UVA irradiated at a dose rate of 0.1kJ/m^2/s. Oligonucleotides were annealed to their complementary strands. 1µl oligonucleotide, 1µl 10X REC Buffer, 1µl Fpg (3U) and 7µl H_2O were incubated at 37°C for 1 hour. 5µl of 3X Alkali Loading Buffer (300mM NaOH, 97% formamide, 0.2% Bromophenol Blue, 0.2% Xylene Cyanol) was added, and samples heated to 95°C for 5 minutes. 5µl was loaded onto a pre-run 15% PAGE gel, run at 50W, 90A and 2150V. After separation, the gel was dried, and ^{32}P labelled products visualised by autoradiography using Kodak Biomax MS film.

2.7.3.2 Aag

The assay was performed as with Fpg, with some changes. In place of TOP-Oxo^{8}G, TOP-I was used. After the first 1hour incubation, 1.5µl of *E. coli* Endo IV and 1µl 10mM $MgCl_2$ were added, and incubated at 37°C for a further 1 hour. Samples were analysed by electrophoresis and autoradiography as above.

2.8 Analysis of PCNA State after 6-TG/UVA

2.8.1 PCNA Mono-Ubiquitination

HCT 116 cells were grown in 6-TG for 48 hours, plated out and exposed to UVA as described earlier. Cells were harvested between 1 and 9 hours post UVA. Whole protein extracts were prepared and analysed by Western blot with an anti-PCNA antibody (PC10).

2.8.2 Immunoprecipitation of PCNA

HCT 116 cells were treated as above. Soluble and chromatin bound extracts were prepared as described. Samples were pre-cleared by the addition of 50µl of Protein A-Sepharose bead slurry (25µl beads in 25µl of IP Buffer (50mM Tris (pH8.0), 150mM NaCl, 10% Glycerol, 0.5% Triton X-100, 1 Protease Inhibitor Tablet)) and incubation

for 1hour at 4°C with gentle rotation. Samples were centrifuged at 2,000 rpm for 5 minutes. Supernatant was transferred to a clean eppendorf tube. 20µl dH_2O and 5µl of Loading Buffer (60mM Tris-HCl (pH6.8), 2% SDS, 20% Glycerol, 1mg/ml Bromopheno Blue, 5% β-mercaptoethanol) was added to the pelleted beads, boiled for 5 minutes, and stored at -80°C.

To the supernatant, 2µg of PC10 antibody was added per 200-500µg of total protein, and incubated overnight at 4°C. 50µl of Protein A-Sepharose beads (1/2 in IP Buffer) was added, and samples incubated at 4°C for 3 hours. Samples were centrifuged at 2,000rpm for 5 minutes, and supernatant was removed and stored for later analysis. Beads were washed three times in 500µl IP Buffer. Beads were resuspended in 20µl IP Buffer, and 5µl of 5X Loading Buffer, boiled for 5 minutes and analysed by SDS PAGE followed by Western blot with anti-PCNA (PC10) or anti-ubiquitin (P4D1) antibodies, as previously described.

2.8.3 Rapid Lysis and Analysis after UVA

HCT 116 cells were grown in 6-TG for 48 hours. Cells were washed and gently scraped into suspension in PBS. Cells were concentrated to around 10^5 cells in 10µl PBS. Cell suspensions were UVA irradiated, at a dose rate of 0.5kJ/m^2/s, with 1kJ/m^2/s. Cells were lysed between 2 and 60 seconds post UVA by addition of 40µl RIPA Buffer (150mM NaCl, 1.5% NP40, 0.5% deoxycholate, 0.1% SDS, 50mM Tris), boiled for 5 minutes, and analysed by SDS PAGE and Western blot with anti-PCNA antibody (PC10).

2.8.4 Glutaraldehyde Crosslinking of PCNA

Chromatin bound protein pellet was resuspended in 200µl Chromatin Lysis Buffer. Gluataraldehyde was added to a final concentration of 0.1%, and incubated for 20 minutes at 4°C. Reaction was stopped by addition of Lysine to a final concentration of 0.1M.Samples were analysed by SDS Page and Western blot with anti-PCNA antibody (PC10).

2.9 Quantification of 6-TG from Patient Samples

DNA extracts were prepared from skin biopsies using the QIAGEN DNeasy Tissue Kit. DNA was depurinated, neutralised and DNA 6-TG quantified by RP-HPLC coupled to A_{342nm} and A_{260nm} detection.

3 Results I : UVA Photochemistry of 6-Thioguanine

3.1 Introduction

6-TG and 6-MP are antileukaemic agents. Their mechanism of action, although not fully understood, appears to depend on the ultimate incorporation of 6-TG into DNA in place of guanine, although 6-MP has also been shown to inhibit *de novo* nucleotide synthesis. Substitution of guanine by 6-TG has the important effect of introducing a UVA chromophore into DNA. Both 6-TG and 6-MP have a much lower oxidation potential than the standard DNA bases. Oxidation products of 6-MP have been detected in the urine of 6-MP treated humans and mice (Chan et al. 1990).

3.1.1 Chemical Oxidation of 6-TG and 6-MP

Extensive characterisation of 6-MP and 6-TG oxidation products has been described in a number of publications (Elion et al. 1958; Doerr et al. 1961; Rackwitz et al. 1974). Rapid oxidation of 6-MP and 6-TG solutions by iodine leads to the formation of thiol dimers of these compounds (R-S-S-R) (Fig 3.1A). These compounds are mildly acid and base labile, and after cleavage in an alkali solution, can react with O_2 to generate sulfinate derivatives (RSO_2^-) (Fig 3.1B III). The same sulfinate products can be formed by incubation of 6-TG or 6-MP with a mild base for four to five days. The sulfinate is itself subject to oxidation leading to the generation of a sulfonate product (RSO_3^-) (Fig 3.1B IV). The sulfonates are also produced by oxidation of 6-TG or 6-MP with $KMnO_4$, or by oxidation of 6-chloro-purine/guanine with sodium sulfite (Fig 3.1B V). The same oxidative reactions also occur with 6-MP and 6-TG ribosides and deoxyribosides. This work also demonstrated that the sulfonate derivatives are fluorescent, a fact which has since been used to develop a sensitive 6-TG quantification technique (Finkel 1975).

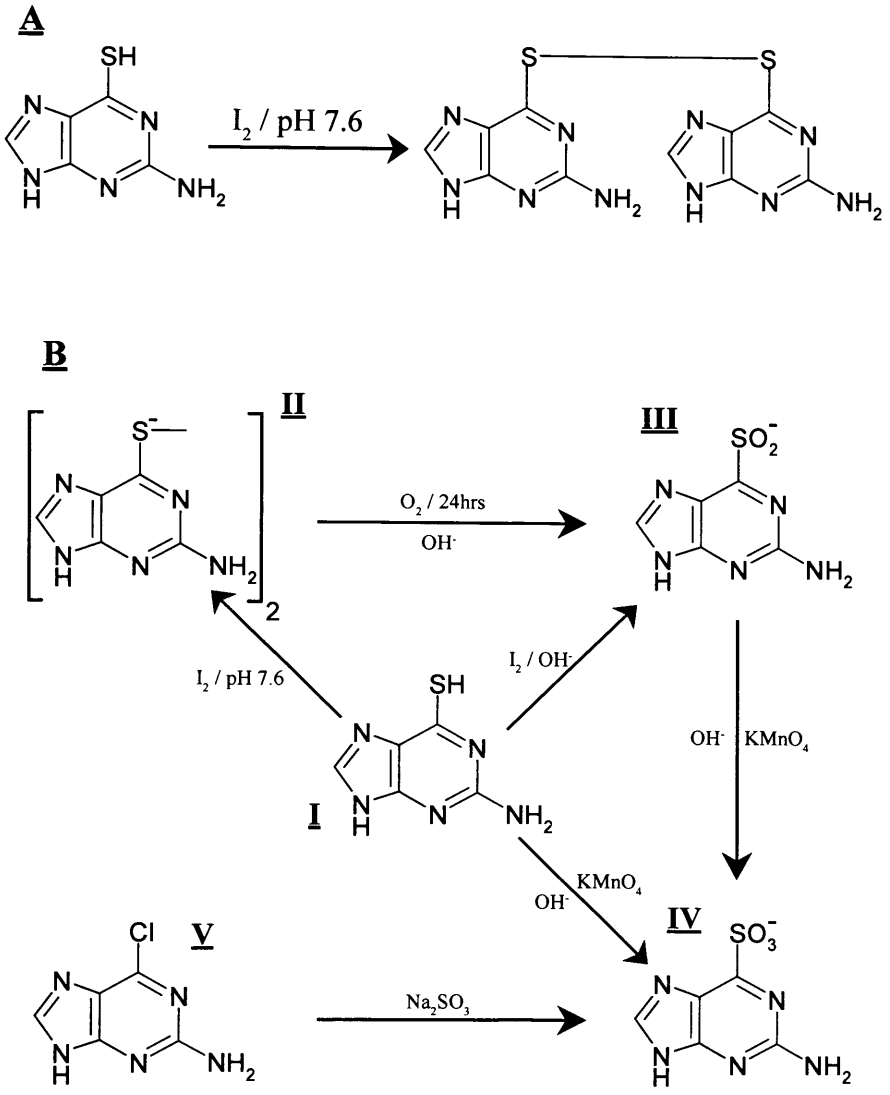

Fig 3.1 Chemical Oxidation Products of 6-TG. **A** Rapid oxidation of 6-TG by I_2 generates the guanine-6-thioguanine dimer. **B** Formation of guaine-6-sulfinate and guanine-6-sulfonate by chemical oxidation. (Adapted from Doerr 1961).

3.1.2 UVA Photo-oxidation of 6-MP

In an aqueous solution, 6-MP can undergo photochemical reactions with UVA. These reactions have been studied in detail (Hemmens et al. 1984; 1986; 1986; Moore et al. 1994), and a brief description will be provided here. In an aqueous, oxygenated solution, 6-MP is destroyed by UVA irradiation. Destruction is accompanied by the formation of two stable photoproducts. A single intermediate has also been isolated. The intermediate is purine-6-sulfinate, and the two stable photoproducts are purine-6-sulfonate and hypoxanthine. Hypoxanthine is a minor product of these reactions, but levels increase as the pH of the irradiated 6-MP solution decreases. Purine-6-sulfinate is a major product of very short UVA irradiations, and retains some absorbance of UVA (at 340nm). As a result of this, it can further react with UVA leading to generation of purine-6-sulfonate. Purine-6-sulfonate does not absorb in the UVA region, and as such, is stable to further irradiation.

O_2 is critical for these reactions. The ratio of oxygen consumption to 6-MP destruction (1:1) suggests oxidation to the sulfinate is by addition of a single molecule of oxygen. From experiments using Methylene Blue, Rose Bengal and Rhodamine ($^1O_2$ sources), sodium azide (a $^1O_2$ quencher) and D_2O (prolongs the lifetime of $^1O_2$), it has been inferred that singlet oxygen is responsible for formation of purine-6-sulfinate, but has no impact on the further oxidation of this to the sulfonate. This study suggests that 6-MP may act as both a Type I and a Type II photosensitiser. Experiments in which $^1O_2$ produced after UVA of 6-MP reacts with histidine, which in turn quenches reactions with the compound *p*-nitrosomethylanaline (RNO), confirm a Type II mechanism. Irradiation of 6-MP in the presence of glutathione (GSH) suggests that oxidation can also occur independently of ROS, by formation of a thiyl-purine radical that can react directly with oxidisable compounds in a Type I photosensitisation reaction.

In a deoxygenated solution, 6-MP photoexcitation leads to the direct loss of an electron, which if no electron accepting compound is present will simply reform 6-MP, but if an acceptor is present, will lead to one electron oxidation of this molecule. Electron transfers can also occur in an oxygenated solution as is illustrated by the generation of $\bullet O_2^-$, which, as described in Chapter 1, may lead to the production of •OH.

3.1.3 Detection of 6-TG

Quantification of 6-TG has been a priority because of the clinical use of thiopurines. The efficacy of thiopurine treatments is dependent on the levels of 6-TdGTP and/or DNA 6-TG. A number of methods have been developed for the detection of 6-TG nucleotides and DNA 6-TG. These all rely on separation by high performance liquid chromatography (HPLC) to isolate 6-TG from other cellular and DNA components prior to its detection. Quantification has been described using the A_{342nm} of 6-TG (Cuffari et al. 1996; Erb et al. 2003). Fluorescence detection of 6-TG sulfonate has been utilised after oxidation of 6-TG by $KMnO_4$ (Erdmann et al. 1990; Pike et al. 2001). The most sensitive optical detection techniques developed so far involve the chemical labelling of 6-TG with fluorescent compounds which then allow highly sensitive detection (Warren et al. 1993; Warren et al. 1995). The development of HPLC coupled mass spectrometry has the potential to allow far more sensitive detection and quantification of 6-TG.

In this chapter I describe the experiments performed to analyse the UVA photochemical reactions of 6-TG. The major photoproducts of these reactions are identified, and a mechanism for their formation is proposed. Finally, I validate a 6-TG detection technique based on a mild oxidation of 6-TG to the sulfonate which does not affect the standard DNA bases, unlike oxidation by $KMnO_4$.

3.2 Results

3.2.1 Detection and Quantification of 6-Thioguanine

In order to study the UVA photochemistry of 6-TG, it was necessary to set up and validate a sensitive and accurate system for its detection and quantification. For this purpose, C_{18} reversed phase high performance liquid chromatography (RP-HPLC) was used. The eluate from the HPLC column was monitored by absorbance at 260nm and 342nm for detection of the standard DNA bases and 6-TG respectively. Following injection of a solution of 6-TG in 0.1N KOH, or H_2O, a single peak with absorbance at 342nm was observed. This A_{342nm} peak was well separated from adenine and guanine in a sample of depurinated DNA spiked with 6-TG (Appendix Fig 7.1). This RP-HPLC separation followed by monitoring A_{342nm} was therefore routinely used to detect and quantify 6-TG in free solution and in depurinated DNA samples.

To determine the limits of detection of this method, a calibration curve of 6-TG A_{342nm} peak area versus the amount of 6-TG was constructed. Depurinated DNA spiked with various amounts of 6-TG was analysed by RP-HPLC (Fig 3.2). 6-TG was detected following injection of as little as 500fmoles. The limit for accurate and reproducible quantification of 6-TG was found to be 1.0pmole, however.

Several attempts to increase the 6-TG detection sensitivity were made. These included use of ion exchange chromatography, electrochemical detection, and fluorescent labelling of 6-TG prior to HPLC analysis. None of these produced the required increased sensitivity coupled with reproducibility, and detection by A_{342nm} was used for all subsequent analyses of 6-TG UVA photochemistry.

3.2.2 UVA Photochemistry of 6-Thioguanine

The effect of UVA on 6-TG in solution was investigated. 6-TG solutions were UVA irradiated and the products analysed by RP-HPLC coupled to A_{342nm}. Without UVA irradiation, a single peak with A_{342nm} was observed, as described above. 5.0kJ/m^2 UVA caused a decrease in 6-TG peak and between 5.0 and 50kJ/m^2, there was a UVA dose dependent destruction of 6-TG (Fig 3.3). These data are summarised in Table 3.1.

UVA (kJ/m^2)	A_{342nm} Peak Area (μVs)	6-TG (moles x 10^{-10})
0	366469	1.2
5	130548	0.44
10	60813	0.21
20	15158	0.06
50	3293	0.02

Table 3.1 UVA Dependent Destruction of 6-TG

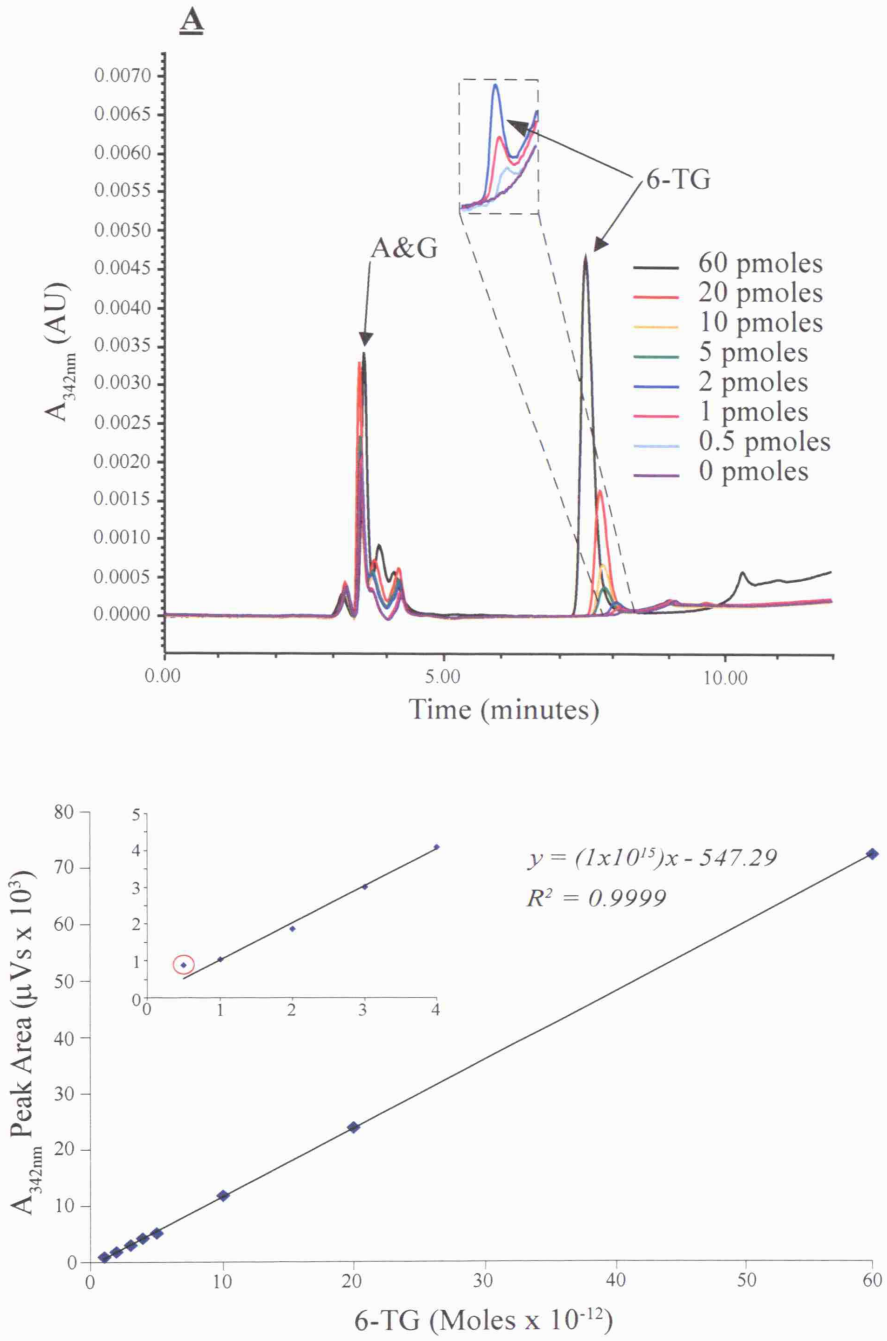

Fig 3.2 Quantification of 6-TG by C_{18} RP-HPLC Coupled to A_{342nm} Detection. DNA samples depurinated by acid hydrolysis were spiked with known amounts of 6-TG and analysed by RP-HPLC coupled to A_{342nm} detection. 6-TG peak area was determined by integration. **A** 6-TG was clearly resolved from other components of the hydrolysate. 1.0pmoles injected could be quantified accurately and reproducibly. **B** Standard curve of A_{342nm} peak area versus amount of 6-TG injected. Inset, lowest 6-TG concentrations expanded. 500fmoles is detectable (circled), but quantification is not accurate or reproducible.

The UVA dependent destruction of 6-TG was accompanied by the formation of two significant photoproducts, P1 and P2, that were resolved by RP-HPLC and detected by A_{342nm}, A_{260nm} or fluorimetry. P1 eluted earlier than 6-TG and P2 eluted later. Both were generated in a UVA dose dependent manner, which correlated well with 6-TG destruction (Fig 3.3A). Analysis of data collected by RP-HPLC monitored by fluorimetry showed P1 to be highly fluorescent (Fig 3.3B). The relationship between 6-TG destruction and photoproduct formation is summarised in Table 3.2

UVA (kJ/m^2)	6-TG (moles)	Corrected P1 Peak Area (μVs)	P2 Peak Area (μVs)
0	1.2×10^{-10}	0	0
5	4.4×10^{-11}	21851	14910
10	2.1×10^{-11}	37635	19644
20	6.0×10^{-12}	48535	28486
50	2.0×10^{-12}	50998	28737

Table 3.2 Relationship Between 6-TG Destruction and Photoproduct Formation

Samples of P1 and P2 were purified by HPLC and their spectral characteristics determined. The absorbance maximum of each photoproduct was determined by spectrophotometry. The fluorescence excitation and emission maxima were determined using a scanning fluorescence spectrophotometer. These data are shown in Table 3.3. Briefly, the wavelength of the absorbance maximum of P1 was shifted down by 20nm from that of 6-TG to 324nm, while that of FP1 was reduced to 331nm.

	A_{max} (nm)	λ_{ex} (nm)	λ_{em} (nm)
P1	324	324	408
P2	331	n/a	n/a

Table 3.3 Spectral Properties of 6-TG/UVA Photoproducts

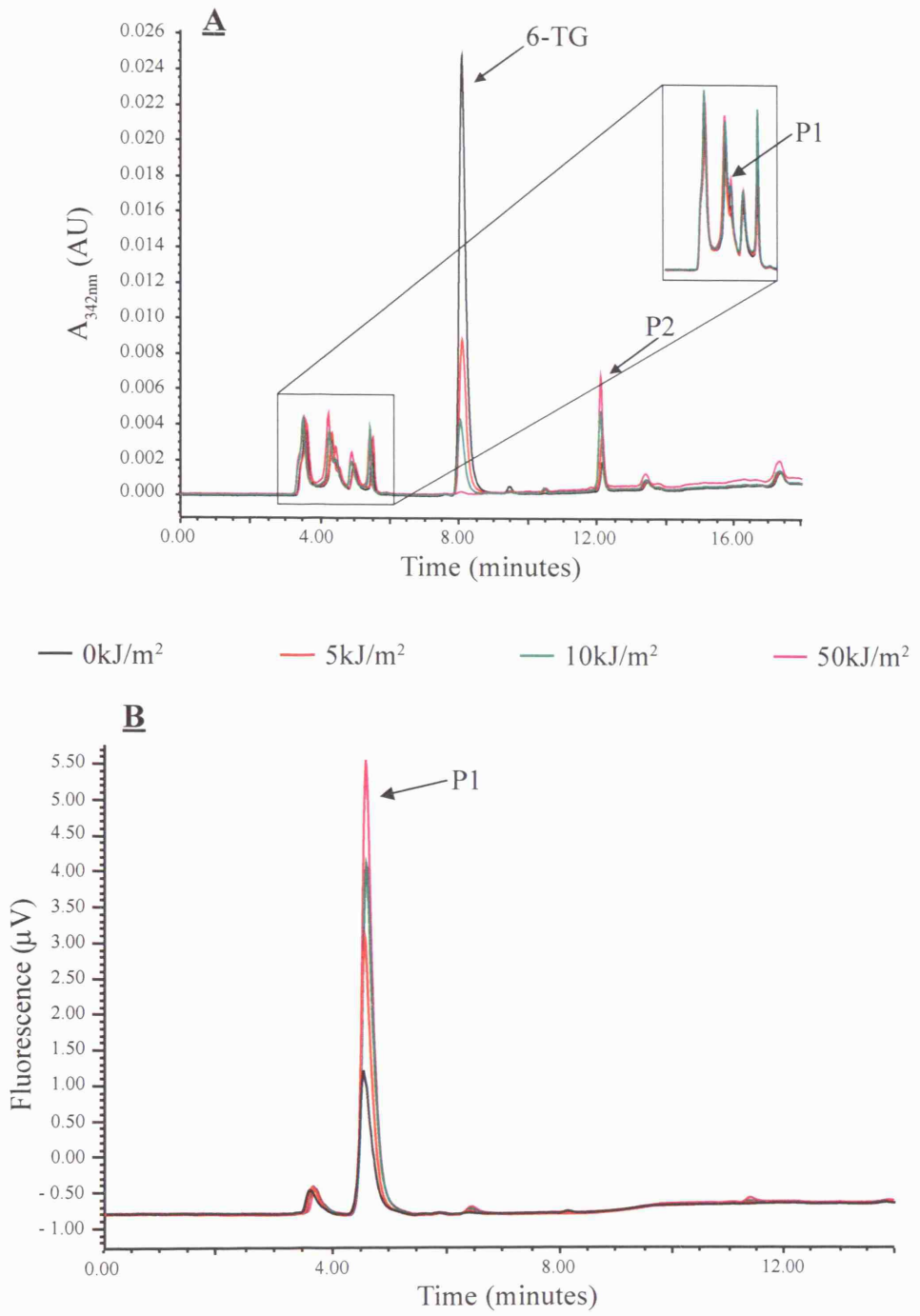

Fig 3.3 UVA Mediated 6-TG Destruction and Photoproduct Formation. An aqueous 0.1mM solution of 6-TG was UVA irradiated at a dose rate of 0.1kJ/m²/s. Samples were analysed by RP-HPLC coupled to A_{342nm}. **A** 6-TG A_{342nm} signal is diminished on UVA irradiation. Two photoproducts are observed by A_{342nm}. P1 elutes earlier than the parent compound, P2 elutes later. Both are formed in a UVA dose dependent manner. Other peaks are column and buffer artifacts that remain constant in every injection. **B** Fluorescence detection of P1. P1 exhibits fluorescence at 408nm with excitation at 324nm.

The identity of P1 and P2 was investigated. Published work has shown that 6-mercaptopurine (6-MP) becomes oxidised during UVA irradiation and that one product of this oxidation was purine-6-sulfonate (P-6-SO_3). Significantly, this compound was shown to be fluorescent. I therefore suspected that P1 may be the analogous guanine-6-sulfonate (G-6-SO_3). Using a published protocol for P-6-SO_3 synthesis, G-6-SO_3 was prepared by $KMnO_4$ oxidation of 6-TG (as described in Materials and Methods).

As can be seen in Fig 3.3B, some P1 was present in a solution of 6-TG before UVA treatment. The level of P1 increased as solutions aged. This is most likely due to the spontaneous oxidation of 6-TG as a result of intermittent exposure to natural light.

The full fluorescence emission spectrum for G-6-SO_3 was determined, and is compared to that of P1 in Fig 3.4A. Both compounds have an excitation maximum of 324nm and their emission spectra were very similar, with a maximum at 408nm. P-6-SO_3 is also reported to be acid labile. Treatment of UVA irradiated 6-TG with 0.1N HCl completely abolished the fluorescence signal (Fig 3.4B). This provided further evidence that P1 is likely to be G-6-SO_3.

A more detailed analysis, using mass spectrometry (MS) and nuclear magnetic resonance (NMR), by my colleagues Dr.Y.-Z. Xu and Dr. X. Zhang confirmed the identity of P1 as G-6-SO_3. The same techniques identified P2 as the 6-TG dimer, guanine-6-thioguanine (G-S-G). The chemical structures of G-6-SO_3 and G-S-G are shown in Fig 3.5.

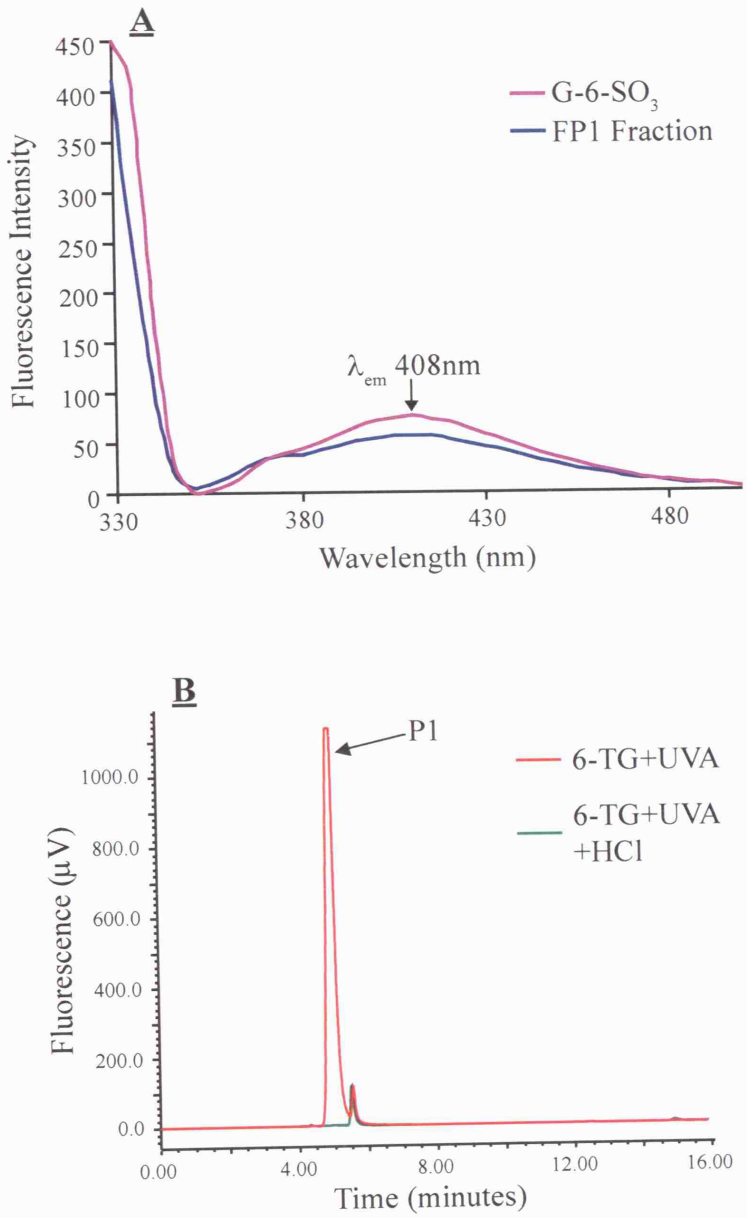

Fig 3.4 Fluorescence Spectrum and Acid Lability of P1. **A** Authentic G-6-SO_3 was prepared by $KMnO_4$ treatment of 6-TG. P1 was obtained by collection of the fluorescent fraction after RP-HPLC. Fluorescence emission spectra were obtained using a standard scanning spectrofluorimeter, with an excitation wavelength of 324nm. The emission maximum of P1 is at 408nm. **B** An aqueous 0.1mM solution of 6-TG was UVA irradiated with 50kJ/m^2, and treated with 0.1N HCl for 5 minutes, at room temperature. Resulting solutions were analysed by RP-HPLC. Acid treatment abolished the P1 fluorescence peak.

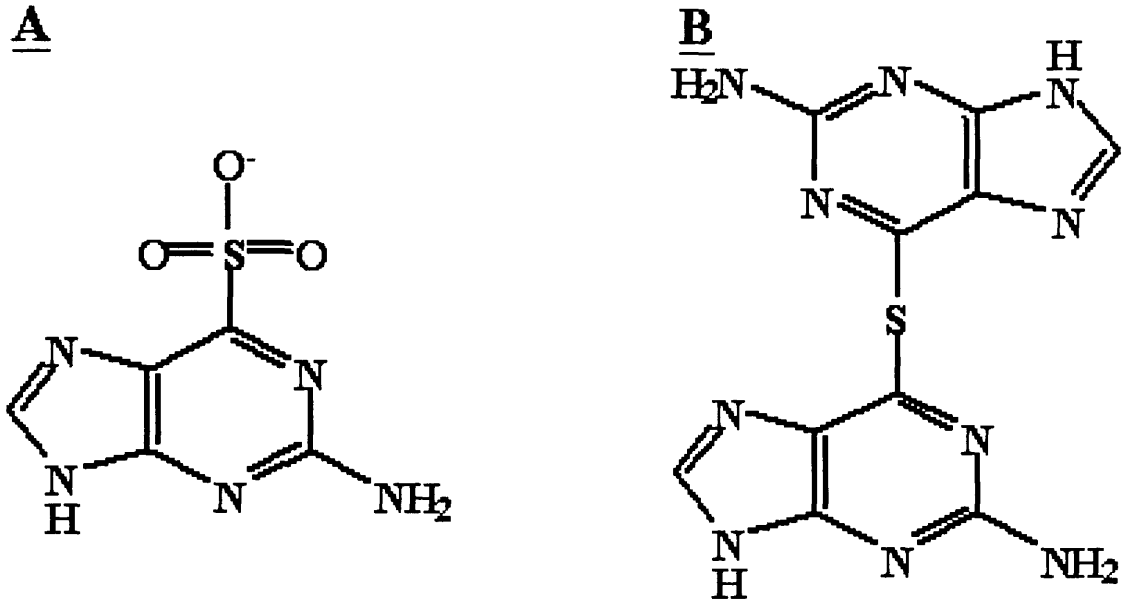

Fig 3.5 Chemical Structures of G-6-SO_3 (A) and G-S-G (B)

3.2.3 Mechanisms of 6-TG/UVA Photoproduct Formation

The mechanisms of 6-TG UVA photoproduct formation were investigated. The first step was to determine the kinetics of 6-TG destruction and photoproduct formation. A solution of 6-TG was irradiated at a dose rate of 0.1kJ/m^2/s, and sampled at intervals. Samples were analysed by RP-HPLC coupled to A_{342nm} and fluorescence detection (Fig 3.6). 6-TG was rapidly destroyed with approximately linear kinetics over the first 2.5 minutes corresponding to a half life ($t_{1/2}$) for 6-TG of around 1.5minutes. The kinetics of formation of G-6-SO_3 were sigmoidal, and became linear only after an initial lag. The lag suggests the formation of reaction intermediates. The intermediate(s) appear to be reactive since no accumulation was detected. There was also a lag in G-S-G formation, again consistent with the formation of reactive intermediates.

Since G-6-SO_3 is an oxidised form of 6-TG, I examined whether anti-oxidants protected against its formation. The addition of N-acetyl cysteine (NAC) during UVA irradiation decreased the rate of 6-TG destruction. The $t_{1/2}$ of 6-TG increased approximately 1.5- to 2-fold, to 2.5 minutes. The rates of formation of G-6-SO_3 and G-S-G were also decreased (Appendix Fig 7.2). Similar results were obtained when the anti-oxidant glutathione (GSH) was used in place of NAC (Appendix).

Molecular oxygen is required for 6-TG oxidation. Following my initial experiments, Dr. Y.-Z. Xu analysed the kinetics of the photoreactions in 6-TG solutions purged of oxygen. He found that the rate of 6-TG destruction was more than 4-fold lower when he replaced O_2 with He. Taken together, the data suggest that reactive oxygen species generated by photoactivation of molecular oxygen are required for destruction of 6-TG by UVA, and for the formation of G-6-SO_3 and G-S-G.

3.2.4 UVA Photochemistry of 6-Thioguanine Deoxyriboside and 6-TG in DNA

The UVA photoreactions of 6-TGdR were also examined. An aqueous solution of 6-TGdR was UVA irradiated and analysed by RP-HPLC coupled to A_{342nm} and fluorescence detection (Fig 3.7). 6-TGdR could be detected by this method, and UVA irradiation caused a dose dependent decrease in A_{342nm} from 6-TGdR. This decrease was accompanied by the formation of two photoproducts, one of which eluted later than 6-TGdR and exhibited A_{342nm}. The second eluted earlier and showed strong fluorescence at the wavelengths used for G-6-SO_3 detection. These photoproducts have been identified as the deoxyriboside derivatives of G-6-SO_3 and G-S-G, by HPLC elution times together with absorbance and fluorescence spectroscopy (Dr. Y.-Z. Xu). In addition to these photoproducts, a small amount of deoxyguanosine was also formed.

The kinetics of 6-TGdR destruction and photoproduct formation were examined (Appendix Fig 7.3). 6-TGdR was destroyed at a slower rate than 6-TG, and its $t_{1/2}$ was 2.5 minutes at a dose rate of 0.1.kJ/m^2/s. Furthermore, the extent of the initial lags preceding sulfonate and dimer formation were correspondingly longer with 6-TGdR. This suggests that the presence of a deoxyribose moiety stabilises UVA excited 6-TG.

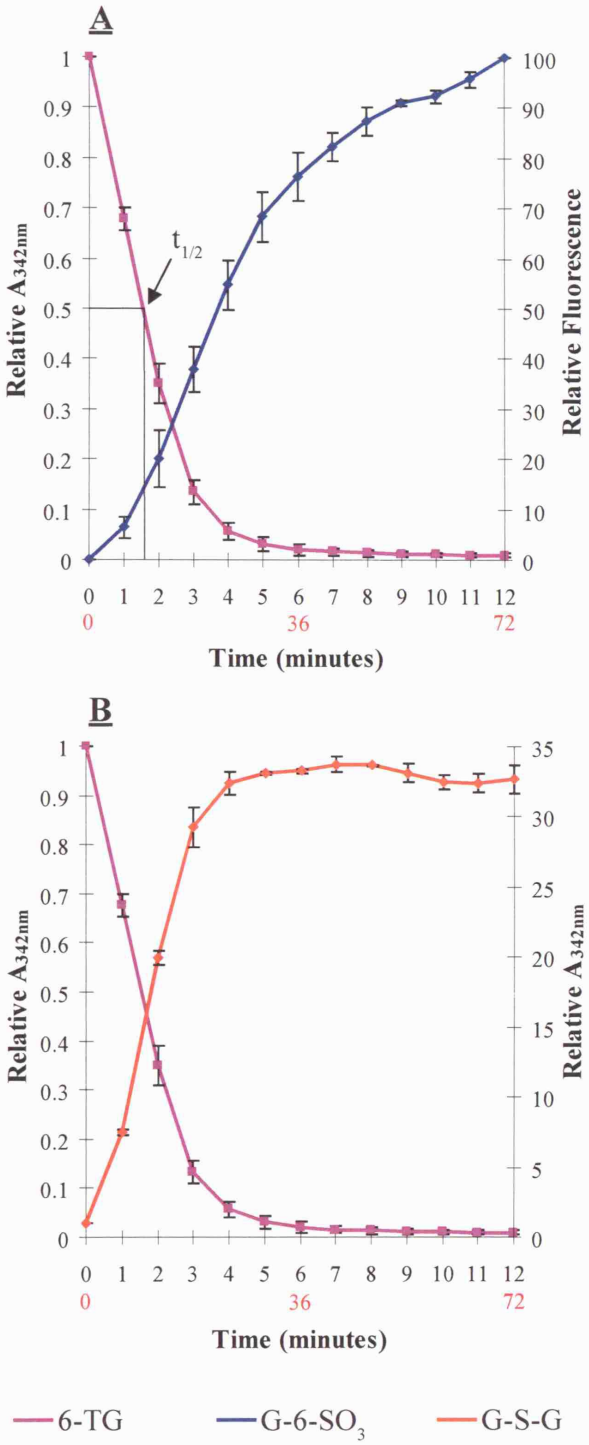

Fig 3.6 Kinetics of 6-TG/UVA Photoreactions. An aqueous solution of 6-TG was irradiated at a dose rate of 0.1kJ/m^2/s. Samples were taken every 60 seconds and analysed by RP-HPLC coupled to A_{342nm}, A_{260nm} and fluorescence detection. UVA doses, in kJ/m^2, are shown in red. **A** 6-TG destruction (pink) and G-6-SO_3 formation (blue). **B** Formation of G-S-G (orange).

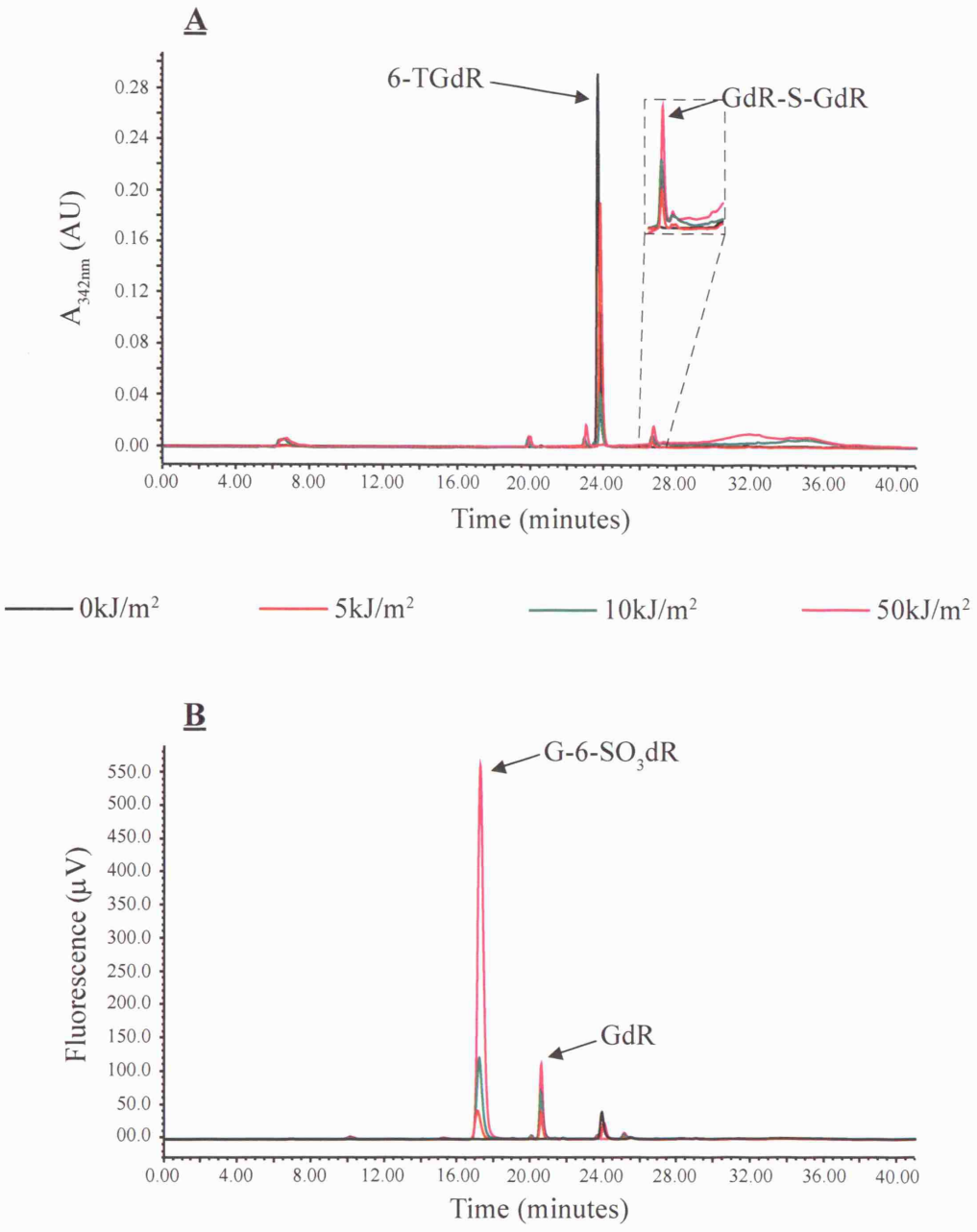

Fig 3.7 6-TGdR/UVA Photochemical Reactions. Aqueous 6-TGdR was UVA irradiated at a dose rate of 0.1kJ/m²/s. Samples were analysed by RP-HPLC coupled to A_{342nm} (**A**) and fluorescence detection (**B**). Peaks were identified by comparison of elution times with authentic standards.

I next examined the photoreactions of 6-TG in DNA. For this, a synthetic 18mer oligonucleotide containing a single 6-TG was used (ThioG1). Following RP-HPLC, ThioG1 gave a single peak with absorbance at both 260nm and 342nm. UVA irradiation reduced the A_{342nm} signal (Fig 3.8A). This was accompanied by an increase in fluorescence at the same elution position (Fig 3.8B). The overall A_{260nm} signal was essentially unchanged, suggesting that the oligonucleotide was not degraded (Fig 3.8C).

Irradiated oligonucleotides were digested to deoxynucleosides by successive nuclease P1 and acid phosphatase treatment. Digests were analysed by RP-HPLC coupled to A_{342nm}, A_{260nm} and fluorescence detection. A control oligonucleotide, containing G in place of 6-TG, generated five peaks with A_{260nm} (Appendix Fig 7.4 & Table 3.4). Comparison with authentic standards revealed deoxyadenosine was not present in these digests. Instead a product that eluted at the position of deoxyinosine was found. Further investigation revealed that this was due to a contaminating adenosine deaminase activity in the acid phosphatase. Since deamination appeared to be selective and complete, quantification of deoxyinosine was substituted for deoxyadenosine. The presence of uracil in the digests was independent of incubation with AP, suggesting the generation of UdR from CdR during synthesis and deprotection of the oligonucleotide.

	A_{260nm}Peak Area (μVs)	**Expected Base Composition**	**Experimental Base Composition**
GdR	364909	4	4
AdR(IdR)	530297	6	5
TdR	432539	7	7
CdR/UdR	60290	1	1

Table 3.4 Digestion of Oligonucleotides to Deoxynucleosides

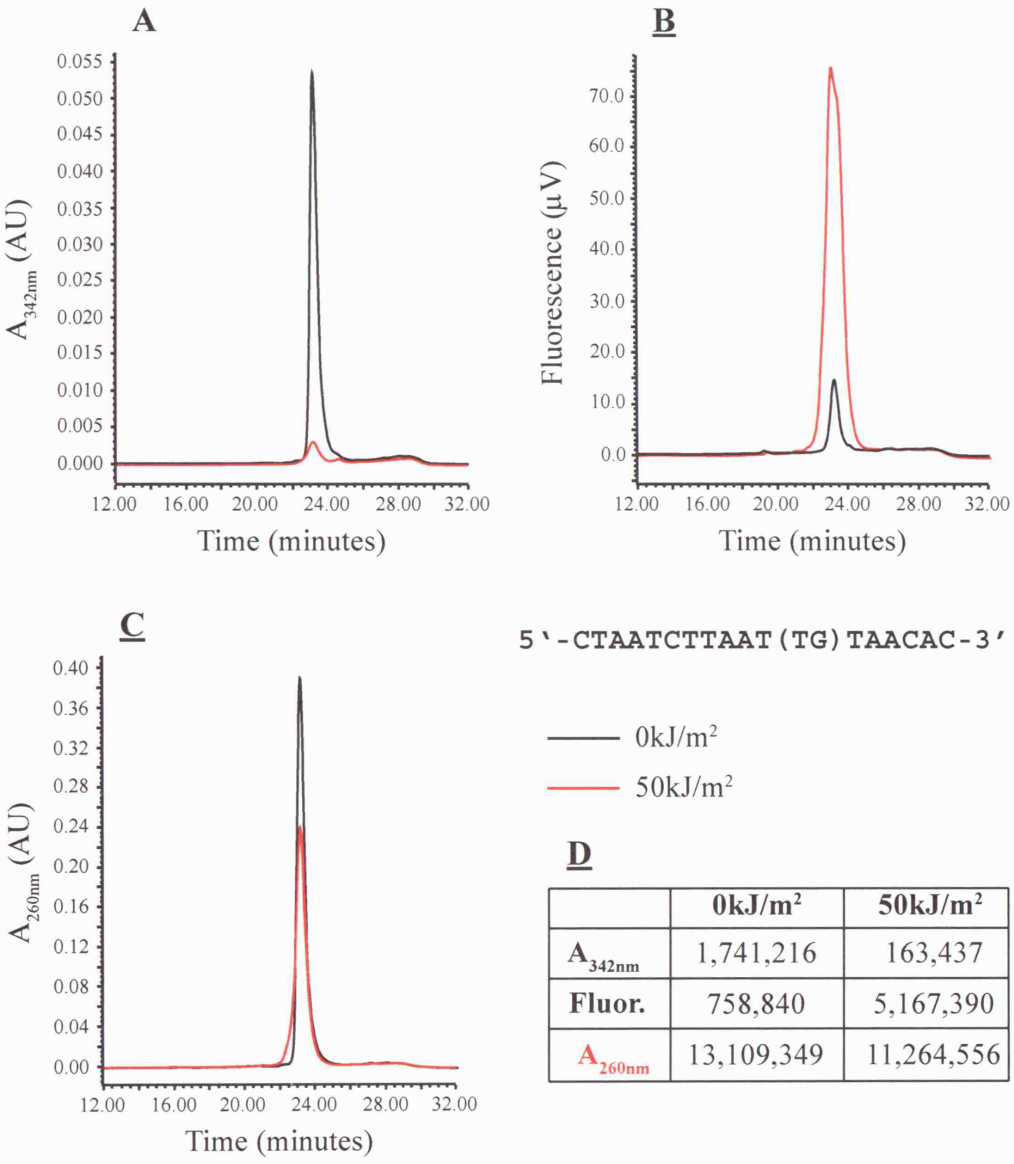

D

	0kJ/m²	50kJ/m²
A_{342nm}	1,741,216	163,437
Fluor.	758,840	5,167,390
A_{260nm}	13,109,349	11,264,556

Fig 3.8 UVA Irradiation of 6-TG Containing Oligonucleotides. A synthetic 18mer oligonucleotide of the sequence shown, containing a single 6-TG residue was irradiated with 50kJ/m² UVA. After UVA irradiation, the oligonucleotide solution was analysed by RP-HPLC coupled to A_{342nm}, A_{260nm} and fluorescence detection. A_{342nm} (**A**), fluorescence (**B**) and A_{260nm} (**C**) traces before (black) and after (red) UVA irradiation. A_{342nm} peak decreases after UVA, fluorescence peak increases and A_{260nm} peak area is unchanged. **D** Summary of peak area data from **A**, **B** and **C**.

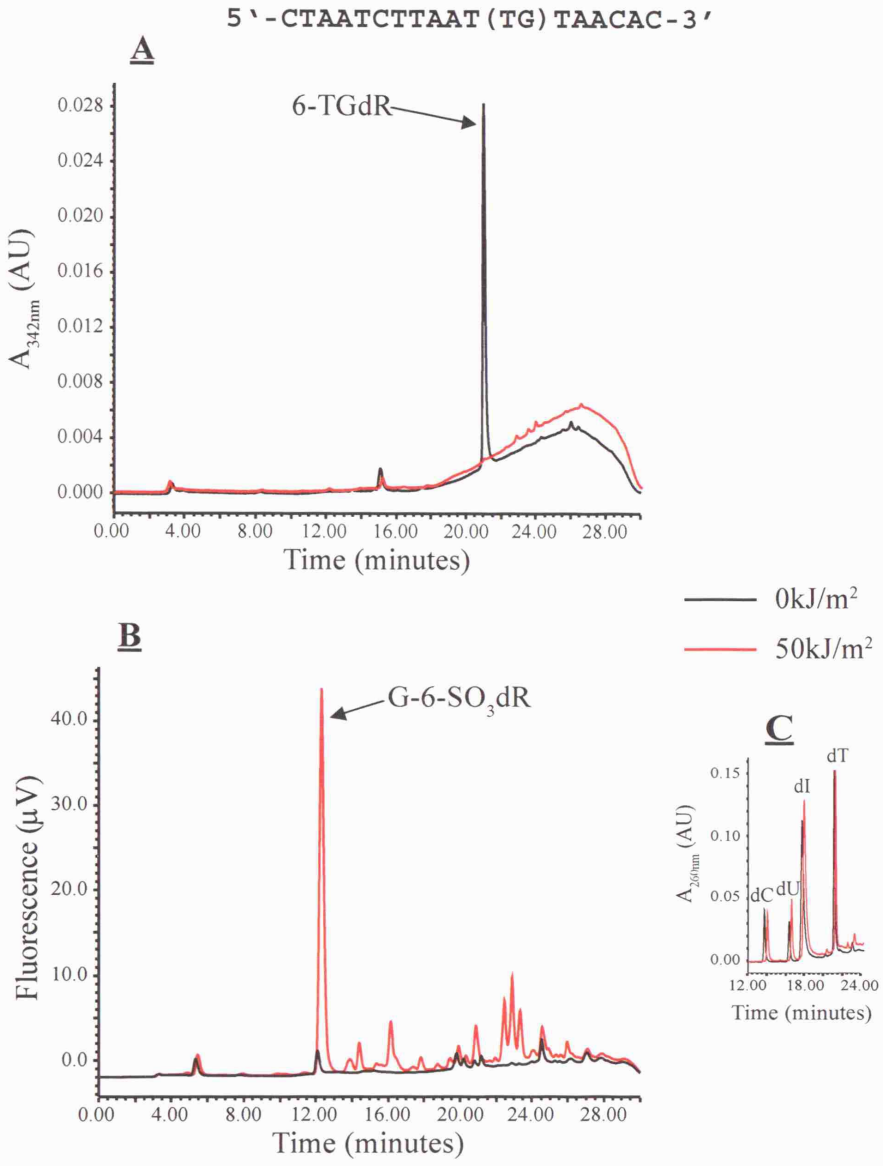

Fig 3.9 6-TG/UVA Photoreactions in ssDNA. An 18mer oligonucleotide containing a single 6-TG was enzymatically digested prior to (black) and post (red) 50kJ/m^2 UVA. The digest was analysed by RP-HPLC coupled to A_{342nm}, A_{260nm} and fluorescence detection. **A** DNA 6-TG is destroyed by UVA. The A_{342nm} peak for 6-TGdR is diminished after UVA. **B** DNA 6-TG photoreacts with UVA to form G-6-SO_3dR. After UVA, a fluorescence peak corresponding to G-6-SO_3dR is observed. **C** UVA does not alter the standard DNA deoxynucleosides in the oligonucleotide, as observed by A_{260nm}.

When the ThioG1 oligonucleotide was digested, an additional peak was observed with strong A_{342nm}. This peak corresponded to 6-TGdR and co-eluted with an authentic marker close to TdR. Its A_{342nm} allows selective 6-TGdR detection. When the same oligonucleotide was UVA irradiated (50kJ/m^2) prior to digestion, the A_{342nm} signal was diminished (Fig 3.9A) and an early eluting, fluorescent photoproduct eluted at the expected G-6-SO_3dR position (Fig 3.9B). A number of minor, unidentified peaks were also present. There was no detectable formation of the GdR-S-GdR dimer.

The effect of UVA on dsDNA was also examined. For these experiments the same 6-TG containing oligonucleotide was annealed to a complementary strand that placed a C opposite 6-TG. After irradiation, the dsDNA was digested to deoxynucleosides and analysed as described above. The A_{342nm} signal of 6-TG was again reduced by UVA treatment. An early eluting fluorescent product that eluted coincident with a G-6-SO_3dR marker was again observed. There was no detectable formation of late eluting products retaining A_{342nm} (AppendixFig 7.5).

3.2.5 Quantification of 6-TG by Fluorescence Detection of G-6-SO_3

Dr.Y.-Z. Xu and Dr. X. Zhang developed a mild oxidation treatment using MMPP (magnesium monoperoxyphthalate). Treatment of 6-TG with MMPP leads to complete conversion to G-6-SO_3 (Fig 3.10A). Furthermore, MMPP is particularly useful in this regard as it does not oxidise the normal DNA bases. For quantification of 6-TG in a DNA hydrolysate, 6-TG was added to DNA extracted from cells. The DNA was depurinated by acid hydrolysis, the mixture neutralised and treated with MMPP (see Materials and Methods). The limit of detection of G-6-SO_3 was 50fmoles, and G-6-SO_3 could be quantified accurately down to 200fmoles by RP-HPLC coupled to fluorescence detection (Fig 3.10B).

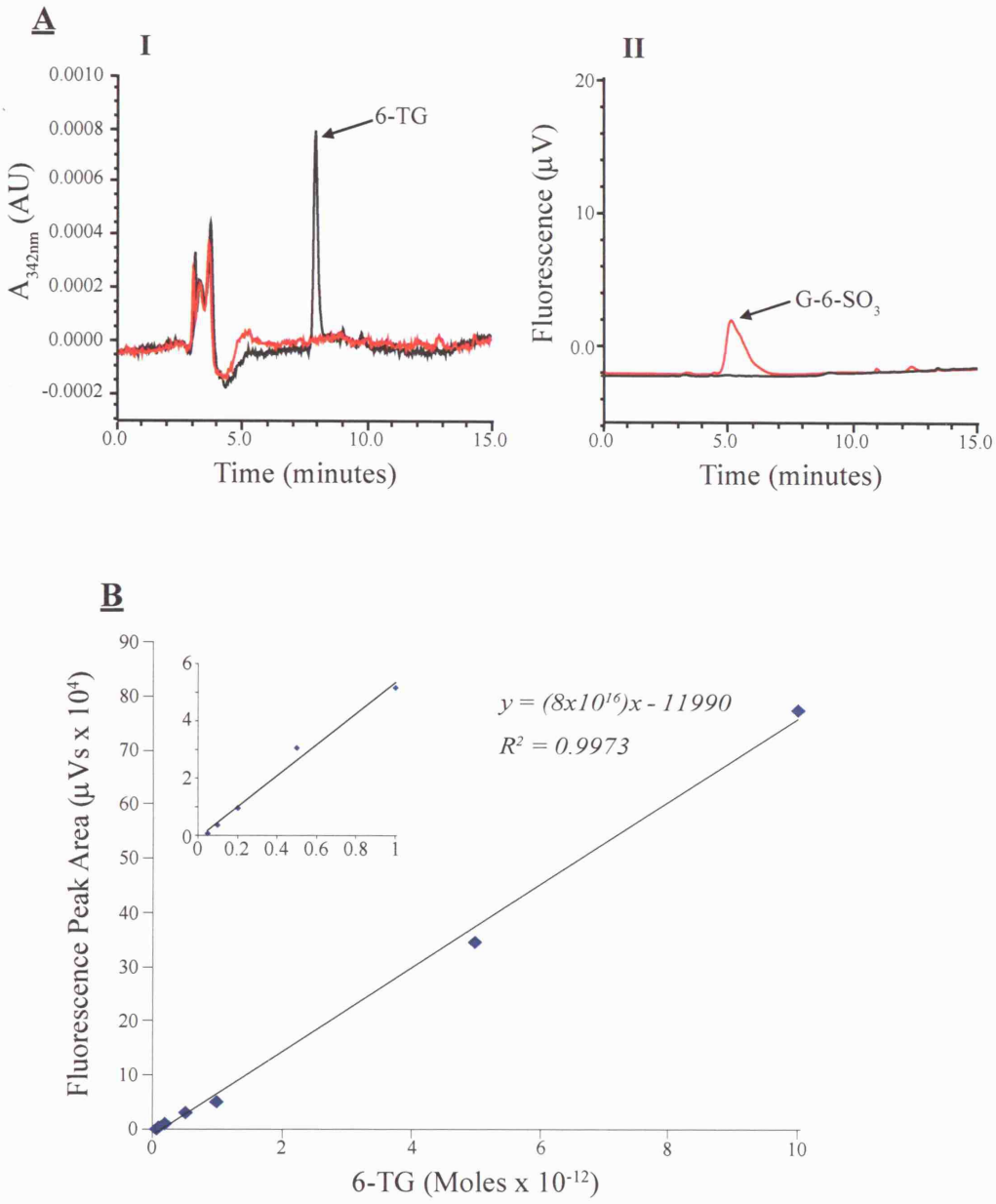

Fig 3.10 DNA 6-TG Quantification by Conversion to G-6-SO_3. **A** A solution of 2.5pmoles 6-TG was treated with 1.0mM MMPP at room temperature for 30 minutes prior to analysis by RP-HPLC coupled to A_{342nm} (**I**) and fluorescence (**II**) detection. MMPP treated (red), untreated (black). **B** A solution of DNA was spiked with 6-TG and depurinated. The solution was neutralised, and treated with 1.0mM MMPP as in A. Resulting mixture was analysed by RP-HPLC coupled to A_{342nm} and fluorescence detection. Fluorescence peak area was plotted against oxidised 6-TG injected. Inset, expanded plot of low 6-TG data points.

3.3 Discussion

A sensitive 6-TG detection technique was set up and validated using A_{342nm} detection following separation by RP-HPLC. This method is capable of detecting and quantifying 1.0pmole of 6-TG in free solution and in DNA hydrolysates. Several attempts were made to find a more sensitive detection system, but these offered little improvement. An alternative method in which 6-TG released from DNA is quantitatively oxidised by treatment with a mild oxidising agent, MMPP, to a fluorescent product provided a measurable improvement in sensitivity of around 5-fold. This chemical treatment was subsequently adopted as standard for measurement of DNA 6-TG in biological samples.

6-TG has a maximum absorbance at 342nm, in the UVA region. The normal DNA bases absorb in the UVC and UVB regions and their photochemistry has been extensively studied. Since 6-TG absorbs UVA, there is an increased probability of UVA-related photoreactions. I found that 6-TG in solution is rapidly destroyed by UVA irradiation in a dose dependent manner. Relatively low UVA doses, around $50kJ/m^2$, were sufficient to destroy almost all of the 6-TG. Two photoproducts were isolated and characterised. The first eluted later from RP-HPLC than 6-TG and retained significant A_{342nm}. Dr. Y.-Z. Xu subsequently identified this as the 6-TG dimer G-S-G. While G-S-G is a significant photoproduct of free 6-TG, its biological relevance may be less, since its formation is via a bimolecular reaction involving two 6-TG molecules.

The early eluting photoproduct, P1, did not exhibit appreciable A_{342nm}, but was highly fluorescent. Working with Dr. Y.-Z. Xu, P1 was identified as G-6-SO_3, an oxidised form of 6-TG. This parallels the published data which show that P-6-SO_3 is a major UVA photoproduct of 6-MP.

The kinetics of destruction of 6-TG were rapid. Photoproduct formation exhibited sigmoidal kinetics, suggesting the formation of reactive intermediates. The photochemical conversion of 6-TG to G-6-SO_3 requires O_2 and involves ROS. The presence of anti-oxidants during irradiation significantly reduced the rate of G-6-SO_3 formation. Hemmens and Moore proposed that for 6-MP, UVA-induced oxidation proceeded via sulfenate (P-6-SO) and sulfinate (P-6-SO_2) intermediates. Dr. Y.-Z. Xu

has demonstrated that molecular oxygen is essential for G-6-SO_3 formation after UVA and has implicated singlet oxygen ($^1O_2$) in the oxidation process. Specifically, the photosensitiser Rose-Bengal, which with visible light is a known $^1O_2$ source, promotes G-6-SO_3 formation. The rate of formation is faster in deuterium oxide (D_2O) than in H_2O. This is consistent with the increased $t_{1/2}$ of $^1O_2$ in D_2O which allows $^1O_2$ more time to react with 6-TG. Finally, azide, a known quencher of $^1O_2$, reduced the rate of G-6-SO_3 production. These findings allow us to propose a mechanism for 6-TG UVA photoproduct formation (Fig 3.11). 6-TG acting as a Type II photosensitiser, produces $^1O_2$ on UVA irradiation. This oxidises 6-TG to 6-TG-sulfenate (G-6-SO), a highly reactive intermediate. G-6-SO may react with 6-TG to form G-S-G, H_2O to form guanine, or it may be further oxidised to 6-TG-sulfonate (G-6-SO_3).

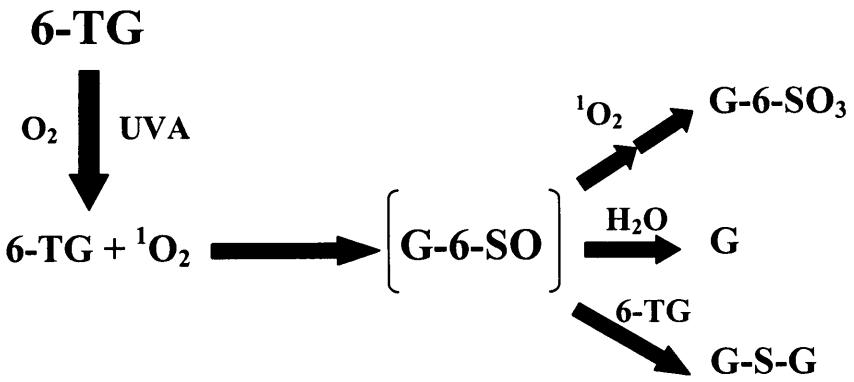

Fig 3.11 Proposed Mechanism for 6-TG/UVA Photreactions

Interestingly, there is protection of 6-TG from UVA as the complexity of the system increases. Free 6-TGdR is more sensitive to UVA than ssDNA 6-TG, which is more sensitive than dsDNA 6-TG (Table 3.5). This is consistent with protection afforded by stacking in duplex DNA or intramolecular folding in ssDNA.

Free 6-TGdR	ssDNA 6-TG	dsDNA 6-TG
0.9%	1.5%	20%

Table 3.5 Percent A_{342nm} Peak Area Remaining after 50kJ/m^2 UVA Irradiation

Use of the sulfonate for quantification of 6-TG increased sensitivity by 5-fold. Fluorescence is an inherently more sensitive detection technique than absorbance (although it is often subject to interference), and the procedure for 6-TG oxidation is a relatively simple one. This makes use of this system especially suitable for patient samples from which very small amounts of DNA are available.

I have shown that UVA interacts with 6-TG in ssDNA and dsDNA resulting in the production of G-6-SO_3. G-S-G was not formed to a significant degree in DNA suggesting that it may have less biological relevance. The requirement for two 6-TG molecules to be correctly juxtaposed for such a bimolecular reaction reduces the likelihood of its formation in DNA. In contrast, G-6-SO_3 is readily formed in DNA. This bulky, charged lesion significantly disrupts the stability of the DNA double helix. Dr. Y.-Z. Xu has demonstrated that the T_m of G-6-SO_3 containing DNA is significantly reduced. In a synthetic double stranded 11mer oligonucleotide with a T_m of 55°C, a 6-TG:C base pair reduces this slightly, to 49°C. Oxidation of the 6-TG to G-6-SO_3, giving a G-6-SO_3:C base pair, reduced the T_m to 35°C. Similar effects were found with A, G and T opposite G-6-SO_3. This disruption may have implications for DNA repair mechanisms, cell survival and mutation.

4 Results II – Biological Effect of 6-Thioguanine/UVA

4.1 Introduction

6-TG, 6-MP and Azathioprine are pharmaceuticals (Elion 1989,; Aarbakke et al. 1997). While 6-TG and 6-MP themselves are purine analogues, Azathioprine must first undergo cleavage to generate 6-MP. 6-MP and 6-TG are subsequently metabolised to 6-TdGTP, which is believed to be responsible for most of their biological effects (Fig 4.1). 6-TG and 6-MP are primarily used in the clinic for treatment of leukaemia (AML and ALL respectively). Azathioprine has found a greater variety of uses. Although originally developed as an immunosuppressant for use in organ transplantations, it is now increasingly used for treatment of inflammatory bowel diseases (IBDs), multiple sclerosis, rheumatoid arthritis, lupus, and other disorders. 6-TdGTP formed after Aza treatment has a half life in cells of approximately 13 days (Chan et al. 1990). Standard Aza immunosuppression involves daily administration, and so over a short period high levels of 6-TG nucleotides may accumulate in cells, and a steady state of 6-TdGTP appears to be reached after only four weeks of therapy (Derijks et al. 2004).

The activity of 6-TG, 6-MP and various intermediates is regulated by the thiopurine methyltransferase (TPMT) enzyme (Relling et al. 2001; Krynetski et al. 2003). TPMT transfers a methyl group onto the thiol group of these compounds, rendering them inactive. TPMT polymorphisms are relatively common with 10% of the population being heterozygous for a defective copy, and 0.3% being homozygous. This can lead to serious complications during 6-MP, 6-TG or Aza therapy, as homozygous individuals are hypersensitive to these agents, while heterozygotes show an intermediate response.

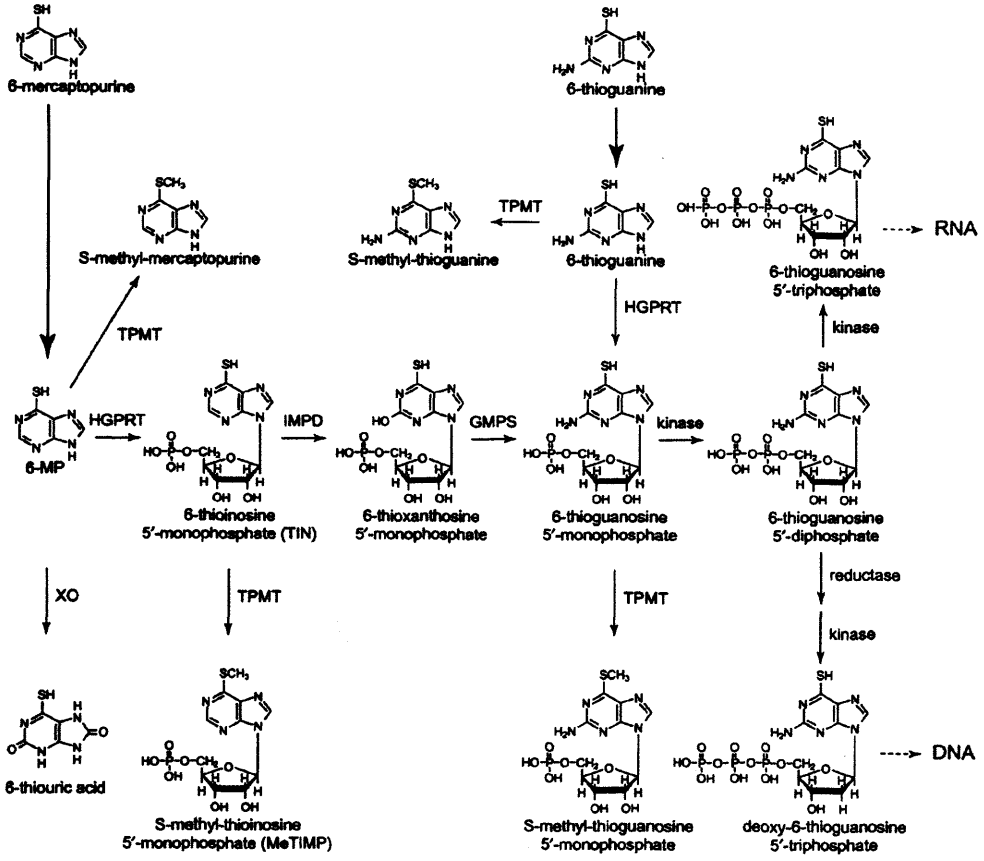

Fig 4.1 Metabolism of 6-MP and 6-TG. Both drugs are incorporated into DNA via the purine salvage pathway. 6-MP is catabolised by xanthine oxidise (XO)and methylation is catalysed by thiopurine methyltransferase (TPMT). GMPS, guanosine monophosphate synthetase. HGPRT, hypoxanthine guanine phosphoribosyl transferase. IPMD, inosine monophosphate dehydrogenase. (Adapted from Aarbakke 1997).

4.1.1 Modes of Action of Thiopurines and Azathioprine

The direct toxicity of 6-TG has been discussed in Chapter 1. The incorporation of 6-TG into DNA has been considered to be the primary immunosuppressive mechanism of Aza. It is proposed that the rapidly dividing precursors of immune effector cells incorporate 6-TG into their DNA, and so suffer its toxic effects. In addition to this, Aza metabolites also inhibit *de novo* purine synthesis. The effect of 6-TG on dNTP synthesis may contribute to immunosuppression, since the dNTP pool of T-cells is normally increased upon their activation (purines 2-fold, pyrimidines up to 8-fold) (Fairbanks et al. 1995), and this is necessary for subsequent immune functions. 6-TdGTP can also alter the synthesis of membrane glycoproteins, including many T-cell receptors critical for their function, although the mechanism behind this activity is not known. 6-TG and 6-MP treatment, in cultured cells and chick embryos, also attenuates angiogenesis (Presta et al. 2002).

More recently, an alternative, and quite distinct, mechanism for the primary immunosuppressive mechanism of Aza has been proposed. In 2003, it was demonstrated that 6-TdGTP can significantly alter signalling pathways in activated T-cells (Tiede et al. 2003; Poppe et al. 2006). Activated T-cells are in a constant state of apoptosis prevention using the Rac-initiated signalling pathway to activate the apoptosis inhibitor bcl-x_L. Rac1 and Rac2 are Rho GTPases which are activated by binding and hydrolysis of a GTP molecule to generate GDP. Exchange of GDP for another GTP molecule is stimulated by the Vav protein. It has been observed that 6-TdGTP can bind to Rac proteins in place of GTP and can be hydrolysed to 6-TdGDP. Vav fails to stimulate the exchange of 6-TdGDP for GTP or 6-TdGTP, thereby inactivating Rac. Hence, the downstream signalling pathway is silenced, and bcl-x_L is not activated, permitting apoptosis. This has the effect of removing T-cells which have been activated, leading to tolerance of the foreign antigens from the graft. This mechanism elegantly proposes a answer to the long standing question of why T-cells are specifically affected by 6-MP, 6-TG or Aza treatment, since several rapidly dividing tissues in the body are unaffected by Aza treatment. It also provides an explanation as to why the levels of 6-

TG found in patients are below those required for disruption of nucleotide synthesis and DNA 6-TG mediated toxicity (Quemeneur et al. 2003).

4.1.2 Structural Effects of 6-TG

6-TG in DNA disrupts the local double helix structure. The thermal stability of 6-TG:C base pairs is lower than that of G:C base pairs (Somerville et al. 2003). Base pairs in duplex DNA are in a constant state of flux between open and closed states (where the base pair is fully formed). A 6-TG:C base pair has been shown to spend more than 17-fold less time in the closed conformation compared to G:C (Bohon et al. 2005). While it has been proposed that this base pairing disruption is largely responsible for the biological effects of 6-TG, this appears unlikely due the plethora of other effects on cellular function that have been observed due to 6-TG, and the large body of evidence implicating MMR in 6-TG cytotoxicity.

4.1.3 6-TG and 6-MP Sensitisation to UV and Ionising Radiation

In 1960, Greer reported that growth of *E. coli* in the DNA base analogue 5-bromouracil (BU) sensitised the bacteria to UV radiation (Greer 1960). This triggered investigations into the UV sensitising effects of base and nucleoside analogues. UV sensitisation by BU and purine analogues was subsequently demonstrated in mammalian cells (Djordjevic et al. 1960; Kaplan et al. 1961). 6-TG and 6-MP were found to sensitise *E. coli* to UV and X-rays This effect was primarily due to 6-TG incorporated into DNA. DNA 6-TG induced X-ray sensitisation required oxygen (Kaplan et al. 1962), and irradiation following thiopurines treatment did not increase lethality under N_2.

Free, unincorporated 6-MP also sensitises cells to UVA radiation (Komeda et al. 1997). uvrA *E. coli* (NER deficient) and recA *E. coli* (recombination, SOS response deficient) strains were particularly sensitive to UVA/6-MP. UVA/6-MP induced the SOS response in wild type cells and mutation was entirely recA dependent. These experiments highlight the ability of thiopurines to interact with UVA to cause potentially cytotoxic and mutagenic DNA lesions. In this particular case, effects are observed even in the absence of incorporation into DNA.

6-TG induced radiosensitisation may also be important clinically. In cohorts undergoing 6-MP treatment for ALL, cranial radiotherapy is often performed prophylactically. An increased incidence of brain tumours, especially glioblastomas, has been reported in these patients (Relling et al. 1999). This combination of treatments has now been removed from clinical use.

4.1.4 Biological Effects of UVA Irradiation

UVA induced DNA damage is described in Chapter 1. In addition to DNA damage, UVA affects a number of cellular processes, many of which involve apoptotic signalling. Many of these effects, including DNA damage, are likely to be relevant clinically, since more UVA passes through the epidermis than UVB, and a substantial proportion of incident UVA can enter the dermis (Lademann et al. 2004). The gene expression profiles for UVA treated cells are currently conflicting. Some groups observe a small of number of expression changes, and others a high number (Koch-Paiz et al. 2004; Wertz et al. 2005). High dose UVA can certainly activate DNA damage signalling pathways, such as the ERK/MAPK pathways (He et al. 2004; Hildesheim et al. 2004; Schieke et al. 2005). These trigger ERK, which provides an anti-apoptotic signal to prevent UVA mediated apoptosis. Exposure to UVA may also affect the rates of DNA repair (Sheehan et al. 2002), and is known to induce the production of melanin, which acts to protect skin against further damage by absorption of UVA (Agar et al. 2005). UVA irradiation also leads to clustering and ligand-independent activation of death and growth receptors at the cell membrane. Recently, it was observed that the caspase-independent AIF (Apoptosis Inducing Factor) apoptotic pathway is activated by UVA (Yuan et al. 2004), as is the Nrf2 pathway (Hirota et al. 2005).

4.1.5 Mutagenicity of UVA

Although UVA is generally accepted as being the least mutagenic of the UV bands, it is moderately mutagenic in cultured cell lines and in rodents (Kino et al. 2005; Pfeifer et al. 2005). UVA mutagenicity may be implicated in the aetiology of malignant melanoma (de Gruijl 1999). There is controversy with regard to the mutation spectrum induced by UVA. An analysis of UVA induced *APRT* mutations in hamster cells demonstrated a 3 to 5 fold increase over the spontaneous mutation frequency after

500kJ/m^2 (Drobetsky et al. 1995). A:T to C:G changes were the most frequent, comprising 37% of the total induced mutations. These were mostly at dipyrimidine sites, and over half were found in a single pyrimidine run in exon 2 of the gene. It has been proposed that CPDs may be responsible for these A:T to C:G transversions (Rochette et al. 2003).

Another study, in mouse embryonic fibroblasts, reported a decrease in A:T to C:G mutations after UVA treatment (180 and 360kJ/m^2)(Besaratinia et al. 2004). The mutation spectrum consisted primarily of G:C to T:A transversions (30%) and small tandem deletions. G:C to T:A mutations were also increased in *E. coli* after UVA irradiation, and the frequency was increased a further 7-fold in an Fpg deficient strain (Palmer et al. 1997). Fpg is responsible for the excision of oxo^{8}G and FapyG, as well as other base lesions, and strongly implicates oxidative DNA damage in the generation of G:C to T:A transversions.

In this chapter I present the work undertaken to decipher the mechanism(s) of 6-TG induced UVA sensitisation. I present data showing that combined 6-TG/UVA treatment is mutagenic, and that the mutation spectrum is different from previously published spontaneous and UVA spectra. 6-TG/UVA is shown to place cells under considerable oxidative stress. The presence of 6-TG in DNA is shown to be a particular hazard during DNA replication at UVA treatment, and induces a novel type of photodamage to the proteins at the replication complex. This is associated with an abrupt inhibition of replication. Finally, I will demonstrate that 6-TG is present at detectable levels in the skin cells of Azathioprine treated patients. These cells are continuously exposed to UVA and the possible implications for skin cancer development in these patients are discussed.

4.2 Results

4.2.1 Quantification of 6-TG Incorporation in DNA

HCT 116 human colon tumour cells were used to study the biological effects of 6-TG/UVA. HCT 116 cells are MMR deficient and can tolerate a high level of DNA 6-TG without suffering direct toxic effects. To measure the level of DNA substitution by

6-TG, HCT 116 cells were cultured in the presence of 6-TG for 48 hours. DNA was extracted, acid hydrolysed, and analysed by RP-HPLC coupled to A_{342nm} and A_{260nm} detection (Fig 4.2A+B). Quantification of 6-TG was performed using the standard curve as described in the Chapter 3. Under these conditions, growth in 1.0μM 6-TG, resulted in substitution of approximately 0.1% of DNA guanine. Over a ten-fold concentration range (0.1 to 1.0μM), substitution of guanine by 6-TG was dependent on the 6-TG dose with which cells were treated (Fig 4.2C). Maximum substitution of 6-TG obtained was 0.1%. All human cell lines used in this work (HCT 116, A2780-SCA5, XP12RO, MRC5-VA) incorporated 6-TG at similar levels, with 0.01% substitution after 48 hours growth in 0.1μM 6-TG

4.2.2 Quantification of 6-TG in Aza Treated Patients

Biopsies of morphologically normal skin were obtained from patients on a standard Azathioprine regimen. Controls from untreated patients were also obtained. DNA from the biopsies was depurinated, and 6-TG quantified by RP-HPLC coupled to A_{342nm} and A_{260nm} detection. In each of the three Aza treated patients, there was approximately 0.02% substitution of DNA guanine by 6-TG (Table 4.1). No signal was obtained in the untreated controls, corresponding to less than 0.007% substitution of DNA guanine.

	Patient A	**Patient B**	**Patient C**	**Patient D**	**Patient E**
Aza(mg/day)	100	50	50	None	None
Guanine(nmoles)	4.5	7.5	7.0	6.0	5.0
6-TG(pmoles)	1.0	1.4	1.6	≤0.4	≤0.4
6-TG(%Guanine)	0.022	0.019	0.023	≤0.007	≤0.008

Table 4.1 Quantification of DNA-6-TG in Skin from Aza Treated Patients

4.2.3 6-TG Sensitises Cells to UVA

Treatment with 1.0μM 6-TG for 48 hours sensitised HCT 116 cells to otherwise non-lethal UVA doses. Without 6-TG, UVA doses up to 30kJ/m^2 were not detectably lethal, nor was 1.0μM 6-TG. After 6-TG treatment, 10kJ/m^2 UVA resulted in greater than 99% lethality (Fig 4.3A). Cell survival after 3.0kJ/m^2 was approximately 20%, and the estimated D_{37} for UVA was 2.5kJ/m^2. The sensitising effect is plotted as a function of DNA guanine substitution by 6-TG in Fig 4.3B.

6-TG sensitisation to UVA was not confined to MMR deficient cells. The fully DNA repair proficient human ovarian carcinoma cell line A2780-SCA5 was grown in a lower 6-TG concentration (0.3μM/48 hours) to avoid MMR-related 6-TG toxicity. Under these conditions, 6-TG substitution of guanine was approximately 0.04%. A2780-SCA5 cells were sensitised to UVA by this treatment. There was no significant difference in the induced UVA sensitivity between A2780-SCA5 and HCT 116 cells. Both cell lines exhibited 20 to 30% survival after 10kJ/m^2 (Fig 4.3C).

6-TG is incorporated into both DNA and RNA. The contribution of DNA 6-TG to the induced UVA sensitivity was determined. HCT 116 cells were treated with the replication inhibitor hydroxyurea (HU) to prevent 6-TG incorporation into DNA but allow substitution of RNA guanine. HU (1mM) was added to cells 30 minutes prior to 6-TG (5μM). Cells were maintained in these conditions overnight, washed, and UVA irradiated. Cells treated with HU showed a diminished UVA sensitivity (Fig 4.3D). Greater than 90% survival was observed following 20kJ/m^2 UVA. In non-HU treated cells, survival was less than 45%. These findings indicate that DNA 6-TG plays a major role in the induced UVA sensitivity

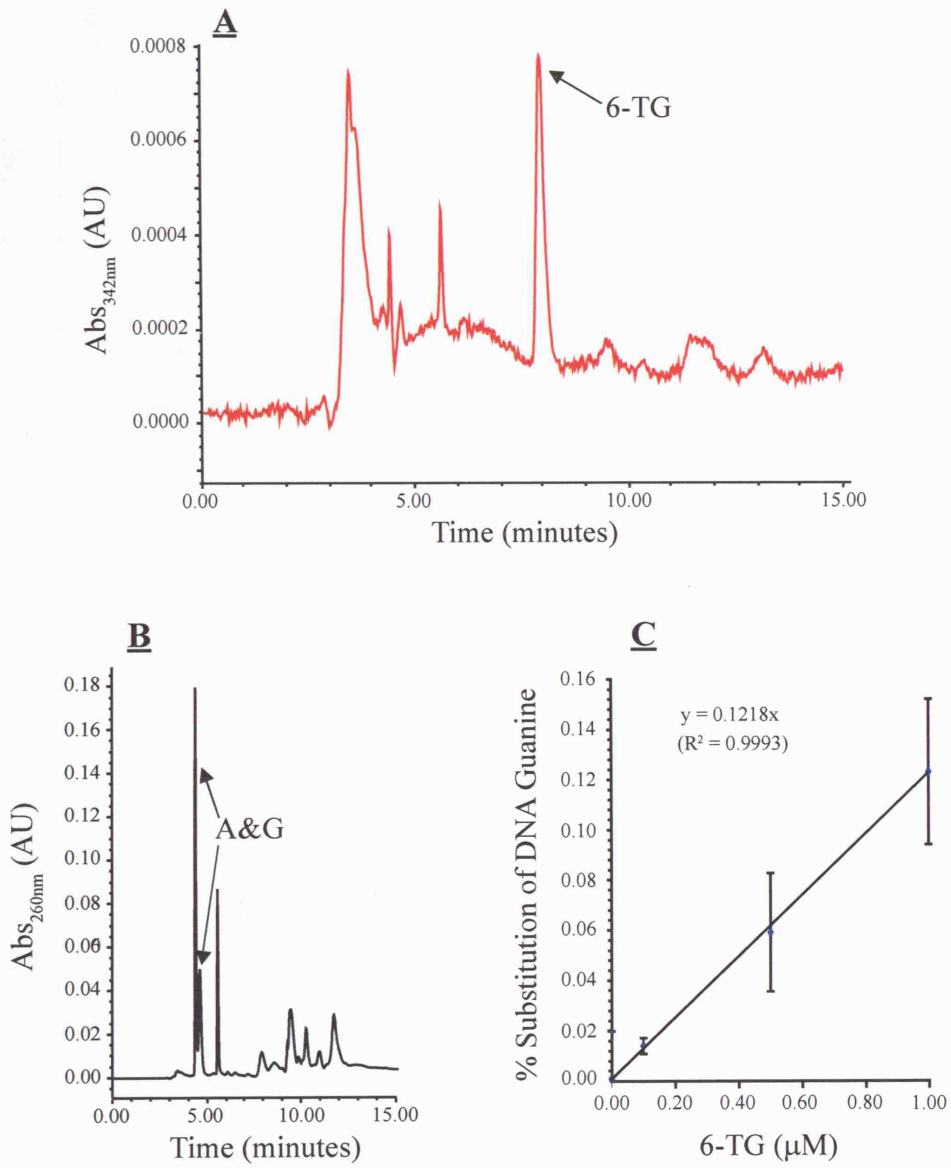

Fig 4.2 Incorporation of 6-TG into DNA in HCT 116. **A** HCT 116 cells were cultured in the presence of 1.0μM 6-TG for 48 hours. Genomic DNA was extracted. DNA extracts were depurinated by acid hydrolysis (0.1N HCl, 70°C, 30 minutes). The depurinated mixture was neutralised and analysed by RP-HPLC coupled to A_{342nm}. 6-TG is the major A_{342nm} peak. **B** A_{260nm} trace of samples from **A**. Adenine and guanine elute early, and are used for quantification of DNA. **C** HCT 116 cells were cultured in the indicated doses of 6-TG, and DNA 6-TG quantified by A_{342nm} after RP-HPLC separation. 6-TG incorporation is dependent on the dose of 6-TG.

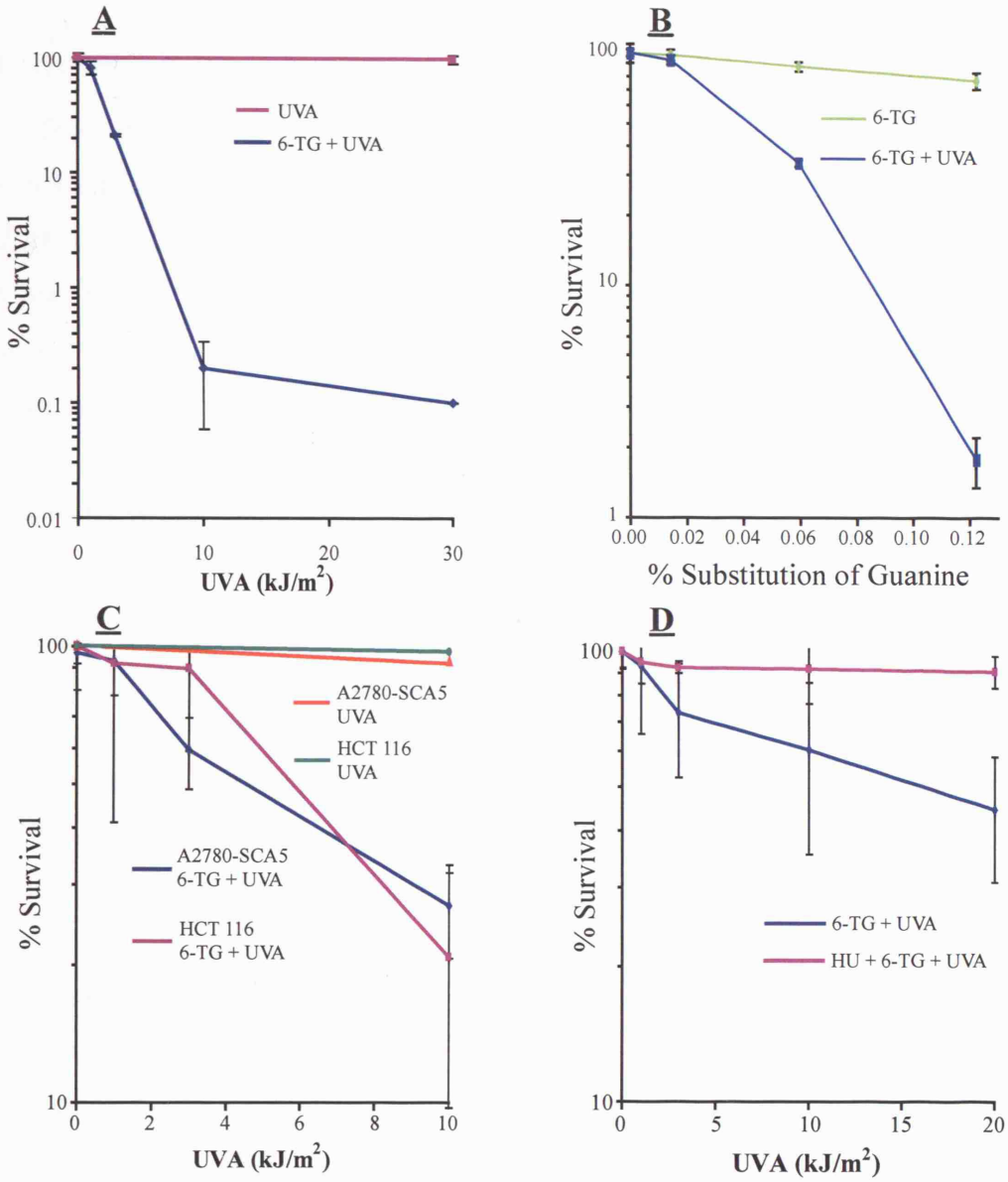

Fig 4.3 6-TG Sensitises Cells to UVA. **A** Treatment with 6-TG sensitises HCT 116 cells to UVA. HCT 116 cells were cultured in the prescence (blue) or absence (pink) of 1.0μM 6-TG for 48 hours and exposed to the indicated dose of UVA. **B** 6-TG induced sensitisation to UVA is dependent on the level of 6-TG incorporation. HCT 116 cells were cultured in the presence of 0, 0.1, 0.5 and 1.0μM 6-TG and exposed to 10kJ/m^2 UVA (blue) or left unirradiated (green). Before UVA, DNA was extracted from a sample of cells and DNA 6-TG quantified by RP-HPLC coupled to A_{342nm}. **C** MMR does not play a role in 6-TG induced UVA sensitivity. HCT 116 (MMR-) and A2780-SCA5 (MMR+) cells were treated with 0.3μM 6-TG for 48 hours and exposed to the indicated dose of UVA. Both cell lines are similarly sensitised to UVA. **D** DNA 6-TG is required for 6-TG induced UVA sensitivity. HCT 116 cells were treated with 5.0μM 6-TG overnight in the presence (pink) or absence (blue) of the replication inhibitor hydroxyurea and UVA irradiated. In all cases survival was determined by clonogenic assay. Results are average of three experiments, in quadruplicate.

4.2.4 Synergistic Mutagenicity of 6-TG and UVA

The potential mutagenicity of combined 6-TG/UVA was examined at the *APRT* locus of Chinese hamster cells. These cells were used as they are hemizygous for the *APRT* gene. Preliminary experiments indicated that in CHO D422 cells neither 1.0kJ/m^2 UVA nor 0.1μM 6-TG caused detectable cell death. The combination of these doses was also non-lethal (Appendix Fig 7.6). Neither 6-TG nor UVA alone increased the mutation frequency over the spontaneous (4.1 x 10^{-6}, n = 5, range: 2.1 x 10^{-6} to 6.0 x 10^{-6}) (P=0.1/0.13 for 6-TG and UVA respectively). Combined, 6-TG and UVA induced a 3.5 fold increase over spontaneous frequency (Fig 4.4A). This was a significant increase (n = 5, range: 2.4 to 4.8, P = 0.005).

In order to investigate the types of mutation induced by 6-TG/UVA, the *APRT* mutation spectrum was determined. After 6-TG/UVA treatment (0.1μM, 1.0kJ/m^2), genomic DNA was extracted from 44 independent *APRT* mutants selected by growth in 8-azaadenine, and the *APRT* locus sequenced in two fragments after amplification of the *APRT* locus by PCR (Fig 4.4A and Appendix Fig 7.7). The first fragment contained exons 1 and 2, and the second exons 3, 4 and 5. The full mutation spectrum is presented in Appendix Table 7.1.

Of the 44 *APRT* mutants sequenced, 40 contained single nucleotide changes. There were 4 deletions (2 single base deletions, 1 codon deletion, and one 20 base pair deletion). Nine mutations were found in exon 1. Two of these were in the start codon (A394G, A394C). A G to T mutation (G400T) resulted in the introduction of a stop codon. There were three T to C mutations at position 447. The 20bp deletion affected bases 466 to 486. Thirteen mutations were found in exon 2. All of these were point mutations. C640T introduced a premature stop codon. Four A703T mutations were found. An apparently silent mutation was also found at position 708 (A708C), and this may affect RNA splicing as it is predicted to be within an exonic splice enhancer. The remaining mutations all resulted in amino acid changes.

Seven *APRT* mutants contained point mutations in exon 3. Three of these were G1698T mutations, in which methionine replaced arginine. A mutation in the intron

between exons 3 and 4 (T1952C) was also found. This maps to a putative splice site. Exon 4 contains 6 mutations. One of these is a codon deletion, resulting in the loss of a tyrosine. Two mutants show the G2031C mutation. An intronic mutation (C2157G) was also found, and like the previous intronic mutation, is at a putative splice site. The remaining seven mutations were found in exon 5. All were point mutations. One of these, A2305G disrupts the stop codon, replacing it with a tryptophan codon

The frequency of each class of mutation was determined. These data are shown in Table 4.2. This spectrum was compared to the previously published spectra of spontaneous mutations in *APRT* (de Jong 1988; Phear 1989) Comparisons were made using a paired t-test. For most mutations, there was no change in frequency compared to the spontaneous spectra. There was a significant increase in A to C and G to C transversions (p-values of 0.005 and 0.02 respectively). There was also a decrease in GC to AT transitions (p-value of 0.02). When compared to previously published UVA induced mutation spectra, A to C tranversions were significantly less frequent, indicating these may be a result of direct absorption of UVA by DNA.

Mutation	**Spontaneous** (de Jong 1988)	**UVA** (Drobetsky et al. 1995)	**6-TG + UVA**	**Corrected 6-TG + UVA**
GC to AT	0.37 (*0.02*)	0.22 (*0.8*)	0.18	0.63
AT to GC	0.08 (*0.08*)	0.09 (*0.2*)	0.18	0.63
A to T	0.03 (*0.2*)	0.02	0.09	0.32
G to T	0.13 (*0.6*)	0.04 (*0.4*)	0.09	0.32
G to C	0.08 (*0.02*)	0.09	0.23	0.8
A to C	0.02 (*0.005*)	0.37	0.14	0.49
Frameshift	0.06 (*0.1*)	0.02	0.04	0.14
Other	0.22 (*0.009*)	0.15	0.05	0.18

Table 4.2 Spontaneous, UVA and 6-TG + UVA Mutation Spectra (p-values compared to 6-TG + UVA in *italics*, within 95% confidence interval are underlined)

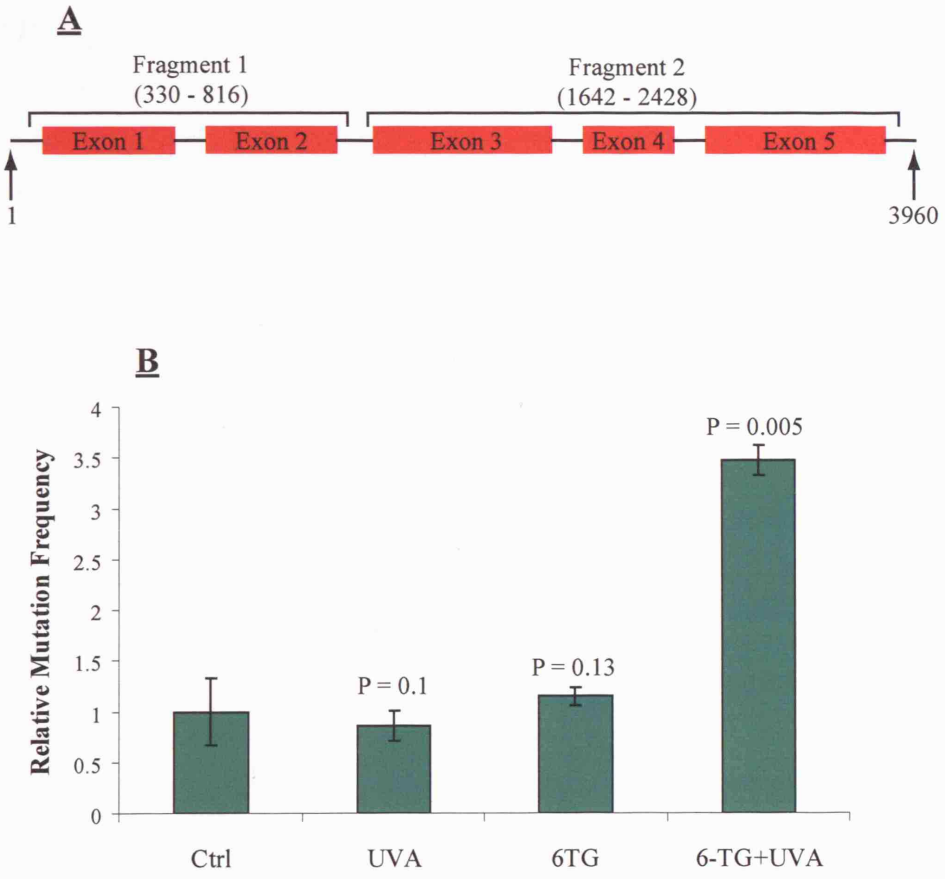

Fig 4.4 6-TG and UVA are Synergistically Mutagenic. **A** Structure of the APRT locus in CHO D422 cells. Sequence numbered according to GenBank X03603. Positions of fragments amplified by PCR and sequenced are highlighted. **B** CHO D422 was cultured for 48 hours in 0.1μM 6-TG and exposed to 1.0kJ/m^2 UVA After 7 days recovery in E4 medium supplemented with 10% FCS, cells were plated out at a density of 1.0 x 10^6 cells/plate in medium containing 4.0mM 8-azaadenine, for selection of APRT$^-$ mutants. Mutation frequency is expressed as the fold increase over spontaneous frequency at this locus. Spontaneous frequency was 4.1 x 10^{-6}. P-values were calculated by a student's paired t-test, n=5.

4.2.5 6-TG/UVA Treatment Generates Reactive Oxygen Species

In vitro, 6-TG is oxidised by singlet oxygen produced on UVA irradiation. I investigated whether DNA 6-TG could act as a source of intracellular ROS on exposure to UVA. HCT 116 cells cultured in the presence of 1.0μM 6-TG for 48 hours were labelled with the ROS reactive dye CM-H_2DCFDA prior to exposure to 3.0kJ/m^2 UVA. This dye is activated by cellular esterases and produces green fluorescence on reaction with reactive oxygen species. Cells were analysed by FACS. A low background fluorescence was observed in untreated cells (Fig 4.5A). Neither 6-TG nor UVA alone resulted in detectably increased intracellular ROS levels (Fig 4.5C and D). Treatment with 0.03% H_2O_2, a known source of ROS, increased the mean fluorescence intensity almost 10 fold over background levels (Fig 4.5B). Combined 6-TG/UVA treatment caused a similarly dramatic increase in intracellular ROS (Fig 4.5E). Cells were also visualised by fluorescence microscopy after this treatment. This confirmed a substantial increase in ROS (Fig 4.6).

ROS production increased as a function of 6-TG concentration. HCT 116 cells were cultured for 48 hours in 6-TG concentrations ranging from 0.01μM to 1.0μM. They were then labelled with CM-H_2DCFDA, irradiated with 3.0kJ/m^2 UVA and fluorescence measured by FACS. The FACS profiles are shown in Fig 4.7A.

Since 6-TG is incorporated into both DNA and RNA, the separate contribution of DNA 6-TG to ROS production was examined. HCT 116 were treated with 1.0mM HU, or 10μM Aphidicolin (both replication inhibitors) for 30 minutes before addition of 6-TG to a final concentration of 5.0μM. Cells were maintained in these conditions overnight. HU or Aphidicolin treatment reduced the mean UVA-induced fluorescence intensity observed by FACS (Fig 4.7B and C). Inspection of these cells by fluorescence microscopy revealed that exclusion of 6-TG from DNA selectively diminished nuclear ROS production, as confirmed by nuclear staining with DAPI (Fig 4.7D).

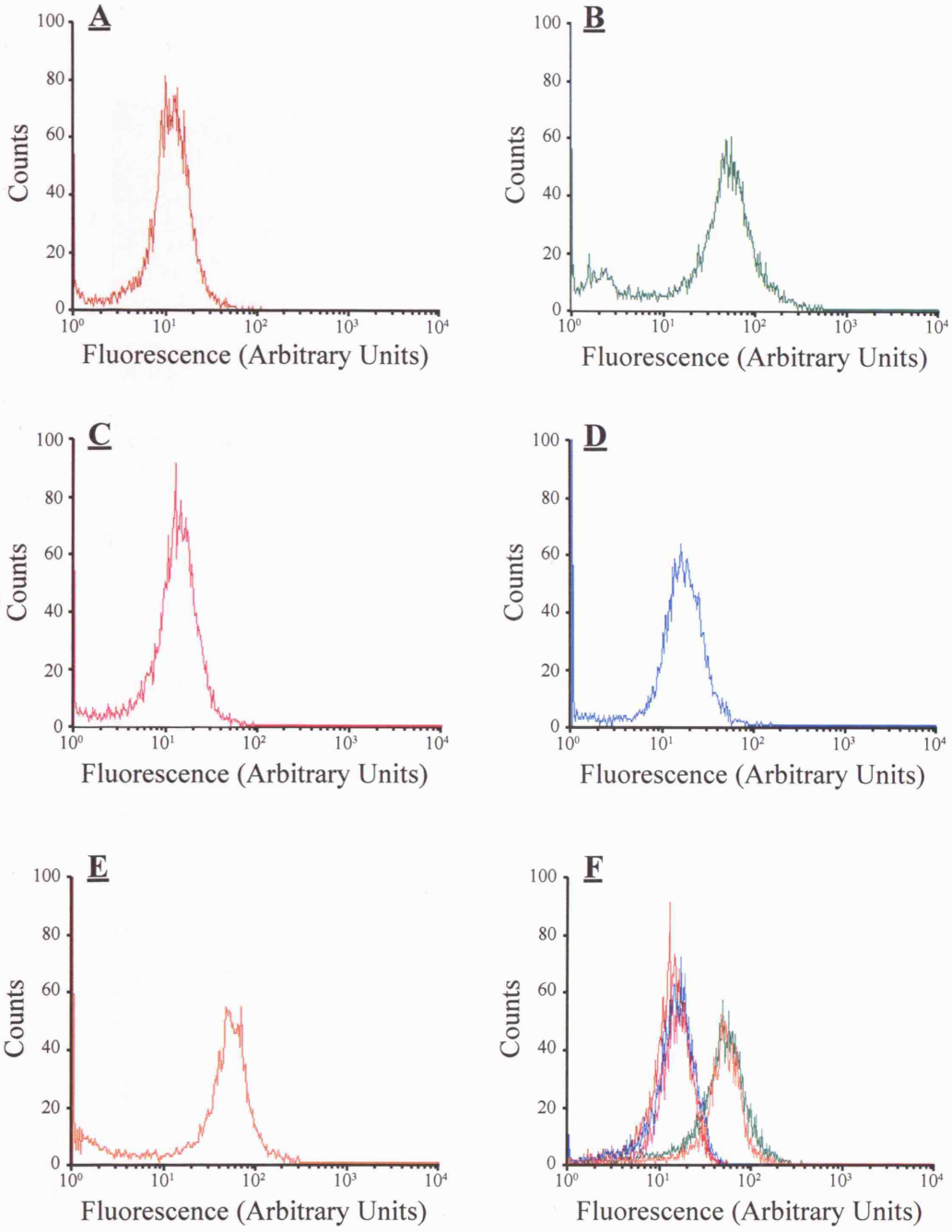

Fig 4.5 UVA and DNA 6-TG Combine to Generate ROS. HCT 116 cells cultured in the presence of 1.0μM 6-TG for 48 hours were labelled with the ROS reactive dye CM-H_2DCFDA, irradiated with 3.0kJ/m^2 UVA, and analysed by FACS. Fluorescence is due to ROS. **A** Untreated cells, background fluorescence. **B** H_2O_2 treated cells. Mean fluorescence intensity increases 10-fold over background. **C** & **D** Neither 6-TG nor UVA alone lead to detectably increased levels of ROS. **E** Combined 6-TG UVA treatment increases mean fluorescence intensity. **F** Traces A through E, overlayed.

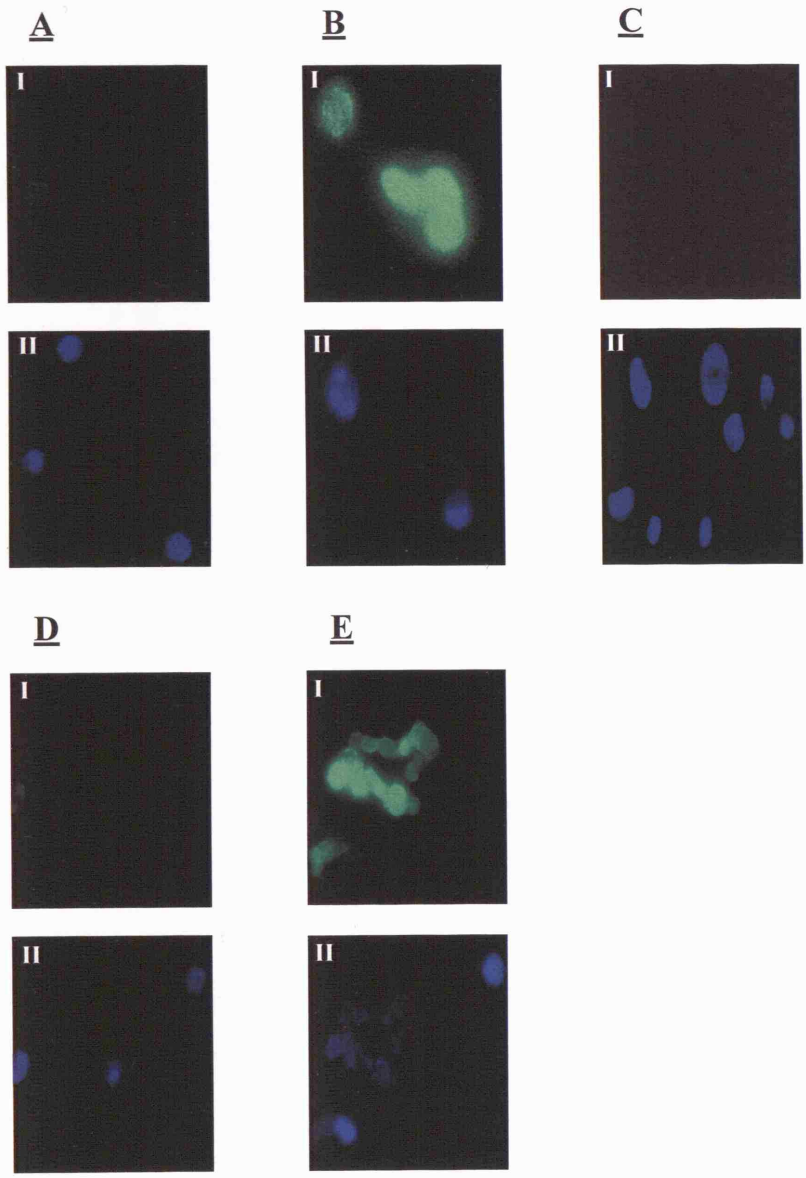

Fig 4.6 Fluorescence Microscopy Analysis of 6-TG/UVA Induced ROS in HCT 116. HCT 116 cells cultured in 1.0μM 6-TG for 48 hours were labelled with CM-H_2DCFDA. Cells were exposed to 3.0kJ/m^2 UVA, counterstained with DAPI and visualised by fluorescence microscopy. Nuclei were visualised using blue fluorescence of DAPI (II), and ROS visualised by green fluorescence (I) **A** Untreated cells show a low level of background fluorescence. **B** Treatment with 0.03% H_2O_2 produces high levels of intracellular ROS. **C** and **D** Neither 1.0μM 6-TG (C) nor 3.0kJ/m^2 UVA (D) produce a detectable increase in ROS. **E** 6-TG/UVA generates ROS.

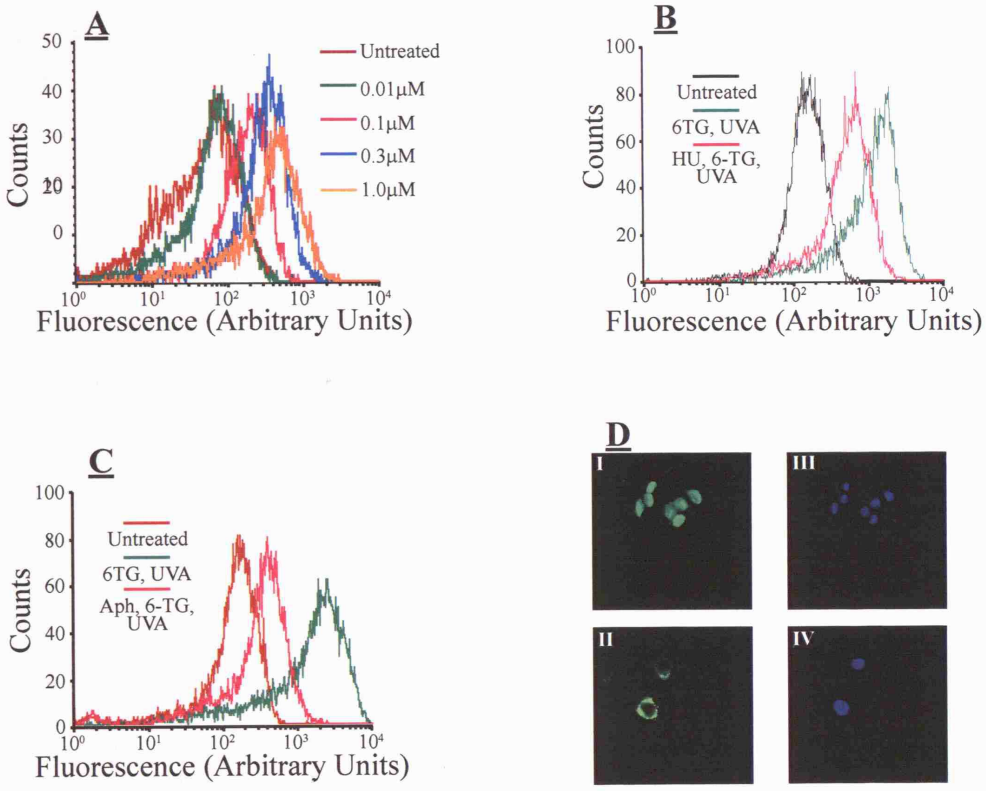

Fig 4.7 DNA 6-TG Dependence of ROS Production in HCT 116. **A** 6-TG UVA induced ROS production is dependent on 6-TG dose. HCT 116 cells cultured in the indicated concentrations of 6-TG for 48 hours, were labelled with CM-H_2DCFDA, exposed to 3.0kJ/m^2 UVA and analysed by FACS. **B** DNA 6-TG plays a role in 6-TG UVA induced ROS production. HCT 116 was treated with 5.0μM 6-TG overnight in the presence or absence of 1.0mM hydroxyurea (HU). Cells were labelled with CM-H_2DCFDA, exposed to 3.0kJ/m^2 UVA, and analysed by FACS. **C** Performed as in B but with 10μM Aphidicolin (Aph) in place of HU. **D** Exclusion of 6-TG from DNA diminishes nuclear ROS after UVA. HCT 116 were treated as in B. After UVA nuclei were stained using DAPI. Cells were visualised by fluorescence microscopy. Green fluorescence indicates ROS (**I** and **II**), blue fluorescence indicates nuclei (**III** and **IV**). **I** and **III**, 6-TG + UVA, **II** and **IV**, HU + 6-TG + UVA.

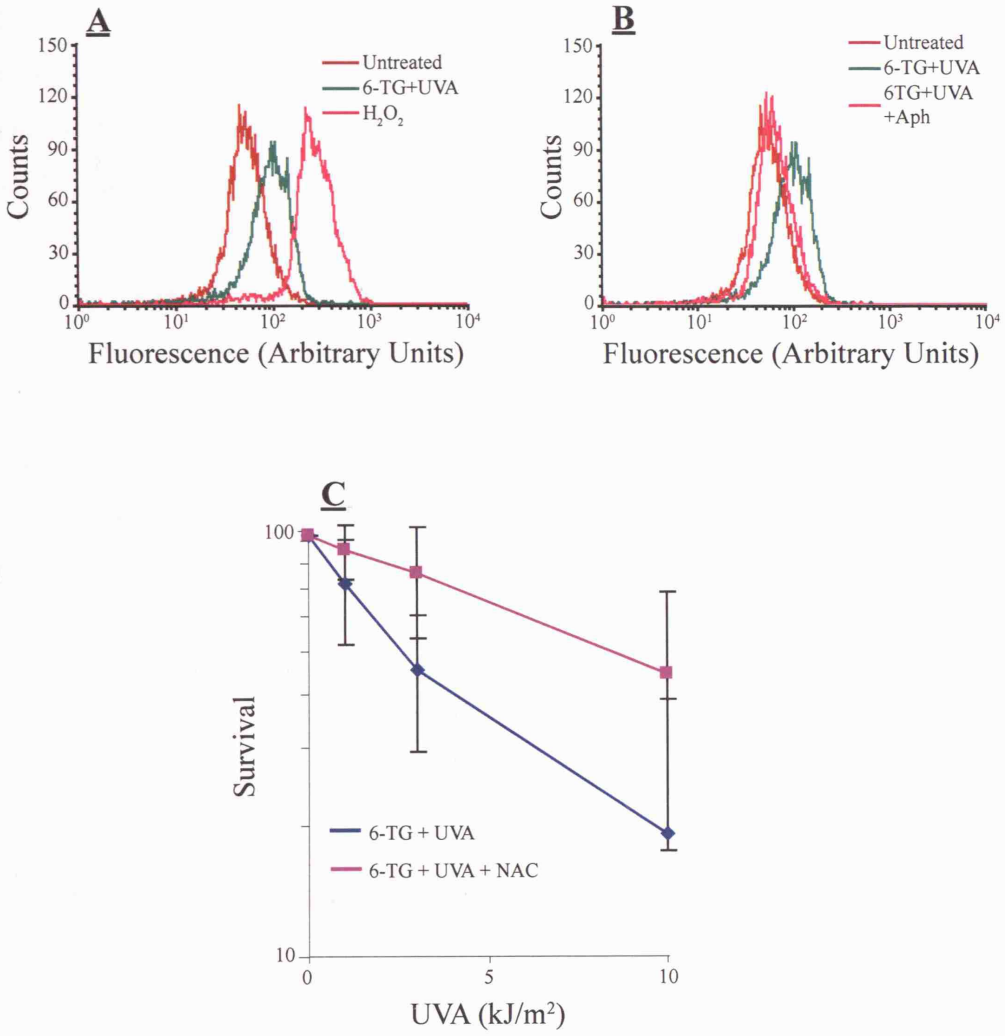

Fig 4.8 6-TG/UVA Induced ROS Production in CHO D422 Cells . A Sublethal, but mutagenic 6-TG UVA treatment induces measurable ROS. CHO D422 cells were cultured for 48 hours in the presence of 0.1μM 6-TG and labelled with CM-H_2DFCDA. Following exposure to 1.0kJ/m^2 UVA, they were analysed by FACS. **B** DNA 6-TG is responsible for most of the ROS induction in CHO D422. Cells were treated with 1.0μM 6-TG overnight in the presence or absence of 10μM Aphidicolin (Aph) to prevent 6-TG incorporation into DNA, and labelled and analysed as in A. **C** Induction of ROS plays a role in 6-TG induced UVA sensitivity. CHO D422 was treated with 0.1μM 6-TG for 48 hours. Cells were exposed to UVA after a 3 hour incubation with 10mM NAC. Survival was determined by clonogenic assay. Data shown is the average of three independent experiments.

The 6-TG/UVA treatments used to investigate ROS production in HCT 116 cells resulted in significant lethality (70%). CHO D422 was used to test whether ROS production could be observed after exposure to the non-lethal treatments that had been used to induce mutations. CHO D422 cells were treated under the conditions described for *APRT* mutant isolation (0.1μM 6-TG, 1.0kJ/m^2 UVA). Before irradiation, cells were labelled with CM-H_2DCFDA, and analysed post-UVA by FACS. This 6-TG/UVA combination caused a 4-fold increase in mean fluorescence intensity over untreated controls (Fig 4.8A). Again, neither 6-TG nor UVA alone induced ROS production. In this case, prevention of 6-TG incorporation by Aphidicolin reduced mean fluorescence intensity to background levels (Fig 4.8B). These cells were also visualised by fluorescence microscopy (Appendix Fig 7.8). Thus, the 6-TG/UVA combination used to induce *APRT*, mutations was also a significant source of ROS in DNA.

The contribution of induced ROS to the lethality of 6-TG UVA was investigated by the use of antioxidants. CHO D422 cells were treated with 0.1μM 6-TG for 48 hours and were incubated with the anti-oxidant NAC for three hours before UVA irradiation. Survival was determined by clonogenic assay. Inclusion of NAC in medium before irradiation afforded measurable protection from lethality (Fig 4.8C). At a UVA dose of 10kJ/m^2, survival was increased 3-fold, from 15% to 45%.

4.2.6 Potential Repair of 6-TG/UVA Photodamage

6-TG and UVA combine to produce the bulky DNA lesion G-6-SO_3. Nucleotide excision repair (NER) removes a wide variety of similar lesions. A possible role for NER in the repair of potentially lethal 6-TG/UVA photoproducts was investigated using the SV40 transformed XPA cell line XP12RO. As a repair proficient control, the similarly transformed cell line MRC5-VA was used. Cells were cultured for 48 hours in 0.5μM 6-TG, a non-lethal concentration for both XPA and control cells. They were then UVA irradiated, and survival determined by clonogenic assay. The sensitivities of the NER proficient and deficient cells were similar. After 10kJ/m^2 UVA, XP12RO and MRC5-VA cells showed around 2.0% survival (Fig 4.9A). Since UVA sensitivity is related to the extent of DNA substitution by 6-TG, DNA 6-TG levels in the two cell

lines was compared. At a 6-TG dose of 1.0μM, both XP12RO and MRC5-VA substituted around 0.1% of guanine with 6-TG. Because XP12RO was not hypersensitive to 6-TG/UVA, its XP phenotype was confirmed in a separate experiment. XP12RO cells were, as expected, more sensitive to UVC than MRC5-VA. Their D_{37} values were 0.8J/m^2 and 7.0J/m^2 respectively (Fig 4.9B). It appears that NER is not significantly involved in the excision of any potentially cytotoxic 6-TG UVA photoproducts. The survival of XP12RO and MRC5-VA is also very similar to that of HCT 116 and A2780-SCA5 cells (Fig 4.3).

BER removes a number of oxidised DNA bases. Reaction of 6-TG with UVA leads to the production of singlet oxygen, which may oxidise guanine bases. The formation of oxidised guanine may play a more important role than the formation of G-6-SO_3, although this is itself an oxidation product. Since oxidised guanine (oxo^{8}G) is removed by the OGG1 DNA glycosylase, I attempted to examine the sensitivity of Ogg1$^{-/-}$ mouse embryonic fibroblasts (MEF) to 6-TG/UVA. Surprisingly, Ogg1 deficient F1.2 cells proved to be extremely resistant to 6-TG concentrations up to 30μM (Fig 4.9C). For the heterozygous (Ogg1$^{-/+}$) F11.1 cells the D_{37} for 6-TG was 1.5μM. When DNA 6-TG was quantified from these cells, F11.1 showed 0.02% substitution of guanine after growth in 0.1μM 6-TG whereas no 6-TG was detected in DNA from F1.2 cells after the same treatment. This suggests that F1.2 cells have a deficiency in the HPRT pathway required for 6-TG incorporation into DNA, or have upregulated levels of 6-TG catabolic enzymes. Whatever the reason, these cells were clearly unsuitable for the study of the biological effects of 6-TG/UVA.

Since the potential contribution of OGG1 to 6-TG/UV lethality could not be analysed in the Ogg1$^{-/-}$ cell line, a preliminary investigation was carried out *in vitro*. A UVA irradiated 18mer oligonucleotide containing a single 6-TG was used as a substrate for two candidate BER glycosylases. The *E. coli* enzyme Fpg (MutM) is a homologue of human OGG1. Fpg is responsible for the removal of oxidised purines from DNA, primarily oxo^{8}G and FaPy products (discussed in Chapter 1). After cleavage of the base-sugar bond, Fpg also cleaves the sugar-phosphate DNA backbone, resulting in a single strand nick. Labelling of an Fpg substrate containing synthetic oligonucleotide with ^{32}P allows this second cleavage to be observed by autoradiography after gel electrophoresis,

as the ^{32}P labelled cleavage product migrates faster through a polyacrylamide gel. As a positive control, an oligonucleotide of the same sequence, but with an oxo^{8}G in place of the 6-TG was also synthesised.

Irradiation with 50kJ/m^2 UVA was found to convert the majority (>90%) of 6-TG in the oligonucleotide to G-6-SO_3, as determined by RP-HPLC coupled to A_{342nm} and fluorescence detection. When this UVA irradiated 6-TG oligonucleotide was annealed to a complementary oligonucleotide and incubated with Fpg, no product of increased mobility on PAGE was observed (Fig 4.10B) The control oxo^{8}G containing oligonucleotide was efficiently cleaved by Fpg, resulting in a ^{32}P labelled 12mer. No cleavage was observed with a G containing oligonucleotide. UVA itself did not affect cleavage of the G or oxo^{8}G oligonucleotides. A UVA dose response was performed, and it was found that none of the UVA doses tested led to detectable Fpg activity on a 6-TG oligonucleotide (Fig 4.10C). Irradiation in the presence of free 6-TG as a source of ROS was performed using 6-TG and oxo^{8}G oligonucleotides. There was still no Fpg mediated cleavage observed with the 6-TG oligonucleotide, while cleavage of an oxo^{8}G oligonucleotide was unaffected (Fig 4.10D). These results suggest that G-6-SO_3 is not a substrate for Fpg. It is possible that the ROS generated by 6-TG/UVA could lead to oxidation of the normal DNA bases. To investigate this possibility, the complementary strand to the 6-TG containing oligonucleotide was ^{32}P radiolabelled and Fpg activity after UVA determined. Again, no cleavage by Fpg was observed (Fig 4.10E).

A second candidate BER glycosylase, Aag, was also tested. Aag acts on a number of alkylkated purines and inosine (hypoxanthine). Unlike Fpg, Aag does not possess an intrinsic AP lyase activity, and does not cleave the DNA backbone after removal of the altered base. After incubation with Aag, oligonucleotides were subsequently incubated with *E. coli* EndoIV, which cleaves the sugar-phosphate backbone at AP sites. Apart from this additional step, experiments with Aag were performed as described for Fpg. An oligonucleotide with inosine in place of 6-TG was used as the positive control. After UVA, cleavage of guanine and inosine containing oligonucleotides was unaffected. UVA irradiation of the 6-TG oligonucleotide did not generate a substrate for Aag (Fig 4.11).

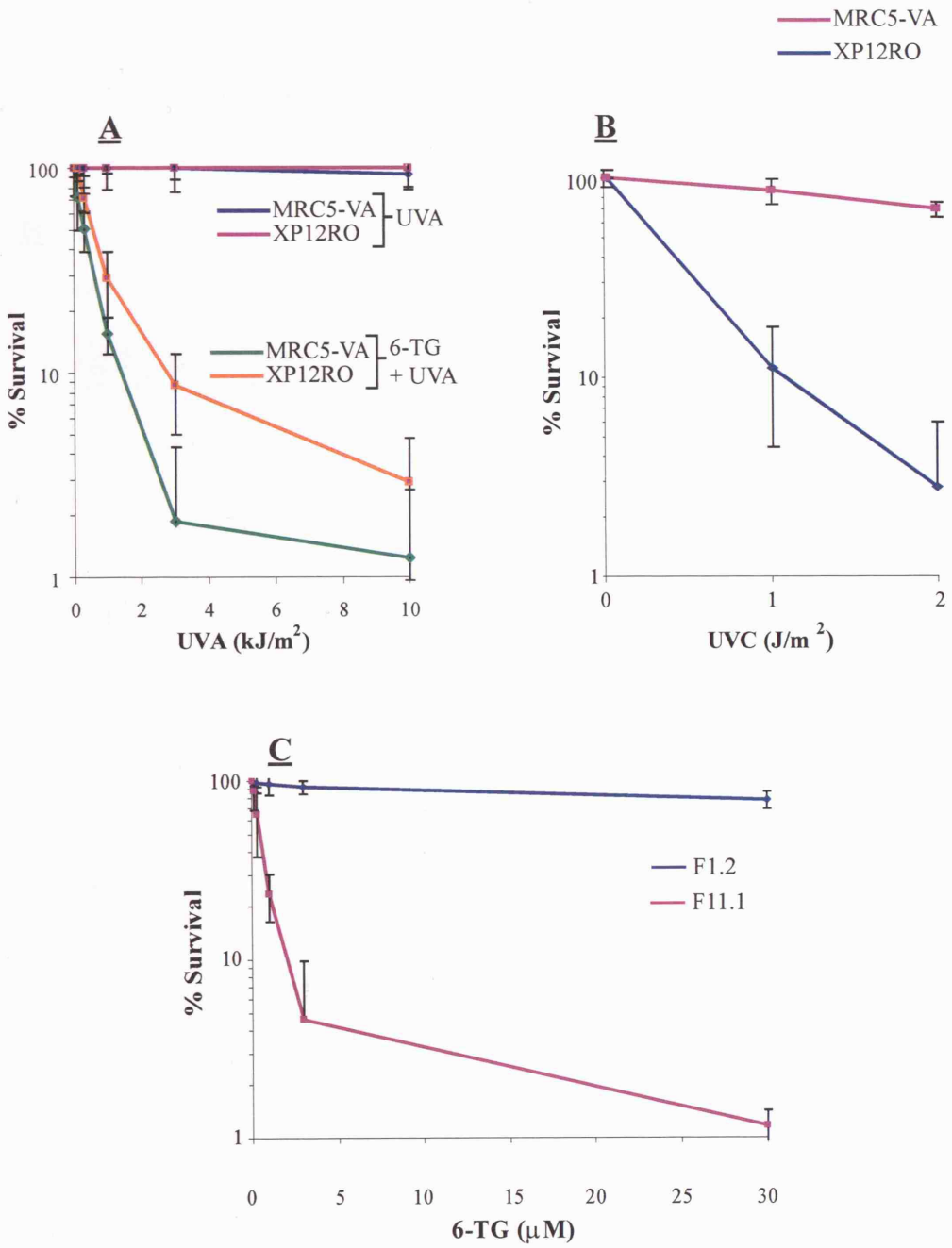

Fig 4.9 NER and Excision of Lethal 6-TG/UVA Photodamage. **A** NER deficient cells are not hypersensitive to 6-TG UVA. XP12RO (NER-) and MRC5-VA (NER+) cells were cultured for 48 hours in 0.5μM 6-TG, UVA irradiated, and survival determined by clonogenic assay. **B** Confirmation of NER deficient XP phenotype of XP12RO. XP12RO and MRC5-VA cells were irradiated with UVC as indicated. Survival was determined by clonogenic assay. **C** $OGG1^{-/-}$ F1.2 cells are highly resistant to 6-TG. F1.2 and wild type F11.1 cells were grown in the presence of 6-TG as indicated for 10 days. Survival was measured by clonogenic assay. Data shown is average of three independent experiments.

A

TOP 5′-CTAATCTTAAT*TAACAC-3′

BOT 5′-GATTAGAATTACATTGTG-3′

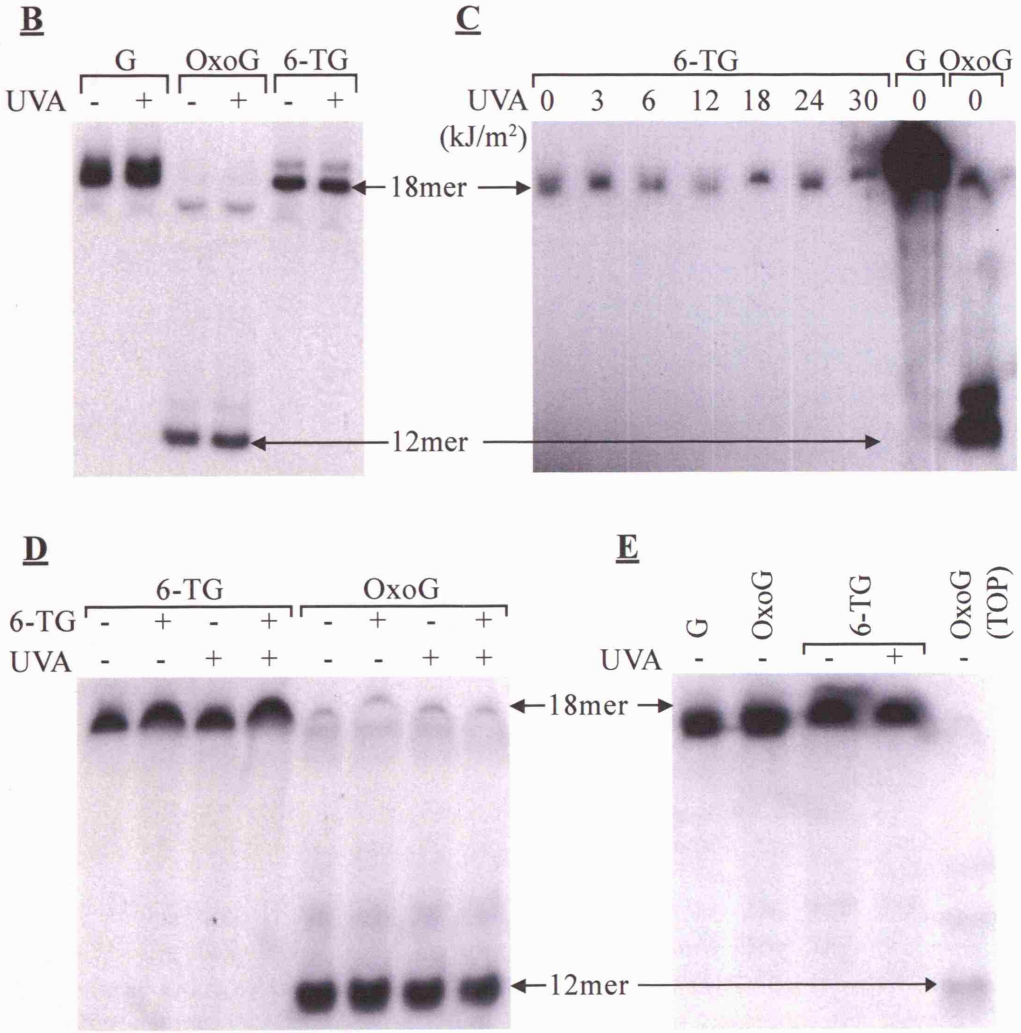

Fig 4.10 Fpg Activity on UVA Irradiated 6-TG Containing Oligonucleotides. Oligonucleotides used for these experiments are shown in **A**. * in TOP represents G, 8-OxoG or 6-TG. Oligonucleotides were annealed to BOT prior to UVA irradiation. Fpg activity results in cleavage of the lesion containing 18mer oligonucleotide into a ^{32}P labelled 12mer, visualised by autoradiography after separation by electrophoresis. TOP is labelled in B, C, and D. BOT is labelled in E **B** There is no detectable Fpg activity on UVA irradiated 6-TG conatining oligonucleotide. ^{32}P labelled oligonucleotide was exposed to 50kJ/m^2 UVA. **C** Fpg activity is not observed at low UVA doses. **D** Irradiation of oligonucleotide in a solution of 6-TG does not yield an Fpg recognised product. The ^{32}P labelled oligonuclotide was UVA irradiated (50kJ/m^2) in a solution of 0.1mM 6-TG. **E** Fpg recognisable damage does not occur in the complementary BOT strand after UVA irradiation. BOT was ^{32}P labelled prioir to annleaing to TOP. Labelled oligonucleotide was exposed to 50kJ/m^2 UVA and Fpg activity assayed.

A

TOP 5′-CTAATCTTAAT*TAACAC-3′

BOT 5′-GATTAGAATTACATTGTG-3′

B

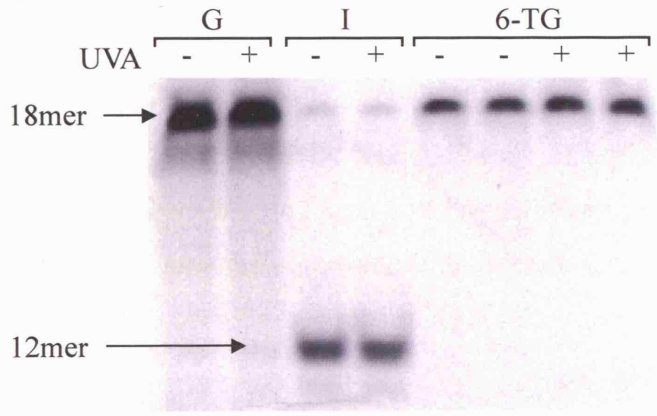

Fig 4.11 Aag Activity on UVA Irradiated 6-TG Containing Oligonucleotides. Oligonucleotides of the sequence shown in **A** were used for these experiments. * represents guanine (G), inosine (I) or 6-TG. TOP oligonucleotides were 5' ^{32}P labelled and after Aag incubation, were incubated with *E. coli* Endonuclease IV to cleave the Aag products. Aag activity was visualised by autoradiogram after separation of products by electrophoresis. **B** No Aag activity was observed on UVA irradiated 6-TG containing oligonucleotides. ^{32}P labelled oligonucleotides were exposed to 50kJ/m^2 UVA irradiation, and Aag activity assayed.

4.2.7 Effects of 6-TG/UVA on Replication

Work performed by my colleagues Dr. Conal Perrett and Dr. Beatriz Montaner has shown that UVA irradiation of 6-TG treated cells causes a rapid and substantial decrease in DNA replication. Using a simple primer extension assay, Dr. Perrett has also shown that *in vitro* G-6-SO_3 acts as block to the exo$^-$ Klenow fragment of *E. coli* DNA polymerase I (PolI). This block is overcome by translesion synthesis (TLS) using human Polη or a similar archaeal Y-family polymerase (DPO4). TLS involves switching from the replicative to a TLS polymerase, which, as described in Chapter 1, involves mono-ubiquitination of PCNA.

Based on these observations, I investigated whether PCNA becomes mono-ubiquitinated after 6-TG/UVA treatment. In a control experiment, HCT 116 cells were exposed to 10J/m^2 UVC and incubated for various times. Samples were analysed by SDS-PAGE followed by Western blotting with a PCNA antibody. At 3 hours post UVC, a slow migrating form of PCNA was observed, with an estimated molecular weight of 40kDa (Fig 4.12A). This form corresponds to mono-ubiquitinated PCNA ($PCNA^{Ubq}$).

I next examined whether 6-TG or UVA separately induced PCNA mono-ubiquitination, Extracts of HCT 116 cells cultured in 1.0μM 6-TG for 48 hours or exposed to 3.0kJ/m^2 UVA and allowed to recover in fresh medium for various times were analysed by SDS-PAGE followed by Western blotting. No slow migrating PCNA band was seen up to 9 hours after UVA irradiation or after 6-TG treatment (Fig 4.12B). Combined 6TG/UVA did induce PCNA mono-ubiquitination, however, and a band migrating at the position of $PCNA^{Ubq}$ could be seen 3 hours after irradiation and persisted for up to 9 hours (Fig 4.12C).The formation of mono-ubiquitinated PCNA was dependent on the 6-TG concentration and approached maximal at 5nM (Fig 4.13A). At higher 6-TG concentrations the level of $PCNA^{Ubq}$ did not increase further. This 40kDa product was confirmed as mono-ubiquitinated PCNA by immunoprecipitation followed by Western blotting with antibodies against PCNA and ubiquitin (Fig 4.13B). Similar results were obtained with the CEM leukaemia cell line.

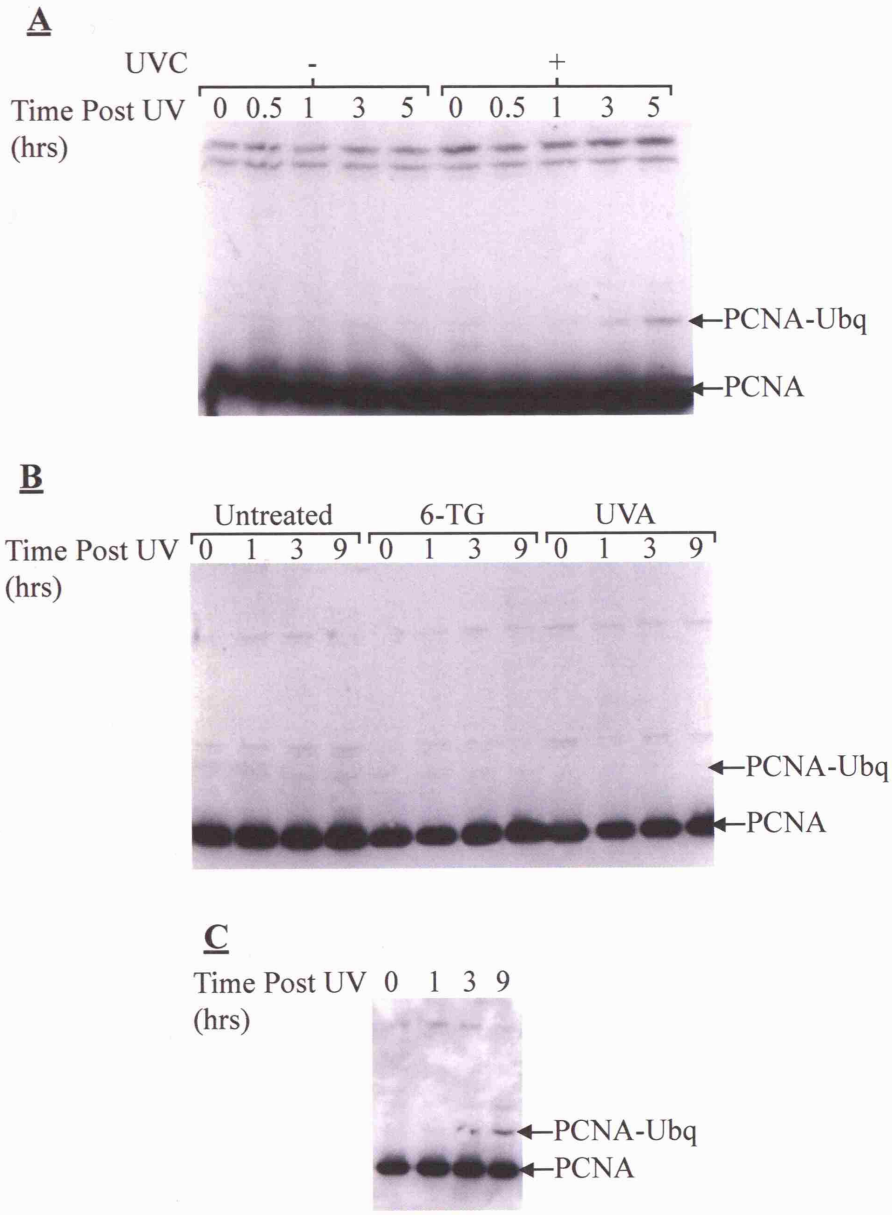

Fig 4.12 PCNA Modification after 6-TG/UVA. A PCNA mono-ubiquitination in UVC irradiated HCT 116 cells. HCT 116 cells were exposed to 10J/m^2 UVC, allowed to recover in fresh E4 medium. At the indicated timepoints cells were harvested, and analysed by Western blotting with an anti-PCNA antibody. **B** Neither 6-TG nor UVA alone induce PCNA mono-uniquitination. Extracts from HCT 116 cells grown in the presence or absence of 1.0μM 6-TG for 48 hours or UVA irradiated with 3.0kJ/m^2 were analysed as above. **C** 6-TG/UVA treatment induces PCNA mono-ubiquitiaton. HCT 116 cells were cultured in the presence of 1.0μM 6-TG for 48 hours and irradiated with 3.0kJ/m^2 UVA. Extracts were prepared at the indicated timepoints and analysed as in A.

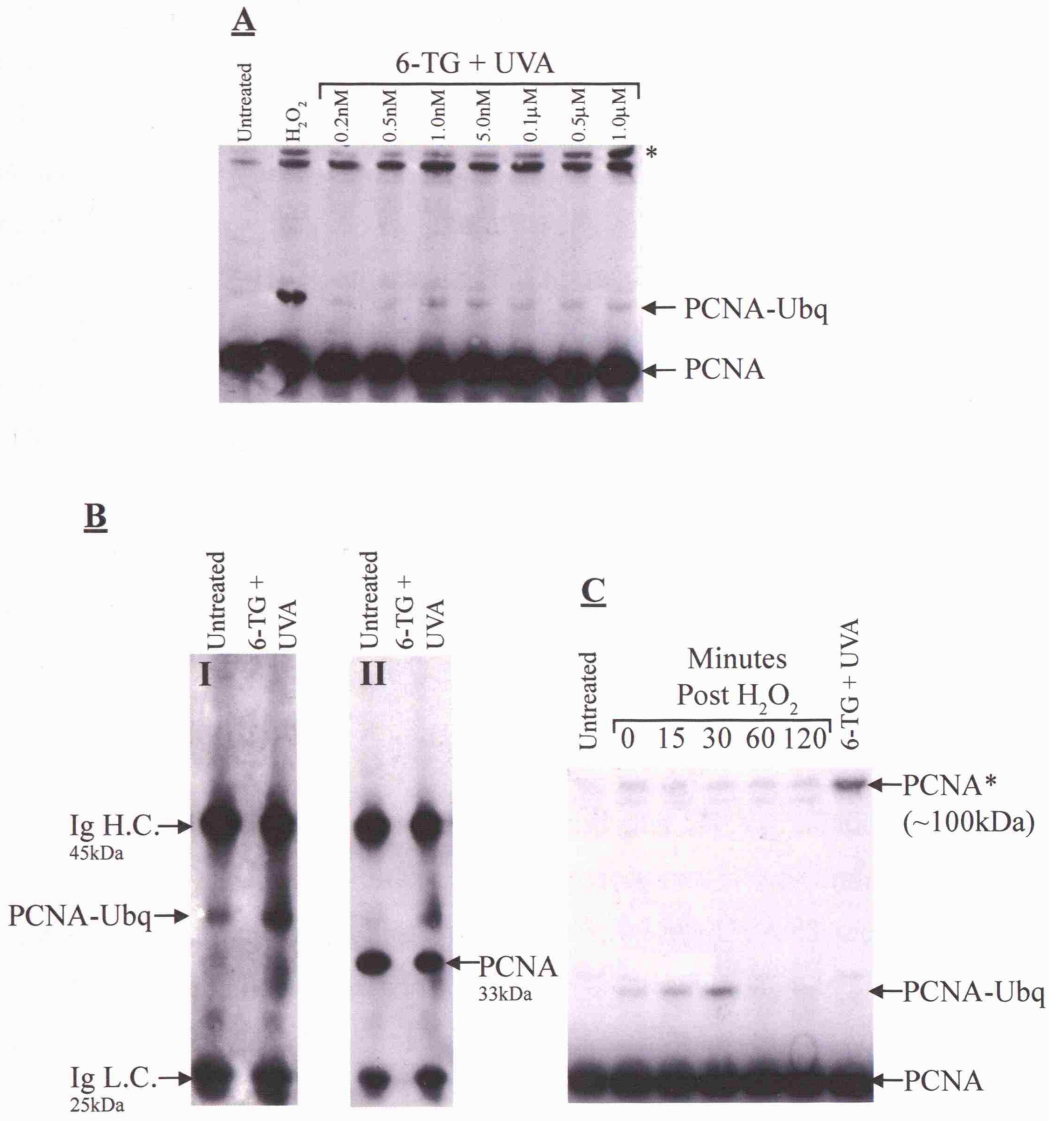

Fig 4.13 PCNA Modification: Mono-Ubiquitination. A PCNA mono-ubiquitination is 6-TG dose dependent. HCT 116 cells cultured for 48 hours in the presence of the indicated concentrations of 6-TG were UVA irradiated (3.0kJ/m^2) and allowed to recover for 6 hours in fresh medium. PCNA was analysed by Western blotting with an anti-PCNA antibody. **B** HCT 116 cells cultured for 48 hours in the presence of 5.0nM 6-TG were UVA irradiated (3.0kJ/m^2)and allowed to recover for 6 hours. PCNA was immunoprecipitated from these extracts, and the precipitated proteins analysed by Western blotting with an anti-ubiquitin antibody (I). This membrane was stripped and reprobed for PCNA (II). **C** H_2O_2 induces rapid and transient PCNA mono-ubiquitination in addition to variable levels of PCNA*. HCT 116 cells were treated with 0.03% H_2O_2 for 2 minutes, and allowed to recover in fresh medium. At various times post H_2O_2 treatment, extracts were prepared. PCNA was analysed as in A and B.

One striking feature of the Western blots was the formation of second PCNA containing species. This product, which migrated at a position corresponding to a size of approximately 100kDa, was also formed in a 6-TG dose dependent manner (Fig 4.13A, PCNA*). PCNA* was observed at 6-TG concentrations of 0.5nM and greater. In contrast to mono-ubiquitinated PCNA, PCNA* continued to accumulate at concentrations above 5nM. This modified PCNA form was also observed after treatment with 0.03% H_2O_2 suggesting PCNA* may be an oxidation product of PCNA. It should, be noted here that the level of PCNA* formed by H_2O_2 treatment was variable. Interestingly, robust but transient mono-ubiquitination of PCNA was consistently observed after a short exposure to H_2O_2 (2 minutes) In this instance, $PCNA^{Ubq}$ reaches a maximum level within 30 minutes, and is not observed after 60 minutes. This observation of PCNA mono-ubiquitination with such rapid kinetics is novel. Neither UVC nor γ-radiation (20Gy) induced detectable formation of PCNA* (Fig 4.14A and B), indicating that it is not a general ROS or DNA damage induced product.

Formation of PCNA* was extremely rapid after UVA irradiation. HCT 116 cells containing 6-TG were UVA irradiated at a high dose rate of $0.5kJ/m^2/s$ to minimise the time between UVA treatment and lysis. After 1.0kJ/m2 UVA (2 seconds), cells were lysed within approximately 2 seconds of end of the irradiation period. Even at this short time, the level of PCNA* had already reached its maximum (Fig 4.15A). The rapidity of PCNA* formation implies that the formation of this product is more likely to be chemical than enzymatic, and is consistent with a possible photochemical crosslinking of PCNA to form PCNA*.

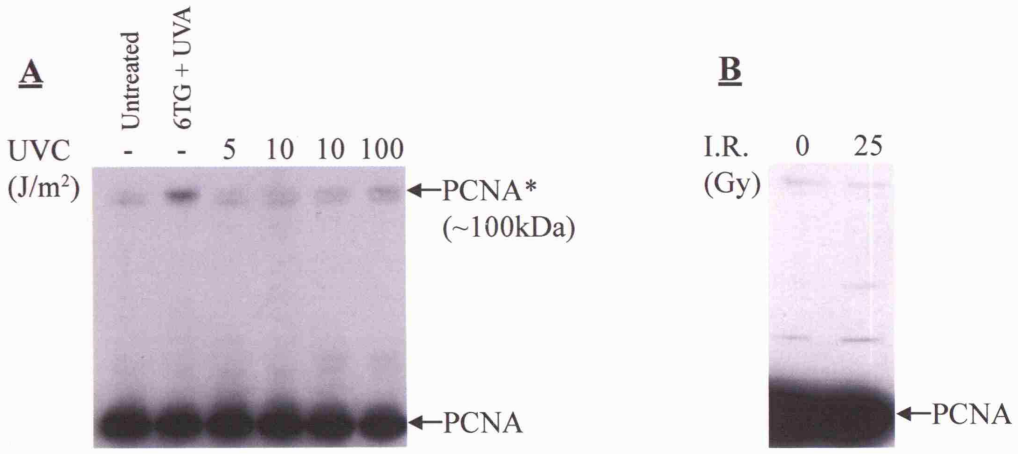

Fig 4.14 PCNA*: Not Induced by Other Forms of DNA Damage. A PCNA* is not formed after UVC irradiation. HCT 116 cells exposed to the indicated dose of UVC were harvested within 5 minutes of irradiation, extracts prepared and anlaysed by Western blotting with an anti-PCNA antibody. **B** Ionising radiation does not induce PCNA* formation. HCT 116 cells were exposed to 25Gy of γ-radiation. Extracts were prepared within 5 minutes of irradiation and analysed as in A.

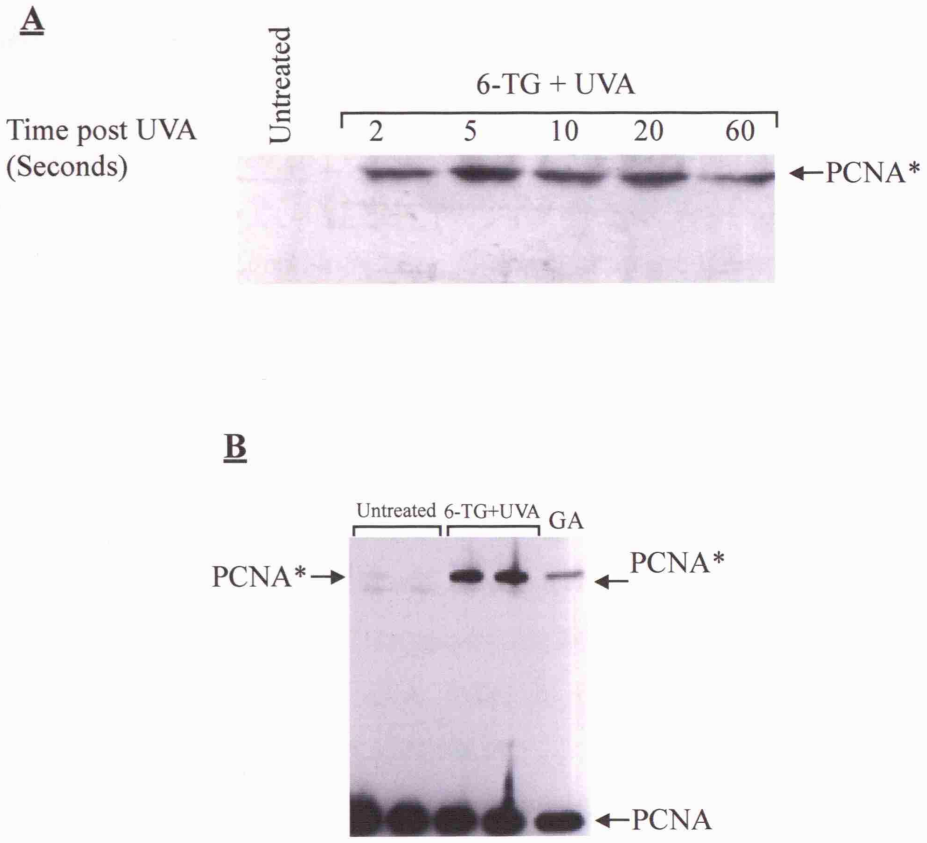

Fig 4.15 Kinetics of PCNA* Formation and Crosslinking of PCNA. **A** PCNA* is formed with extremely fast kinetics. HCT 116 cells grown for 48 hours in 1.0μM 6-TG were UVA irradiated with 1.0kJ/m^2 UVA, at a dose rate of 0.5kJ/m^2/s. At the indicated times, cells were analysed by Western blotting with anti-PCNA antibody. **B** PCNA* is also formed by chemical crosslinking of PCNA. HCT 116 cells were synchronised in S-phase by growth in 1.0mM hydroxyurea. 60 minutes after removal of HU, cells were harvested and chromatin bound protein fraction prepared. This fraction was treated with glutaraldehyde as described in Materials and Methods. Samples were analysed by Western blotting with anti-PCNA.

The size of PCNA*, together with the rapidity, and the potential singlet oxygen dependence of its formation led me to believe that this product might be a PCNA multimer (dimer or trimer) covalently crosslinked by the singlet oxygen produced in DNA after UVA irradiation. To test this hypothesis, crosslinked PCNA was produced by a published method, involving glutaraldehyde crosslinking of a chromatin bound protein fraction. Crosslinking of PCNA in this manner gave a single product observed by Western blotting with an anti-PCNA antibody. This crosslinked PCNA product was found to co-migrate with PCNA* generated after 6-TG/UVA (Fig 4.15B). These data suggest that PCNA* is indeed a PCNA multimer, although the composition (dimer or trimer) remains unclear.

4.3 Discussion

The aim of the work described in this chapter was to investigate the mechanism(s) of 6-TG sensitisation to UVA and to determine some of the biological effects of combined 6-TG/UVA. The experiments undertaken involved:

- Quantification of DNA 6-TG in cultured cells and examining the relationship to UVA sensitisation
- Examination of 6-TG/UVA mutagenicity
- Investigation of ROS generated *in vivo* by 6-TG/UVA
- Preliminary investigation of possible repair of 6-TG/UVA induced DNA damage
- Study of the effects of 6-TG/UVA on DNA replication

4.3.1 6-TG Sensitises Cells to UVA

The mechanism by which 6-TG is toxic has been extensively studied. DNA 6-TG kills cells in an MMR dependent manner. The thiopurine was initially shown to be a UVA sensitiser in XP12ROB4 cells (Massey et al. 2001), which are both NER and MMR deficient. My first priority on beginning this work was to ascertain whether this sensitisation was a general phenomenon. HCT 116 cells are MMR deficient but NER proficient. They were also sensitised to UVA by growth in 6-TG. UVA sensitisation was not confined to MMR defective cells, however. It was also observed in the A2780-SCA5, MRC5-VA and CHO D422 cell lines, all of which are fully repair proficient.

Sensitisation occurs at levels of DNA 6-TG which are in themselves non-toxic. As described in Chapter I, the toxicity of DNA 6-TG is dependent on its methylation by SAM to form 6-meTG. Since this methylation affects approximately 1 in every 10^4 DNA 6-TG residues, there is likely to be a threshold level of DNA 6-TG below which MMR is not activated and the viability of cells in not affected. At these non-toxic levels of DNA 6-TG sensitisation to UVA in MMR proficient cells was observed.

6-TG is incorporated into both DNA and RNA. It is also present in the dNTP pool. There is no reason why the photochemical reactions of 6-TG could not occur with RNA 6-TG, and I have shown that they occur with free 6-TGdR. Might these fractions of intracellular 6-TG contribute significantly the induced UVA sensitivity? HU treatment protected HCT 116 cells against 6-TG/UVA toxicity. This strongly suggests that DNA 6-TG is involved in 6-TG induced UVA sensitivity. It does not completely exclude the other possibilities, however.

4.3.2 Synergistic Mutagenicity of 6-TG and UVA

Both 6-TG and UVA are rather weakly mutagenic (Margison and Santibanez-Koref 2002). 6-TG is mutagenic due to the mismatches that occur during replication of DNA containing 6-TG (as described in Chapter 1). The mutagenicity of UVA is usually measured at high doses, exceeding 200kJ/m^2, and the mechanism of this is currently under debate. It is believed that UVA is absorbed by, as yet unidentified, cellular UVA chromophores. This leads to the production of reactive oxygen species (ROS) via a type II photosensitisation reaction. ROS then causes mutagenic oxidative DNA base damage. Of course, although UVA is absorbed very weakly by DNA itself, it is known to induce UVC- and UVB-type DNA damage, i.e. CPDs.

6-TG/UVA is mutagenic. Although the increase in mutation frequency was relatively modest, it is statistically highly significant. If, as seems possible, the mutagenicity of the treatment is due to ROS production the mechanism of mutagenesis is worthy of further examination

The 6-TG/UVA mutation spectrum differed significantly from published spontaneous spectra at the same locus. The main differences are an increased frequency of G to C and of A to C transversions. There is a compensatory decrease in G to A transitions. The 6-TG/UVA spectrum is also different from two published UVA spectra, although these differ significantly from each other. The fact that the 6-TG/UVA induced spectrum appears different from UVA spectra suggests that the mechanisms of mutagenesis are, at least partially, distinct.

From the high number of G to C transversions it is possible to speculate about a mechanism of mutagenesis. It has recently been shown that oxidised forms of guanine can generate G to C transversions (Henderson et al. 2003). This occurs by attempted replication of DNA guanidinohydantoin (Gh) and spiroiminodihydantoin (Sp) lesions (see Chapter 1). These lesions are formed by further oxidation of oxo^{8}G. Significantly, Sp products can also be formed directly by singlet oxygen mediated oxidation of unmodified guanine. Since $^1O_2$ is formed on UVA irradiation of 6-TG, Sp products, either of 6-TG or guanine may be formed, as well as G-6-SO_3. If formed, these might contribute to the generation of G to C mutation. Alternatively, G-6-SO_3 itself might also cause G to C transversions. This question has been addressed by my colleague Dr. Conal Perrett. Using a simple *in vitro* primer extension assay, he has shown that there is little, if any, incorporation of G opposite G-6-SO_3 by either the exo$^-$ Klenow fragment of *E. coli* Pol I, or two members of the Y-family of bypass polymerases. If the same applies in intact cells, this suggests that G-6-SO_3 might not be directly responsible for the high incidence of G to C mutations.

The increase in A to C transversions may also be explained by the generation of singlet oxygen. A to C transversions are known to occur after high doses of UVA, as a result of the oxidation of DNA adenine to oxo^{8}A, and possibly FapyA and 2-hydroxyadenine. Guanine can be incorporated opposite each of these bases during replication (Kamiya et al. 1995; Kamiya et al. 1995; Delaney et al. 2002). In G to C mutations it may be possible that cytosine is the damaged base. If the mutations are ROS induced, this is unlikely since the oxidation potential of cytosine is higher than that of guanine.

From this work I conclude that G to C and A to C transversions are the signature mutations of 6-TG/UVA. On balance, the data indicate that this is likely to be due to oxidative damage of DNA bases, either normal G/A bases or 6-TG itself. Oxo^{8}G is widely regarded as the most abundant oxidative DNA lesion in cells under oxidative stress. The contribution of DNA oxo^{8}G to 6-TG/UVA induced mutation is probably not significant as there is no detectable increase in G to T transversions, the oxo^{8}G signature mutation.

Overall, the mutation spectrum suggests the involvement of reactive oxygen and oxidative DNA damage. Intracellular ROS in cells under mutagenic 6-TG/UVA conditions was observed. Oxidative stress is also implicated in the lethality of 6-TG/UVA. The anti-oxidant NAC clearly provided protection. This poses an interesting question: would topical antioxidants on sun exposed skin reduce the NMSC incidence in Aza patients? This is already in practice for cosmetic purposes, and the dermatological community is actively promoting topical antioxidant use against photoaging of skin.

4.3.3 Repair of 6-TG/UVA DNA Photodamage?

As mentioned in Chapter 3, Dr. Y.-Z. Xu has demonstrated that G-6-SO_3 disrupts DNA base pairing. It is also charged, and the SO_3^- moiety is large. As NER recognises a number of similarly large DNA adducts, I expected that NER might repair DNA G-6-SO_3. The similar sensitivities to 6-TG/UVA of XP12RO (XPA) and MRC5-VA (wild-type) fibroblasts were therefore unexpected. This does not necessarily mean that NER does not remove DNA G-6-SO_3. We do not know whether this is the lethal lesion induced by 6-TG/UVA treatment. Perhaps NER does remove G-6-SO_3, but if this is not the lethal DNA lesion, then no phenotype would be observed in XP cells.

BER represents another possible mechanism for repair of 6-TG/UVA induced DNA damage. This pathway is involved in the repair of many modified bases, including most oxidised bases, and is discussed in greater detail in Chapter 1. A number of DNA glycosylases, each with its own specific substrate(s), function in BER. One of these, oxo^{8}G-DNA glycosylase (OGG1) excises oxidised and ring opened purines, including oxo^{8}G and FapyG, from DNA. Since G-6-SO_3 is an oxidised purine, I investigated

whether OGG1 excises 6-TG/UVA induced DNA damage. Attempts to use an $OGG1^{-/-}$ MEF line, F1.2, were frustrated by its lack of sensitivity to very high doses of 6-TG. I found that this was due to its inability to incorporate 6-TG into DNA. The reasons for this are not clear. These cells are spontaneously immortalised, and so are likely to be aneuploid, containing multiple copies of some genes and deletions of others. The lack of 6-TG sensitivity could be due to diminished activity of hypoxanthine phosphoribosyl transferase (HPRT), which is the first step in the production of 6-TG dNTP for incorporation into DNA. It could also be due to increased levels of TPMT, which could methylate 6-TG and prevent its incorporation into DNA. Whether or not this is the case, these cells were not suitable for investigating a role for OGG1 in 6-TG/UVA induced DNA damage repair.

Fpg is the E. coli homologue of mammalian OGG1. Fpg was used in an *in vitro* repair assay. No Fpg activity was observed on a 6-TG containing oligonucleotide before or after UVA irradiation. The UVA dose used resulted in around 90% of 6-TG being converted to G-6-SO_3. The fact that no Fpg substrate was formed in any of these experiments suggests that G-6-SO_3 is not recognised by this glycosylase. The lack of activity on a G containing oligonucleotide irradiated in the presence of free 6-TG tells us that either no oxo^{8}G is formed or that if it is , it is further oxidised to a form that isn't recognised by Fpg. The human and mouse 3-methyladenine glycosylases (Aag), act on methylated purines, as well as hypoxanthine and ethenoadenine. As with Fpg, there was no activity of Aag on any 6-TG/UVA substrate.

These two DNA glycosylases seemed to be the most likely candidates for repair of G-6-SO_3, or other oxidised DNA bases after UVA of 6-TG. The fact that 6-TG/UVA DNA damage does not appear to be a substrate for these enzymes raises the question of whether this damage is subject to repair at all. The fact that G-6-SO_3 is a completely novel DNA lesion that can only occur in organisms treated with 6-TG, 6-MP or Aza and UVA may mean that there is no repair mechanism, although this is highly unlikely. Alternatively, perhaps other cellular effects are responsible for the induced UVA lethality. Possible candidates may include lipid peroxidation products, PCNA*, or activation of stress induced signalling pathways leading to necrotic or apoptotic cell death. It may be interesting to analyse how 6-TG/UVA treated cells are dying, i.e. is it apoptosis or necrosis? If it is apoptosis, which apoptotic pathways are involved?

It is important to remember that after UVA of 6-TG treated cells, there will most likely be numerous sites of ROS mediated damage. RNA 6-TG and 6-TdGTP (and its precursors) can produce ROS on UVA irradiation, as evidenced by cytoplasmic ROS induced by 6-TG/UVA in HU treated cells. This cytoplasmic ROS may lead to lipid peroxidation, and mitochondrial disruption, both of which are known to cause cell death. ROS production within the double helix is particularly hazardous, and will oxidise DNA 6-TG to G-6-SO_3 which is a novel DNA lesion. As yet, we do not know the consequences of the presence of G-6-SO_3 in genomic DNA, although it is a replication block *in vitro*. ROS produced in DNA would also be expected to modify other DNA bases either directly or via charge transfer through the double helix. ROS can also lead to protein-DNA or protein-protein crosslinks. There might also be a contribution from non-ROS based mechanisms since 6-TG could act as a Type I photosensitiser, causing the generation of non-oxygen based radicals from various cellular components and macromolecules. This too could result in DNA-protein crosslinks. Hence, hypersensitivity to 6-TG/UVA may only be revealed by screening many repair defective cell types, and cells deficient in more than one form of DNA repair.

4.3.4 Effects of 6-TG/UVA on Replication

My colleagues have shown that G-6-SO_3 is a block to replication *in vitro*. This block can be bypassed, *in vitro*, by the purified translesion synthesis (TLS) DNA polymerase Polη. It has been reported in the literature that the modification of PCNA by ubiquitination on lysine 164 may play a role in switching from the replicative to a TLS polymerase at stalled replication forks.

While neither 6-TG nor UVA alone induced $PCNA^{Ubq}$, when combined there was an induction of mono-ubiquitination. This suggests that there may be an attempt to bypass 6-TG/UVA induced DNA damage. No data has been obtained as to the effects of lesion bypass. Is it necessary for survival? Is bypass actually successful? Could TLS play a role in 6-TG/UVA mutagenesis? All these questions remain unanswered. The biological relevance of lesion bypass after 6-TG/UVA might be best investigated using

an XPV, Polη deficient cell line. Polη may not be the TLS polymerase involved *in vivo*, however,

The formation of the high molecular weight PCNA complex (PCNA*) is a novel and exciting observation. The rapidity of PCNA* formation strongly suggests a chemical (possibly oxygen radical-mediated) rather than an enzymatic reaction. Such rapid reactions are characteristic of ROS, owing to their highly reactive nature. Treatment with H_2O_2 gave varying levels of PCNA*. This inconsistency is not altogether surprising. Whereas the major product of H_2O_2 is •OH, the levels of the less frequent products ($^1O_2$, $•O_2^-$, etc.) can be highly variable. Since my data suggest the involvement of $^1O_2$ in the formation of PCNA*, the inconsistent results with H_2O_2 may reflect this. Colleagues in the laboratory have since found that high doses ($\geq$100kJ/m^2) of UVA alone can induce PCNA* formation. UVA is known to generate $^1O_2$ through Type II photosensitisation reactions. IR and UVC produce minimal $^1O_2$, and so the absence of PCNA* from γ- or UVC-irradiated cells is also consistent with a requirement for $^1O_2$ in PCNA* formation. These finding also signify that PCNA* is not a general marker for DNA damage.

Taken together, I believe my data, and that of my colleagues, to be consistent with oxidative crosslinking of PCNA by $^1O_2$ produced by 6-TG/UVA. A large number of proteins can be found together at a replication fork, where PCNA is proposed to act as a scaffold for the recruitment of replication factors. In one approach to determining which of these may be crosslinked to PCNA in PCNA*, a list of PCNA interacting proteins was constructed using the online BIND database (Appendix Table 7.2, http://www.bind.ca). Those significantly above 70kDa were excluded from consideration since the PCNA monomer is 33kDa, and so a complex of PCNA with any protein greater than 70kDa would give product larger than the estimated molecular weight of PCNA*. DNA damage inducible factors were also excluded because of the rapid kinetics of PCNA* formation, as were DNA repair factors which operate at sites to which PCNA is required only for the final steps in repair. The remaining interacting proteins consisted of the RFC PCNA clamp loader, the Polδ regulatory subunit, and PCNA itself.

Of these, I believe that PCNA crosslinked monomers is perhaps the most likely possibility. When crosslinked PCNA was prepared according to a published protocol, the single product obtained was indistinguishable from the 6-TG/UVA induced PCNA*. The literature suggests that this is a covalently linked circular trimer, but to my knowledge there is no definitive proof that this is indeed a trimer, and not crosslinked PCNA dimer or linear trimer. While a dimer would be expected to migrate through SDS PAGE with an apparent molecular weight of 66kDa, the mobility of any crosslinked PCNA cannot be predicted. Glutaraldehyde crosslinking involves the use of a massive excess of crosslinking agent. Since each crosslinking event is independent, one event would lead to a dimer, two events to a linear trimer, and three events would be required for formation of a circular trimer. It may be unlikely that crosslinking would halt at the dimer, and so only trimer would be formed. There is also a suggestion of a PCNA double trimer formed after formaldehyde crosslinking (Naryzhny et al. 2005).

At present, I am unable to conclude whether PCNA* is a dimer, trimer, or circular trimer of PCNA. I can say, however, that PCNA is the only component of PCNA*. PCNA* has been purified by my colleagues Dr. Olivier Reelfs and Mr. Peter McPherson. Mass spectrometry and 2D gel electrophoresis have shown that PCNA* has an identical pI to PCNA and contains only PCNA. Further analysis is under way to investigate which residues are involved in the crosslinking. Further investigation of the involvement of $^1O_2$ is being undertaken by Mr. Peter McPherson, using Rose Bengal as a $^1O_2$ source.

4.3.5 Azathioprine and UVA

In order to link the work described using 6-TG to dermatological effects I examined whether 6-TG was present in the skin of Aza patients. I found that DNA 6-TG was present in skin biopsies at levels similar to those previously reported in lymphocytes of 6-TG and 6-MP treated patients (Warren et al. 1995; Cuffari et al. 1996). Dr. Conal Perrett has demonstrated that Aza treatment sensitises patients skin specifically to UVA. Minimal erethyma dose (MED) measurements are used to test skin photosensitivity. They quantify the minimum amount of radiation required to induced redness in non-sun exposed skin. Dr. Perrett measured the MED in patients before and during their Aza regimens, and found that although there was no increased sensitivity to

UVB, there was a significant sensitisation to UVA and to SSR (Simulated Solar Radiation), a mixture of UVA, UVB and visible light.

An important unsolved question is the contribution of 6-TG/UVA induced mutation to cancer in Aza patients. At the time of writing of this thesis, a study to address this issue is underway. I have obtained DNA from 40 BCC samples from Aza treated patients (20 with matching blood) and from 20 BCCs from immunocompetent patients (10 with matching blood). Sequencing of the *PTCH* gene in these samples is now underway. *PTCH* is known to be mutated in 60% of BCCs, and this is probably critical for their development. *PTCH* mutation spectra will be obtained An overrepresentation of G to C or A to C transversions in the immunocompromised group would be consistent with a role for DNA 6-TG and Aza in NMSC development in organ transplant recipients. Of course, any differences may be difficult to find, and I anticipate a significant background of UVB mutations

The experiments relating to 6-TG/UVA sensitivity and mutagenicity involved a single treatment of cultured cells with UVA. Azathioprine treated patients may be continuously exposed to UVA irradiation, and since treatment regimens are lengthy this constitutes a serious risk to genome integrity.

In this chapter, I have described some of the biological effects of combined 6-TG and UVA treatment of cultured cells. Lethality is dependent on 6-TG incorporation into DNA. UVA irradiation leads to the production of ROS, probably $^1O_2$, in DNA itself. The production of $^1O_2$ may also be responsible for the 6-TG/UVA mutation spectrum that has been obtained. At the same time, DNA 6-TG is oxidised to G-6-SO_3, a novel DNA lesion that can be bypassed, *in vitro*, by TLS polymerases. This may contribute to mutagenesis. Lethal DNA damage that occurs after 6-TG/UVA does not appear to be repaired by NER. Two candidate BER glycosylases do not recognise G-6-SO_3 *in vitro*. In addition to DNA damage, $^1O_2$ may lead to protein and lipid damage in the cytoplasm since 6-TG can be incorporated into RNA, and exist in the dNTP pool

An important additional finding is the ability of 6-TG/UVA to cause protein oxidation at the replication fork. Protein oxidation has largely been dismissed as a significant factor in the effects of radiation since proteins, unlike DNA, are small targets

and are readily turned over. Oxidative crosslinking of PCNA into PCNA*, possibly a PCNA trimer, could have potentially serious consequences for the cell. How would a crosslinked trimer be removed from DNA? PCNA* is formed rapidly and can represent ~20% of total cell PCNA. Does this affect replication? Might PCNA also become oxidatively croslinked to DNA, posing further problems for the replication fork?

Currently, my colleagues are attempting to address these questions and elucidate the role, if any, of PCNA* in 6-TG induced UVA sensitivity. If such a role is found, this would be the first demonstration that the replication complex itself, rather than DNA, can be a target for oxidative damage, and that this can have biological consequences.

I believe that my finding may have relevance to skin cancer in Aza treated patients. I have shown that skin DNA from these patients contains measurable levels of 6-TG. The presence of DNA 6-TG is associated with a selective sensitisation to UVA. The relevance of the photochemical reactions 6-TG to the pathogenesis of NMSC in organ transplant recipients might prove worthy of further investigation.

5 Future Perspectives

The work presented in this thesis provides a framework with which to investigate further a posible causal role for Azathioprine in NMSC in OTRs. There are, however, many questions and details that, thus far, have remained elusive. Chief amongst these, clinically, is whether 6-TG/UVA induced mutations are responsible for the development of NMSC in these patients. The fact that exposure of DNA 6-TG to UVA leads to mutations in cultured cells might suggest that this is so. The skin is very frequently exposed to UVA, and while the UVA doses may not be high enough to be mutagenic in themselves, DNA 6-TG and UVA act synergistically. The question still remains as to whether G-6-SO_3 or collateral oxidative base damage, or both, cause mutations. The implied importance of $^1O_2$ would point to a mechanism which is similar to that proposed for UVA induced mutagenesis, and may explain the increased A to C changes found after 6-TG/UVA. G to C mutations can also be due to oxidative stress, but possibly also due to G-6-SO_3. The sequencing of *PTCH* gene in BCCs from Aza patients will hopefully help to answer some of these questions.

Aza is now being phased out of immunosuppressive regimens for OTRs. It is finding a far wider clinical use in chronic inflammatory and auto-immune conditions. These treatments can often be long term, though not as long as for immunosuppression in OTRs. OTRs are warned about exposure to sunlight, but rarely about UVA in particular. Perhaps this should be considered by the medical community. It is also worth noting that, generally, glass does not block UVA, and Aza treated patients might need to pay particular attention in the workplace and at home to minimize their UVA exposure.

Protein oxidation is not generally considered a significant cause of lethality in cells because proteins present small targets for radiation damage and any damaged proteins are rapidly turned over. This may not apply in the case of proteins involved in functions essential to DNA replication or maintenance of genome integrity. Can cells simply remove the offenders, recruit replacements, and carry on? The serendipitous discovery of PCNA*, reported here, addresses this possibility. Preliminary indications from my colleagues suggest that PCNA* is responsible for at least some of the toxicity of 6-TG/UVA. PCNA* is only formed when DNA 6-TG is at or close to an active

replication fork. It is possible that PCNA* is a crosslinked trimer of PCNA. If this is the case, then one can imagine how it might contribute to cytotoxicity. How would such a trimer be removed from DNA? Could such a trimer carry out its normal functions in DNA replication or does it play a significant part in the abrupt inhibition or replication after 6-TG/UVA? The migration of PCNA in SDS PAGE might be consistent with either a linear or circular trimer. Intuitively the former is difficult to explain. Why would such crosslinking only occur at two sites in the native PCNA trimer to form a linear molecule, and not all three? These questions may prove difficult to answer, since it is very hard to isolate the formation of PCNA* from the generation of DNA damage. In spite of these questions, the formation of PCNA*, and its apparent impact on cellular functions and survival remains an intriguing phenomenon.

The effects of Azathioprine in patients are multiple. They comprise immunosuppression, DNA damage, protein damage, and interactions thereof. The fact that this drug has been in use for so long while so little was known about its mechanisms of action is a common theme in medicine. The mechanisms of action of many drugs are not known. Most depend on DNA damage or dysregulation of signalling pathways for their effects. This may lead to serious side effects later in life, years, or even decades, after treatment is finished. Nevertheless, these drugs work. This makes the need to elucidate their mechanisms, to help understand the basis of, and possibly eliminate, their harmful side effects, all the greater.

6 References

Aarbakke, J., G. Janka-Schaub and G. B. Elion (1997). "Thiopurine biology and pharmacology." Trends Pharmacol Sci **18**(1): 3-7.

Aas, P. A., M. Otterlei, P. O. Falnes, C. B. Vagbo, F. Skorpen, M. Akbari, O. Sundheim, M. Bjoras, G. Slupphaug, E. Seeberg, et al. (2003). "Human and bacterial oxidative demethylases repair alkylation damage in both RNA and DNA." Nature **421**(6925): 859-63.

Adhikary, A., A. Y. Malkhasian, S. Collins, J. Koppen, D. Becker and M. D. Sevilla (2005). "UVA-visible photo-excitation of guanine radical cations produces sugar radicals in DNA and model structures." Nucleic Acids Res **33**(17): 5553-64.

Agar, N. and A. R. Young (2005). "Melanogenesis: a photoprotective response to DNA damage?" Mutat Res **571**(1-2): 121-32.

Agar, N. S., G. M. Halliday, R. S. Barnetson, H. N. Ananthaswamy, M. Wheeler and A. M. Jones (2004). "The basal layer in human squamous tumors harbors more UVA than UVB fingerprint mutations: a role for UVA in human skin carcinogenesis." Proc Natl Acad Sci U S A **101**(14): 4954-9.

Ahnesorg, P., P. Smith and S. P. Jackson (2006). "XLF interacts with the XRCC4-DNA ligase IV complex to promote DNA nonhomologous end-joining." Cell **124**(2): 301-13.

Al-Tassan, N., N. H. Chmiel, J. Maynard, N. Fleming, A. L. Livingston, G. T. Williams, A. K. Hodges, D. R. Davies, S. S. David, J. R. Sampson, et al. (2002). "Inherited variants of MYH associated with somatic G:C-->T:A mutations in colorectal tumors." Nat Genet **30**(2): 227-32.

Alam, M. and D. Ratner (2001). "Cutaneous squamous-cell carcinoma." N Engl J Med **344**(13): 975-83.

Allanson, M. and V. E. Reeve (2005). "Ultraviolet A (320-400 nm) modulation of ultraviolet B (290-320 nm)-induced immune suppression is mediated by carbon monoxide." J Invest Dermatol **124**(3): 644-50.

Aquilina, G., A. M. Giammarioli, A. Zijno, A. Di Muccio, E. Dogliotti and M. Bignami (1990). "Tolerance to O6-methylguanine and 6-thioguanine cytotoxic effects: a cross-resistant phenotype in N-methylnitrosourea-resistant Chinese hamster ovary cells." Cancer Res **50**(14): 4248-53.

Aractingi, S., J. Kanitakis, S. Euvrard, C. Le Danff and E. D. Carosella (2003). "Selective expression of HLA-G in malignant and premalignant skin specimens in kidney transplant recipients." Int J Cancer **106**(2): 232-5.

Athar, M., C. Li, X. Tang, S. Chi, X. Zhang, A. L. Kim, S. K. Tyring, L. Kopelovich, J. Hebert, E. H. Epstein, Jr., et al. (2004). "Inhibition of smoothened signaling prevents ultraviolet B-induced basal cell carcinomas through regulation of Fas expression and apoptosis." Cancer Res **64**(20): 7545-52.

Bale, A. E. and K. P. Yu (2001). "The hedgehog pathway and basal cell carcinomas." Hum Mol Genet **10**(7): 757-62.

Barnes, D. E. and T. Lindahl (2004). "Repair and genetic consequences of endogenous DNA base damage in mammalian cells." Annu Rev Genet **38**: 445-76.

Berman, D. M., S. S. Karhadkar, A. Maitra, R. Montes De Oca, M. R. Gerstenblith, K. Briggs, A. R. Parker, Y. Shimada, J. R. Eshleman, D. N. Watkins, et al. (2003). "Widespread requirement for Hedgehog ligand stimulation in growth of digestive tract tumours." Nature **425**(6960): 846-51.

Besaratinia, A., T. W. Synold, B. Xi and G. P. Pfeifer (2004). "G-to-T transversions and small tandem base deletions are the hallmark of mutations induced by ultraviolet a radiation in mammalian cells." Biochemistry **43**(25): 8169-77.

Bienko, M., C. M. Green, N. Crosetto, F. Rudolf, G. Zapart, B. Coull, P. Kannouche, G. Wider, M. Peter, A. R. Lehmann, et al. (2005). "Ubiquitin-binding domains in Y-family polymerases regulate translesion synthesis." Science **310**(5755): 1821-4.

Bjelland, S. and E. Seeberg (2003). "Mutagenicity, toxicity and repair of DNA base damage induced by oxidation." Mutat Res **531**(1-2): 37-80.

Blackwell, L. J., D. Martik, K. P. Bjornson, E. S. Bjornson and P. Modrich (1998). "Nucleotide-promoted release of hMutSalpha from heteroduplex DNA is consistent with an ATP-dependent translocation mechanism." J Biol Chem **273**(48): 32055-62.

Bodak, N., S. Queille, M. F. Avril, B. Bouadjar, C. Drougard, A. Sarasin and L. Daya-Grosjean (1999). "High levels of patched gene mutations in basal-cell carcinomas from patients with xeroderma pigmentosum." Proc Natl Acad Sci U S A **96**(9): 5117-22.

Bohon, J. and C. R. de los Santos (2005). "Effect of 6-thioguanine on the stability of duplex DNA." Nucleic Acids Res **33**(9): 2880-6.

Bordea, C., F. Wojnarowska, P. R. Millard, H. Doll, K. Welsh and P. J. Morris (2004). "Skin cancers in renal-transplant recipients occur more frequently than previously recognized in a temperate climate." Transplantation **77**(4): 574-9.

Boukamp, P. (2005). "Non-melanoma skin cancer: what drives tumor development and progression?" Carcinogenesis **26**(10): 1657-67.

Bouwes Bavinck, J. N., D. R. Hardie, A. Green, S. Cutmore, A. MacNaught, B. O'Sullivan, V. Siskind, F. J. Van Der Woude and I. R. Hardie (1996). "The risk of skin cancer in renal transplant recipients in Queensland, Australia. A follow-up study." Transplantation **61**(5): 715-21.

Branch, P., M. Masson, G. Aquilina, M. Bignami and P. Karran (2000). "Spontaneous development of drug resistance: mismatch repair and p53 defects in resistance to cisplatin in human tumor cells." Oncogene **19**(28): 3138-45.

Brellier, F., C. Marionnet, O. Chevallier-Lagente, R. Toftgard, A. Mauviel, A. Sarasin and T. Magnaldo (2004). "Ultraviolet irradiation represses PATCHED gene transcription in human epidermal keratinocytes through an activator protein-1-dependent process." Cancer Res **64**(8): 2699-704.

Buck, D., L. Malivert, R. de Chasseval, A. Barraud, M. C. Fondaneche, O. Sanal, A. Plebani, J. L. Stephan, M. Hufnagel, F. le Deist, et al. (2006). "Cernunnos, a novel nonhomologous end-joining factor, is mutated in human immunodeficiency with microcephaly." Cell **124**(2): 287-99.

Cadet, J., T. Douki, D. Gasparutto and J. L. Ravanat (2003). "Oxidative damage to DNA: formation, measurement and biochemical features." Mutat Res **531**(1-2): 5-23.

Cadet, J., E. Sage and T. Douki (2005). "Ultraviolet radiation-mediated damage to cellular DNA." Mutat Res **571**(1-2): 3-17.

Casorelli, I., J. Offman, L. Mele, L. Pagano, S. Sica, M. D'Errico, G. Giannini, G. Leone, M. Bignami and P. Karran (2003). "Drug treatment in the development of mismatch repair defective acute leukemia and myelodysplastic syndrome." DNA Repair (Amst) **2**(5): 547-59.

Chan, G. L., G. R. Erdmann, S. A. Gruber, A. J. Matas and D. M. Canafax (1990). "Azathioprine metabolism: pharmacokinetics of 6-mercaptopurine, 6-thiouric

acid and 6-thioguanine nucleotides in renal transplant patients." J Clin Pharmacol **30**(4): 358-63.

Ciccia, A., A. Constantinou and S. C. West (2003). "Identification and characterization of the human mus81-eme1 endonuclease." J Biol Chem **278**(27): 25172-8.

Claij, N. and H. te Riele (2004). "Msh2 deficiency does not contribute to cisplatin resistance in mouse embryonic stem cells." Oncogene **23**(1): 260-6.

Clark, A. B., F. Valle, K. Drotschmann, R. K. Gary and T. A. Kunkel (2000). "Functional interaction of proliferating cell nuclear antigen with MSH2-MSH6 and MSH2-MSH3 complexes." J Biol Chem **275**(47): 36498-501.

Colussi, C., E. Parlanti, P. Degan, G. Aquilina, D. Barnes, P. Macpherson, P. Karran, M. Crescenzi, E. Dogliotti and M. Bignami (2002). "The mammalian mismatch repair pathway removes DNA 8-oxodGMP incorporated from the oxidized dNTP pool." Curr Biol **12**(11): 912-8.

Couve-Privat, S., B. Bouadjar, M. F. Avril, A. Sarasin and L. Daya-Grosjean (2002). "Significantly high levels of ultraviolet-specific mutations in the smoothened gene in basal cell carcinomas from DNA repair-deficient xeroderma pigmentosum patients." Cancer Res **62**(24): 7186-9.

Couve-Privat, S., M. Le Bret, E. Traiffort, S. Queille, J. Coulombe, B. Bouadjar, M. F. Avril, M. Ruat, A. Sarasin and L. Daya-Grosjean (2004). "Functional analysis of novel sonic hedgehog gene mutations identified in basal cell carcinomas from xeroderma pigmentosum patients." Cancer Res **64**(10): 3559-65.

Crowson, A. N. (2006). "Basal cell carcinoma: biology, morphology and clinical implications." Mod Pathol **19 Suppl 2**: S127-47.

Cuffari, C., E. G. Seidman, S. Latour and Y. Theoret (1996). "Quantitation of 6-thioguanine in peripheral blood leukocyte DNA in Crohn's disease patients on maintenance 6-mercaptopurine therapy." Can J Physiol Pharmacol **74**(5): 580-5.

Cui, C., T. Elsam, Q. Tian, J. T. Seykora, M. Grachtchouk, A. Dlugosz and H. Tseng (2004). "Gli proteins up-regulate the expression of basonuclin in Basal cell carcinoma." Cancer Res **64**(16): 5651-8.

D'Amours, D. and S. P. Jackson (2002). "The Mre11 complex: at the crossroads of dna repair and checkpoint signalling." Nat Rev Mol Cell Biol **3**(5): 317-27.

D'Errico, M., A. Calcagnile, F. Canzona, B. Didona, P. Posteraro, R. Cavalieri, R. Corona, I. Vorechovsky, T. Nardo, M. Stefanini, et al. (2000). "UV mutation signature in tumor suppressor genes involved in skin carcinogenesis in xeroderma pigmentosum patients." Oncogene **19**(3): 463-7.

Dajee, M., M. Lazarov, J. Y. Zhang, T. Cai, C. L. Green, A. J. Russell, M. P. Marinkovich, S. Tao, Q. Lin, Y. Kubo, et al. (2003). "NF-kappaB blockade and oncogenic Ras trigger invasive human epidermal neoplasia." Nature **421**(6923): 639-43.

Daya-Grosjean, L. and A. Sarasin (2000). "UV-specific mutations of the human patched gene in basal cell carcinomas from normal individuals and xeroderma pigmentosum patients." Mutat Res **450**(1-2): 193-9.

De Fabo, E. C., F. P. Noonan, T. Fears and G. Merlino (2004). "Ultraviolet B but not ultraviolet A radiation initiates melanoma." Cancer Res **64**(18): 6372-6.

de Gruijl, F. R. (1999). "Skin cancer and solar UV radiation." Eur J Cancer **35**(14): 2003-9.

de Jong, P. J., Grosovsky, A. J., Glickman, B. W. (1988). "Spectrum of Spontaneous Mutation at the *APRT* Locus of Chinese Hamster Ovary Cells: An Analysis at the DNA Sequence Level." P Natl Acad Sci **85**: 3499 - 503.

Delaney, M. O., C. J. Wiederholt and M. M. Greenberg (2002). "Fapy.dA induces nucleotide misincorporation translesionally by a DNA polymerase." Angew Chem Int Ed Engl **41**(5): 771-3.

Derijks, L. J., L. P. Gilissen, L. G. Engels, L. P. Bos, P. J. Bus, J. J. Lohman, W. L. Curvers, S. J. Van Deventer, D. W. Hommes and P. M. Hooymans (2004). "Pharmacokinetics of 6-mercaptopurine in patients with inflammatory bowel disease: implications for therapy." Ther Drug Monit **26**(3): 311-8.

Djordjevic, B. and W. Szybalski (1960). "Genetics of human cell lines. III. Incorporation of 5-bromo- and 5-iododeoxyuridine into the deoxyribonucleic acid of human cells and its effect on radiation sensitivity." J Exp Med **112**: 509-31.

Doerr, I. L., I. Wempen, D. A. Clarke and J. F. Fox (1961). "Thiation of nucleosides. III. Oxidation of 6-mercaptopurine." J Org Chem **26**: 3401-8.

Douki, T. and J. Cadet (1999). "Modification of DNA bases by photosensitized one-electron oxidation." Int J Radiat Biol **75**(5): 571-81.

Douki, T., A. Reynaud-Angelin, J. Cadet and E. Sage (2003). "Bipyrimidine photoproducts rather than oxidative lesions are the main type of DNA damage involved in the genotoxic effect of solar UVA radiation." Biochemistry **42**(30): 9221-6.

Drablos, F., E. Feyzi, P. A. Aas, C. B. Vaagbo, B. Kavli, M. S. Bratlie, J. Pena-Diaz, M. Otterlei, G. Slupphaug and H. E. Krokan (2004). "Alkylation damage in DNA and RNA--repair mechanisms and medical significance." DNA Repair (Amst) **3**(11): 1389-407.

Drobetsky, E. A., J. Turcotte and A. Chateauneuf (1995). "A role for ultraviolet A in solar mutagenesis." Proc Natl Acad Sci U S A **92**(6): 2350-4.

Duncan, T., S. C. Trewick, P. Koivisto, P. A. Bates, T. Lindahl and B. Sedgwick (2002). "Reversal of DNA alkylation damage by two human dioxygenases." Proc Natl Acad Sci U S A **99**(26): 16660-5.

Eggler, A. L., R. B. Inman and M. M. Cox (2002). "The Rad51-dependent pairing of long DNA substrates is stabilized by replication protein A." J Biol Chem **277**(42): 39280-8.

Ehrhart, J. C., F. P. Gosselet, R. M. Culerrier and A. Sarasin (2003). "UVB-induced mutations in human key gatekeeper genes governing signalling pathways and consequences for skin tumourigenesis." Photochem Photobiol Sci **2**(8): 825-34.

Elion, G. B. (1989). "The purine path to chemotherapy." Science **244**(4900): 41-7.

Elion, G. B., S. Mueller and G. H. Hitchings (1958). "Studies on condensed pyrimidine systems. XXI. The isolation and synthesis of 6-mercapto-2,8-purinediol (6-thiouric acid)." J Am Chem Soc **81**: 3042-5.

Erb, N., U. Haverland, D. O. Harms, G. Escherich and G. Janka-Schaub (2003). "High-performance liquid chromatographic assay of metabolites of thioguanine and mercaptopurine in capillary blood." J Chromatogr B Analyt Technol Biomed Life Sci **796**(1): 87-94.

Erdmann, G. R., L. A. France, B. C. Bostrom and D. M. Canafax (1990). "A reversed phase high performance liquid chromatography approach in determining total red blood cell concentrations of 6-thioguanine, 6-mercaptopurine, methylthioguanine, and methylmercaptopurine in a patient receiving thiopurine therapy." Biomed Chromatogr **4**(2): 47-51.

Esteller, M. (2002). "CpG island hypermethylation and tumor suppressor genes: a booming present, a brighter future." Oncogene **21**(35): 5427-40.

Euvrard, S., J. Kanitakis and A. Claudy (2003). "Skin cancers after organ transplantation." N Engl J Med **348**(17): 1681-91.

Euvrard, S., J. Kanitakis, C. Pouteil-Noble, A. Claudy and J. L. Touraine (1997). "Skin cancers in organ transplant recipients." Ann Transplant **2**(4): 28-32.

Fairbanks, L. D., M. Bofill, K. Ruckemann and H. A. Simmonds (1995). "Importance of ribonucleotide availability to proliferating T-lymphocytes from healthy humans. Disproportionate expansion of pyrimidine pools and contrasting effects of de novo synthesis inhibitors." J Biol Chem **270**(50): 29682-9.

Falnes, P. O., R. F. Johansen and E. Seeberg (2002). "AlkB-mediated oxidative demethylation reverses DNA damage in Escherichia coli." Nature **419**(6903): 178-82.

Fink, D., S. Nebel, P. S. Norris, R. N. Baergen, S. P. Wilczynski, M. J. Costa, M. Haas, S. A. Cannistra and S. B. Howell (1998). "Enrichment for DNA mismatch repair-deficient cells during treatment with cisplatin." Int J Cancer **77**(5): 741-6.

Finkel, J. M. (1975). "Fluorometric assay of thioguanine." J Pharm Sci **64**(1): 121-2.

Fishel, R. (2001). "The selection for mismatch repair defects in hereditary nonpolyposis colorectal cancer: revising the mutator hypothesis." Cancer Res **61**(20): 7369-74.

Fortina, A. B., S. Piaserico, A. L. Caforio, D. Abeni, M. Alaibac, A. Angelini, S. Iliceto and A. Peserico (2004). "Immunosuppressive level and other risk factors for basal cell carcinoma and squamous cell carcinoma in heart transplant recipients." Arch Dermatol **140**(9): 1079-85.

Friedberg, E. C., A. R. Lehmann and R. P. Fuchs (2005). "Trading places: how do DNA polymerases switch during translesion DNA synthesis?" Mol Cell **18**(5): 499-505.

Friedberg, E. C., G. C. Walker and W. Siede (2006). DNA repair and mutagenesis. Washington, D.C., ASM ; [Oxford : Blackwell [distributor].

Fryer, A. A., H. M. Ramsay, T. J. Lovatt, P. W. Jones, C. M. Hawley, D. L. Nicol, R. C. Strange and P. N. Harden (2005). "Polymorphisms in glutathione S-transferases and non-melanoma skin cancer risk in Australian renal transplant recipients." Carcinogenesis **26**(1): 185-91.

Gailani, M. R., M. Stahle-Backdahl, D. J. Leffell, M. Glynn, P. G. Zaphiropoulos, C. Pressman, A. B. Unden, M. Dean, D. E. Brash, A. E. Bale, et al. (1996). "The role of the human homologue of Drosophila patched in sporadic basal cell carcinomas." Nat Genet **14**(1): 78-81.

Gradia, S., D. Subramanian, T. Wilson, S. Acharya, A. Makhov, J. Griffith and R. Fishel (1999). "hMSH2-hMSH6 forms a hydrolysis-independent sliding clamp on mismatched DNA." Mol Cell **3**(2): 255-61.

Greer, S. (1960). "Studies on ultraviolet irradiation of Escherichia coli containing 5-bromouracil in its DNA." J Gen Microbiol **22**: 618-34.

Hahn, H., C. Wicking, P. G. Zaphiropoulous, M. R. Gailani, S. Shanley, A. Chidambaram, I. Vorechovsky, E. Holmberg, A. B. Unden, S. Gillies, et al. (1996). "Mutations of the human homolog of Drosophila patched in the nevoid basal cell carcinoma syndrome." Cell **85**(6): 841-51.

Halliwell, B. and J. M. C. Gutteridge (1998). Free radicals in biology and medicine. Oxford, Oxford University Press.

Haluska, F. G., H. Tsao, H. Wu, F. S. Haluska, A. Lazar and V. Goel (2006). "Genetic alterations in signaling pathways in melanoma." Clin Cancer Res **12**(7 Pt 2): 2301s-2307s.

Harfe, B. D. and S. Jinks-Robertson (2000). "DNA mismatch repair and genetic instability." Annu Rev Genet **34**: 359-399.

Harwood, C. A., J. M. McGregor, C. M. Proby and J. Breuer (1999). "Human papillomavirus and the development of non-melanoma skin cancer." J Clin Pathol **52**(4): 249-53.

Hawn, M. T., A. Umar, J. M. Carethers, G. Marra, T. A. Kunkel, C. R. Boland and M. Koi (1995). "Evidence for a connection between the mismatch repair system and the G2 cell cycle checkpoint." Cancer Res **55**(17): 3721-5.

He, Y. Y., J. L. Huang and C. F. Chignell (2004). "Delayed and sustained activation of extracellular signal-regulated kinase in human keratinocytes by UVA: implications in carcinogenesis." J Biol Chem **279**(51): 53867-74.

Hefferin, M. L. and A. E. Tomkinson (2005). "Mechanism of DNA double-strand break repair by non-homologous end joining." DNA Repair (Amst) **4**(6): 639-48.

Hemmens, V. J. and D. E. Moore (1984). "Photo-oxidation of 6-mercaptopurine in aqueous solution." Chem Soc Perkin Trans II: 209-11.

Hemmens, V. J. and D. E. Moore (1986). "Photochemical sensitization by azathioprine and its metabolites--I. 6-Mercaptopurine." Photochem Photobiol **43**(3): 247-55.

Hemmens, V. J. and D. E. Moore (1986). "Photochemical sensitization by azathioprine and its metabolites--II. Azathioprine and nitroimidazole metabolites." Photochem Photobiol **43**(3): 257-62.

Henderson, P. T., J. C. Delaney, J. G. Muller, W. L. Neeley, S. R. Tannenbaum, C. J. Burrows and J. M. Essigmann (2003). "The hydantoin lesions formed from oxidation of 7,8-dihydro-8-oxoguanine are potent sources of replication errors in vivo." Biochemistry **42**(31): 9257-62.

Henle, E. S. and S. Linn (1997). "Formation, prevention, and repair of DNA damage by iron/hydrogen peroxide." J Biol Chem **272**(31): 19095-8.

Herman, M., T. Weinstein, A. Korzets, A. Chagnac, Y. Ori, D. Zevin, T. Malachi and U. Gafter (2001). "Effect of cyclosporin A on DNA repair and cancer incidence in kidney transplant recipients." J Lab Clin Med **137**(1): 14-20.

Hildesheim, J. and A. J. Fornace, Jr. (2004). "The dark side of light: the damaging effects of UV rays and the protective efforts of MAP kinase signaling in the epidermis." DNA Repair (Amst) **3**(6): 567-80.

Hirota, A., Y. Kawachi, K. Itoh, Y. Nakamura, X. Xu, T. Banno, T. Takahashi, M. Yamamoto and F. Otsuka (2005). "Ultraviolet A irradiation induces NF-E2-related factor 2 activation in dermal fibroblasts: protective role in UVA-induced apoptosis." J Invest Dermatol **124**(4): 825-32.

Hoeijmakers, J. H. (2001). "Genome maintenance mechanisms for preventing cancer." Nature **411**(6835): 366-74.

Ichihashi, M., M. Ueda, A. Budiyanto, T. Bito, M. Oka, M. Fukunaga, K. Tsuru and T. Horikawa (2003). "UV-induced skin damage." Toxicology **189**(1-2): 21-39.

Ikehata, H., S. Nakamura, T. Asamura and T. Ono (2004). "Mutation spectrum in sunlight-exposed mouse skin epidermis: small but appreciable contribution of oxidative stress-mediated mutagenesis." Mutat Res **556**(1-2): 11-24.

Jeggo, P. A. and M. Lobrich (2005). "Artemis links ATM to double strand break rejoining." Cell Cycle **4**(3): 359-62.

Jiricny, J. (2006). "The multifaceted mismatch-repair system." Nat Rev Mol Cell Biol **7**(5): 335-46.

Jiricny, J. and G. Marra (2003). "DNA repair defects in colon cancer." Curr Opin Genet Dev **13**(1): 61-9.

Kamiya, H., H. Miura, N. Murata-Kamiya, H. Ishikawa, T. Sakaguchi, H. Inoue, T. Sasaki, C. Masutani, F. Hanaoka, S. Nishimura, et al. (1995). "8-Hydroxyadenine (7,8-dihydro-8-oxoadenine) induces misincorporation in in

vitro DNA synthesis and mutations in NIH 3T3 cells." Nucleic Acids Res **23**(15): 2893-9.

Kamiya, H., T. Ueda, T. Ohgi, A. Matsukage and H. Kasai (1995). "Misincorporation of dAMP opposite 2-hydroxyadenine, an oxidative form of adenine." Nucleic Acids Res **23**(5): 761-6.

Kannouche, P. L., J. Wing and A. R. Lehmann (2004). "Interaction of human DNA polymerase eta with monoubiquitinated PCNA: a possible mechanism for the polymerase switch in response to DNA damage." Mol Cell **14**(4): 491-500.

Kaplan, H. S., K. C. Smith and P. Tomlin (1961). "Radiosensitization of E. coli by purine and pyrimidine analogues incorporated in deoxyribonucleic acid." Nature **190**: 794-6.

Kaplan, H. S., R. Zavarine and J. Earle (1962). "Interaction of the oxygen effect and radiosensitization produced by base analogues incorporated into deoxyribonuclease acid." Nature **194**: 662-4.

Karagas, M. R., G. L. Cushing, Jr., E. R. Greenberg, L. A. Mott, S. K. Spencer and D. W. Nierenberg (2001). "Non-melanoma skin cancers and glucocorticoid therapy." Br J Cancer **85**(5): 683-6.

Karran, P. (2000). "DNA double strand break repair in mammalian cells." Curr Opin Genet Dev **10**(2): 144-50.

Karran, P. and M. Bignami (1994). "DNA damage tolerance, mismatch repair and genome instability." Bioessays **16**(11): 833-9.

Karran, P. and M. G. Marinus (1982). "Mismatch correction at O6-methylguanine residues in E. coli DNA." Nature **296**(5860): 868-9.

Karran, P., J. Offman and M. Bignami (2003). "Human mismatch repair, drug-induced DNA damage, and secondary cancer." Biochimie **85**(11): 1149-60.

Kennedy, R. D. and A. D. D'Andrea (2005). "The Fanconi Anemia/BRCA pathway: new faces in the crowd." Genes Dev **19**(24): 2925-40.

Kielbassa, C. and B. Epe (2000). "DNA damage induced by ultraviolet and visible light and its wavelength dependence." Methods Enzymol **319**: 436-45.

Kim, M. Y., H. J. Park, S. C. Baek, D. G. Byun and D. Houh (2002). "Mutations of the p53 and PTCH gene in basal cell carcinomas: UV mutation signature and strand bias." J Dermatol Sci **29**(1): 1-9.

Kino, K. and H. Sugiyama (2005). "UVR-induced G-C to C-G transversions from oxidative DNA damage." Mutat Res **571**(1-2): 33-42.

Koch-Paiz, C. A., S. A. Amundson, M. L. Bittner, P. S. Meltzer and A. J. Fornace, Jr. (2004). "Functional genomics of UV radiation responses in human cells." Mutat Res **549**(1-2): 65-78.

Komeda, K., S. Iwamoto, S. Kominami and T. Ohnishi (1997). "Induction of cell killing, mutation and umu gene expression by 6-mercaptopurine or 2-thiouracil with UVA irradiation." Photochem Photobiol **65**(1): 115-8.

Kow, Y. W. (2002). "Repair of deaminated bases in DNA." Free Radic Biol Med **33**(7): 886-93.

Kozmin, S., G. Slezak, A. Reynaud-Angelin, C. Elie, Y. de Rycke, S. Boiteux and E. Sage (2005). "UVA radiation is highly mutagenic in cells that are unable to repair 7,8-dihydro-8-oxoguanine in Saccharomyces cerevisiae." Proc Natl Acad Sci U S A **102**(38): 13538-43.

Krokan, H. E., F. Drablos and G. Slupphaug (2002). "Uracil in DNA--occurrence, consequences and repair." Oncogene **21**(58): 8935-48.

Krynetski, E. and W. E. Evans (2003). "Drug methylation in cancer therapy: lessons from the TPMT polymorphism." Oncogene **22**(47): 7403-13.

Kunkel, T. A. and D. A. Erie (2005). "DNA mismatch repair." Annu Rev Biochem **74**: 681-710.

Lademann, J., U. Jacobi, H. Otberg, H.-J. Weigmann, H. Meffert, H. Schaefer, U. Blume-Peytavi and W. Sterry (2004). "In vivo determination of UV-photons entering into human skin." Laser Physics **14**(2): 234-7.

Laine, J. P., V. Mocquet and J. M. Egly (2006). "TFIIH enzymatic activities in transcription and nucleotide excision repair." Methods Enzymol **408**: 246-63.

Lehmann, A. R. (2002). "Replication of damaged DNA in mammalian cells: new solutions to an old problem." Mutat Res **509**(1-2): 23-34.

Lehmann, A. R. (2005). "Replication of damaged DNA by translesion synthesis in human cells." FEBS Lett **579**(4): 873-6.

Lehmann, A. R. (2006). "Clubbing together on clamps: The key to translesion synthesis." DNA Repair (Amst) **5**(3): 404-7.

Lennard, L., S. Thomas, C. I. Harrington and J. L. Maddocks (1985). "Skin cancer in renal transplant recipients is associated with increased concentrations of 6-thioguanine nucleotide in red blood cells." Br J Dermatol **113**(6): 723-9.

Leppard, J. B., Z. Dong, Z. B. Mackey and A. E. Tomkinson (2003). "Physical and functional interaction between DNA ligase IIIalpha and poly(ADP-Ribose) polymerase 1 in DNA single-strand break repair." Mol Cell Biol **23**(16): 5919-27.

Limoli, C. L., E. Giedzinski, W. M. Bonner and J. E. Cleaver (2002). "UV-induced replication arrest in the xeroderma pigmentosum variant leads to DNA double-strand breaks, gamma -H2AX formation, and Mre11 relocalization." Proc Natl Acad Sci U S A **99**(1): 233-8.

Lin, X. and S. B. Howell (1999). "Effect of loss of DNA mismatch repair on development of topotecan-, gemcitabine-, and paclitaxel-resistant variants after exposure to cisplatin." Mol Pharmacol **56**(2): 390-5.

Lind, M. H., B. Rozell, R. P. Wallin, M. van Hogerlinden, H. G. Ljunggren, R. Toftgard and I. Sur (2004). "Tumor necrosis factor receptor 1-mediated signaling is required for skin cancer development induced by NF-kappaB inhibition." Proc Natl Acad Sci U S A **101**(14): 4972-7.

Lindahl, T. (1993). "Instability and decay of the primary structure of DNA." Nature **362**(6422): 709-15.

Lindahl, T. (2001). "Keynote: past, present, and future aspects of base excision repair." Prog Nucleic Acid Res Mol Biol **68**: xvii-xxx.

Lindahl, T. and R. D. Wood (1999). "Quality control by DNA repair." Science **286**(5446): 1897-905.

Lindelof, B., J. Jarnvik, A. Ternesten-Bratel, F. Granath and M. A. Hedblad (2006). "Mortality and clinicopathological features of cutaneous squamous cell carcinoma in organ transplant recipients: a study of the Swedish cohort." Acta Derm Venereol **86**(3): 219-22.

Ling, G., A. Ahmadian, A. Persson, A. B. Unden, G. Afink, C. Williams, M. Uhlen, R. Toftgard, J. Lundeberg and F. Ponten (2001). "PATCHED and p53 gene alterations in sporadic and hereditary basal cell cancer." Oncogene **20**(53): 7770-8.

Liu, Y. and S. C. West (2004). "Happy Hollidays: 40th anniversary of the Holliday junction." Nat Rev Mol Cell Biol **5**(11): 937-44.

Lobrich, M. and P. A. Jeggo (2005). "Harmonising the response to DSBs: a new string in the ATM bow." DNA Repair (Amst) **4**(7): 749-59.

Lodygin, D., A. S. Yazdi, C. A. Sander, T. Herzinger and H. Hermeking (2003). "Analysis of 14-3-3sigma expression in hyperproliferative skin diseases reveals selective loss associated with CpG-methylation in basal cell carcinoma." Oncogene **22**(35): 5519-24.

Loercher, A., T. L. Lee, J. L. Ricker, A. Howard, J. Geoghegen, Z. Chen, J. B. Sunwoo, R. Sitcheran, E. Y. Chuang, J. B. Mitchell, et al. (2004). "Nuclear factor-kappaB is an important modulator of the altered gene expression profile and malignant phenotype in squamous cell carcinoma." Cancer Res **64**(18): 6511-23.

Lombard, D. B., K. F. Chua, R. Mostoslavsky, S. Franco, M. Gostissa and F. W. Alt (2005). "DNA repair, genome stability, and aging." Cell **120**(4): 497-512.

MacRobert, A. J., S. G. Bown and D. Phillips (1989). "What are the ideal photoproperties for a sensitizer?" Ciba Found Symp **146**: 4-12; discussion 12-16.

Malkhosyan, S., N. Rampino, H. Yamamoto and M. Perucho (1996). "Frameshift mutator mutations." Nature **382**(6591): 499-500.

Margison, G. P. and M. F. Santibanez-Koref (2002). "O6-alkylguanine-DNA alkyltransferase: role in carcinogenesis and chemotherapy." Bioessays **24**(3): 255-66.

Marnett, L. J. (2000). "Oxyradicals and DNA damage." Carcinogenesis **21**(3): 361-70.

Massey, A., Y. Z. Xu and P. Karran (2001). "Photoactivation of DNA thiobases as a potential novel therapeutic option." Curr Biol **11**(14): 1142-6.

McGlynn, P. and R. G. Lloyd (2002). "Recombinational repair and restart of damaged replication forks." Nat Rev Mol Cell Biol **3**(11): 859-70.

McKinnon, P. J. (2004). "ATM and ataxia telangiectasia." EMBO Rep **5**(8): 772-6.

Middleton, M. R. and G. P. Margison (2003). "Improvement of chemotherapy efficacy by inactivation of a DNA-repair pathway." Lancet Oncol **4**(1): 37-44.

Milligan, J. R., Limoli, C.L., Wu, C.C.L., Ng, J.Y.-Y., Ward, J.F. (1995). Radiation damage in DNA : structure/function relationships at early times : International workshop : Papers. Columbus, Ohio, Battelle Press.

Mitchell, J. R., J. H. Hoeijmakers and L. J. Niedernhofer (2003). "Divide and conquer: nucleotide excision repair battles cancer and ageing." Curr Opin Cell Biol **15**(2): 232-40.

Moore, D. E., R. H. Sik, P. Bilski, C. F. Chignell and K. J. Reszka (1994). "Photochemical sensitization by azathioprine and its metabolites. Part 3. A direct EPR and spin-trapping study of light-induced free radicals from 6-mercaptopurine and its oxidation products." Photochem Photobiol **60**(6): 574-81.

Moshous, D., I. Callebaut, R. de Chasseval, B. Corneo, M. Cavazzana-Calvo, F. Le Deist, I. Tezcan, O. Sanal, Y. Bertrand, N. Philippe, et al. (2001). "Artemis, a novel DNA double-strand break repair/V(D)J recombination protein, is mutated in human severe combined immune deficiency." Cell **105**(2): 177-86.

Naryzhny, S. N., H. Zhao and H. Lee (2005). "Proliferating cell nuclear antigen (PCNA) may function as a double homotrimer complex in the mammalian cell." J Biol Chem **280**(14): 13888-94.

Neill, G. W., L. R. Ghali, J. L. Green, M. S. Ikram, M. P. Philpott and A. G. Quinn (2003). "Loss of protein kinase Calpha expression may enhance the tumorigenic potential of Gli1 in basal cell carcinoma." Cancer Res **63**(15): 4692-7.

Newlands, E. S., T. Foster and S. Zaknoen (2003). "Phase I study of temozolamide (TMZ) combined with procarbazine (PCB) in patients with gliomas." Br J Cancer **89**(2): 248-51.

Nicolas, M., A. Wolfer, K. Raj, J. A. Kummer, P. Mill, M. van Noort, C. C. Hui, H. Clevers, G. P. Dotto and F. Radtke (2003). "Notch1 functions as a tumor suppressor in mouse skin." Nat Genet **33**(3): 416-21.

O'Driscoll, M., K. M. Cerosaletti, P. M. Girard, Y. Dai, M. Stumm, B. Kysela, B. Hirsch, A. Gennery, S. E. Palmer, J. Seidel, et al. (2001). "DNA ligase IV mutations identified in patients exhibiting developmental delay and immunodeficiency." Mol Cell **8**(6): 1175-85.

O'Driscoll, M., A. R. Gennery, J. Seidel, P. Concannon and P. A. Jeggo (2004). "An overview of three new disorders associated with genetic instability: LIG4 syndrome, RS-SCID and ATR-Seckel syndrome." DNA Repair (Amst) **3**(8-9): 1227-35.

Oei, S. L. and M. Ziegler (2000). "ATP for the DNA ligation step in base excision repair is generated from poly(ADP-ribose)." J Biol Chem **275**(30): 23234-9.

Offman, J., G. Opelz, B. Doehler, D. Cummins, O. Halil, N. R. Banner, M. M. Burke, D. Sullivan, P. Macpherson and P. Karran (2004). "Defective DNA mismatch repair in acute myeloid leukemia/myelodysplastic syndrome after organ transplantation." Blood **104**(3): 822-8.

Palmer, C. M., D. M. Serafini and H. E. Schellhorn (1997). "Near ultraviolet radiation (UVA and UVB) causes a formamidopyrimidine glycosylase-dependent increase in G to T transversions." Photochem Photobiol **65**(3): 543-9.

Parikh, S. S., C. D. Mol, G. Slupphaug, S. Bharati, H. E. Krokan and J. A. Tainer (1998). "Base excision repair initiation revealed by crystal structures and binding kinetics of human uracil-DNA glycosylase with DNA." Embo J **17**(17): 5214-26.

Pastink, A., J. C. Eeken and P. H. Lohman (2001). "Genomic integrity and the repair of double-strand DNA breaks." Mutat Res **480-481**: 37-50.

Pastoriza Gallego, M. and A. Sarasin (2003). "Transcription-coupled repair of 8-oxoguanine in human cells and its deficiency in some DNA repair diseases." Biochimie **85**(11): 1073-82.

Paunel, A. N., A. Dejam, S. Thelen, M. Kirsch, M. Horstjann, P. Gharini, M. Murtz, M. Kelm, H. de Groot, V. Kolb-Bachofen, et al. (2005). "Enzyme-independent nitric oxide formation during UVA challenge of human skin: characterization, molecular sources, and mechanisms." Free Radic Biol Med **38**(5): 606-15.

Pegg, A. E. (2000). "Repair of O(6)-alkylguanine by alkyltransferases." Mutat Res **462**(2-3): 83-100.

Peltomaki, P. (2003). "Role of DNA mismatch repair defects in the pathogenesis of human cancer." J Clin Oncol **21**(6): 1174-9.

Pfeifer, G. P., Y. H. You and A. Besaratinia (2005). "Mutations induced by ultraviolet light." Mutat Res **571**(1-2): 19-31.

Pike, M. G., C. L. Franklin, D. C. Mays, J. J. Lipsky, P. W. Lowry and W. J. Sandborn (2001). "Improved methods for determining the concentration of 6-thioguanine nucleotides and 6-methylmercaptopurine nucleotides in blood." J Chromatogr B Biomed Sci Appl **757**(1): 1-9.

Ping, X. L., D. Ratner, H. Zhang, X. L. Wu, M. J. Zhang, F. F. Chen, D. N. Silvers, M. Peacocke and H. C. Tsou (2001). "PTCH mutations in squamous cell carcinoma of the skin." J Invest Dermatol **116**(4): 614-6.

Poppe, D., I. Tiede, G. Fritz, C. Becker, B. Bartsch, S. Wirtz, D. Strand, S. Tanaka, P. R. Galle, X. R. Bustelo, et al. (2006). "Azathioprine suppresses ezrin-radixin-moesin-dependent T cell-APC conjugation through inhibition of Vav guanosine exchange activity on Rac proteins." J Immunol **176**(1): 640-51.

Prasad, R., O. I. Lavrik, S. J. Kim, P. Kedar, X. P. Yang, B. J. Vande Berg and S. H. Wilson (2001). "DNA polymerase beta -mediated long patch base excision repair. Poly(ADP-ribose)polymerase-1 stimulates strand displacement DNA synthesis." J Biol Chem **276**(35): 32411-4.

Presta, M., M. Belleri, A. Vacca and D. Ribatti (2002). "Anti-angiogenic activity of the purine analog 6-thioguanine." Leukemia **16**(8): 1490-9.

Qiao, W., A. G. Li, P. Owens, X. Xu, X. J. Wang and C. X. Deng (2006). "Hair follicle defects and squamous cell carcinoma formation in Smad4 conditional knockout mouse skin." Oncogene **25**(2): 207-17.

Quemeneur, L., L. M. Gerland, M. Flacher, M. Ffrench, J. P. Revillard and L. Genestier (2003). "Differential control of cell cycle, proliferation, and survival of primary T lymphocytes by purine and pyrimidine nucleotides." J Immunol **170**(10): 4986-95.

Quinn, A. G. and E. Epstein, Jr. (2003). "Patched, hedgehog, and skin cancer." Methods Mol Biol **222**: 85-95.

Rackwitz, H. R. and K. H. Scheit (1974). "Die synthese von purinnucleosid-6-sulfonaten." Chem Ber **107**: 2284-94.

Raffel, C., R. B. Jenkins, L. Frederick, D. Hebrink, B. Alderete, D. W. Fults and C. D. James (1997). "Sporadic medulloblastomas contain PTCH mutations." Cancer Res **57**(5): 842-5.

Ralf, C., I. D. Hickson and L. Wu (2006). "The Bloom's syndrome helicase can promote the regression of a model replication fork." J Biol Chem.

Ramos, J., J. Villa, A. Ruiz, R. Armstrong and J. Matta (2004). "UV dose determines key characteristics of nonmelanoma skin cancer." Cancer Epidemiol Biomarkers Prev **13**(12): 2006-11.

Reelfs, O., R. M. Tyrrell and C. Pourzand (2004). "Ultraviolet a radiation-induced immediate iron release is a key modulator of the activation of NF-kappaB in human skin fibroblasts." J Invest Dermatol **122**(6): 1440-7.

Reeve, V. E., G. E. Greenoak, C. H. Gallagher, P. J. Canfield and F. J. Wilkinson (1985). "Effect of immunosuppressive agents and sunscreens on UV carcinogenesis in the hairless mouse." Aust J Exp Biol Med Sci **63 (Pt 6)**: 655-65.

Regl, G., G. W. Neill, T. Eichberger, M. Kasper, M. S. Ikram, J. Koller, H. Hintner, A. G. Quinn, A. M. Frischauf and F. Aberger (2002). "Human GLI2 and GLI1 are part of a positive feedback mechanism in Basal Cell Carcinoma." Oncogene **21**(36): 5529-39.

Relling, M. V. and T. Dervieux (2001). "Pharmacogenetics and cancer therapy." Nat Rev Cancer **1**(2): 99-108.

Relling, M. V., J. E. Rubnitz, G. K. Rivera, J. M. Boyett, M. L. Hancock, C. A. Felix, L. E. Kun, A. W. Walter, W. E. Evans and C. H. Pui (1999). "High incidence of secondary brain tumours after radiotherapy and antimetabolites." Lancet **354**(9172): 34-9.

Rochette, P. J., J. P. Therrien, R. Drouin, D. Perdiz, N. Bastien, E. A. Drobetsky and E. Sage (2003). "UVA-induced cyclobutane pyrimidine dimers form predominantly at thymine-thymine dipyrimidines and correlate with the mutation spectrum in rodent cells." Nucleic Acids Res **31**(11): 2786-94.

Rubin, A. I., E. H. Chen and D. Ratner (2005). "Basal-cell carcinoma." N Engl J Med **353**(21): 2262-9.

Sambrook, J. and D. W. Russell (2001). Molecular cloning : a laboratory manual. Cold Spring Harbor, N.Y., Cold Spring Harbor Laboratory Press.

Sampson, J. R., S. Jones, S. Dolwani and J. P. Cheadle (2005). "MutYH (MYH) and colorectal cancer." Biochem Soc Trans **33**(Pt 4): 679-83.

Schieke, S. M., K. Ruwiedel, H. Gers-Barlag, S. Grether-Beck and J. Krutmann (2005). "Molecular crosstalk of the ultraviolet a and ultraviolet B signaling responses at the level of mitogen-activated protein kinases." J Invest Dermatol **124**(4): 857-9.

Sedgwick, B. and T. Lindahl (2002). "Recent progress on the Ada response for inducible repair of DNA alkylation damage." Oncogene **21**(58): 8886-94.

Seeberg, E., L. Luna, I. Morland, L. Eide, B. Johnsen, E. Larsen, I. Alseth, F. Dantzer, K. Baynton, R. Aamodt, et al. (2000). "Base removers and strand scissors: different strategies employed in base excision and strand incision at modified base residues in DNA." Cold Spring Harb Symp Quant Biol **65**: 135-42.

Setlow, R. B., A. D. Woodhead and E. Grist (1989). "Animal model for ultraviolet radiation-induced melanoma: platyfish-swordtail hybrid." Proc Natl Acad Sci U S A **86**(22): 8922-6.

Sheehan, J. M., N. Cragg, C. A. Chadwick, C. S. Potten and A. R. Young (2002). "Repeated ultraviolet exposure affords the same protection against DNA photodamage and erythema in human skin types II and IV but is associated with faster DNA repair in skin type IV." J Invest Dermatol **118**(5): 825-9.

Sinha, R. P. and D. P. Hader (2002). "UV-induced DNA damage and repair: a review." Photochem Photobiol Sci **1**(4): 225-36.

Somerville, L., E. Y. Krynetski, N. F. Krynetskaia, R. D. Beger, W. Zhang, C. A. Marhefka, W. E. Evans and R. W. Kriwacki (2003). "Structure and dynamics of thioguanine-modified duplex DNA." J Biol Chem **278**(2): 1005-11.

Sonntag, C. v. (1987). The chemical basis of radiation biology. London, Taylor & Francis.

Sosman, J. A. and I. Puzanov (2006). "Molecular targets in melanoma from angiogenesis to apoptosis." Clin Cancer Res **12**(7 Pt 2): 2376s-2383s.

Stockfleth, E., C. Ulrich, T. Meyer, R. Arndt and E. Christophers (2001). "Skin diseases following organ transplantation--risk factors and new therapeutic approaches." Transplant Proc **33**(1-2): 1848-53.

Sung, J. S. and B. Demple (2006). "Roles of base excision repair subpathways in correcting oxidized abasic sites in DNA." Febs J **273**(8): 1620-9.

Svejstrup, J. Q. (2002). "Mechanisms of transcription-coupled DNA repair." Nat Rev Mol Cell Biol **3**(1): 21-9.

Svejstrup, J. Q. (2003). "Rescue of arrested RNA polymerase II complexes." J Cell Sci **116**(Pt 3): 447-51.

Swann, P. F., T. R. Waters, D. C. Moulton, Y. Z. Xu, Q. Zheng, M. Edwards and R. Mace (1996). "Role of postreplicative DNA mismatch repair in the cytotoxic action of thioguanine." Science **273**(5278): 1109-11.

Taylor, A. E. and S. Shuster (1992). "Skin cancer after renal transplantation: the causal role of azathioprine." Acta Derm Venereol **72**(2): 115-9.

Thayer, S. P., M. P. di Magliano, P. W. Heiser, C. M. Nielsen, D. J. Roberts, G. Y. Lauwers, Y. P. Qi, S. Gysin, C. Fernandez-del Castillo, V. Yajnik, et al. (2003). "Hedgehog is an early and late mediator of pancreatic cancer tumorigenesis." Nature **425**(6960): 851-6.

Tiede, I., G. Fritz, S. Strand, D. Poppe, R. Dvorsky, D. Strand, H. A. Lehr, S. Wirtz, C. Becker, R. Atreya, et al. (2003). "CD28-dependent Rac1 activation is the molecular target of azathioprine in primary human CD4+ T lymphocytes." J Clin Invest **111**(8): 1133-45.

Todo, T. (1999). "Functional diversity of the DNA photolyase/blue light receptor family." Mutat Res **434**(2): 89-97.

Tournas, J. A., F. H. Lin, J. A. Burch, M. A. Selim, N. A. Monteiro-Riviere, J. E. Zielinski and S. R. Pinnell (2006). "Ubiquinone, idebenone, and kinetin provide ineffective photoprotection to skin when compared to a topical antioxidant combination of vitamins C and E with ferulic acid." J Invest Dermatol **126**(5): 1185-7.

Trewick, S. C., T. F. Henshaw, R. P. Hausinger, T. Lindahl and B. Sedgwick (2002). "Oxidative demethylation by Escherichia coli AlkB directly reverts DNA base damage." Nature **419**(6903): 174-8.

Ulrich, H. D. (2004). "How to activate a damage-tolerant polymerase: consequences of PCNA modifications by ubiquitin and SUMO." Cell Cycle **3**(1): 15-8.

Ulrich, H. D. (2005). "Mutual interactions between the SUMO and ubiquitin systems: a plea of no contest." Trends Cell Biol **15**(10): 525-32.

Ulrich, H. D., S. Vogel and A. A. Davies (2005). "SUMO keeps a check on recombination during DNA replication." Cell Cycle **4**(12): 1699-702.

Van Komen, S., G. Petukhova, S. Sigurdsson and P. Sung (2002). "Functional cross-talk among Rad51, Rad54, and replication protein A in heteroduplex DNA joint formation." J Biol Chem **277**(46): 43578-87.

Varon, R., C. Vissinga, M. Platzer, K. M. Cerosaletti, K. H. Chrzanowska, K. Saar, G. Beckmann, E. Seemanova, P. R. Cooper, N. J. Nowak, et al. (1998). "Nibrin, a novel DNA double-strand break repair protein, is mutated in Nijmegen breakage syndrome." Cell **93**(3): 467-76.

Veness, M. J., D. I. Quinn, C. S. Ong, A. M. Keogh, P. S. Macdonald, S. G. Cooper and G. W. Morgan (1999). "Aggressive cutaneous malignancies following cardiothoracic transplantation: the Australian experience." Cancer **85**(8): 1758-64.

Villemure, J. F., C. Abaji, I. Cousineau and A. Belmaaza (2003). "MSH2-deficient human cells exhibit a defect in the accurate termination of homology-directed repair of DNA double-strand breaks." Cancer Res **63**(12): 3334-9.

Vogt, A., P. T. Chuang, J. Hebert, J. Hwang, Y. Lu, L. Kopelovich, M. Athar, D. R. Bickers and E. H. Epstein, Jr. (2004). "Immunoprevention of basal cell carcinomas with recombinant hedgehog-interacting protein." J Exp Med **199**(6): 753-61.

Wang, H. and J. B. Hays (2004). "Signaling from DNA mispairs to mismatch-repair excision sites despite intervening blockades." Embo J **23**(10): 2126-33.

Ward, J. F. (1994). "The complexity of DNA damage: relevance to biological consequences." Int J Radiat Biol **66**(5): 427-32.

Ward, J. F. (2000). "Complexity of damage produced by ionizing radiation." Cold Spring Harb Symp Quant Biol **65**: 377-82.

Warren, D. J., A. Andersen and L. Slordal (1995). "Quantitation of 6-thioguanine residues in peripheral blood leukocyte DNA obtained from patients receiving 6-mercaptopurine-based maintenance therapy." Cancer Res **55**(8): 1670-4.

Warren, D. J. and L. Slordal (1993). "A high-performance liquid chromatographic method for the determination of 6-thioguanine residues in DNA using precolumn derivatization and fluorescence detection." Anal Biochem **215**(2): 278-83.

Wertz, K., P. B. Hunziker, N. Seifert, G. Riss, M. Neeb, G. Steiner, W. Hunziker and R. Goralczyk (2005). "beta-Carotene interferes with ultraviolet light A-induced gene expression by multiple pathways." J Invest Dermatol **124**(2): 428-34.

West, S. C. (2003). "Molecular views of recombination proteins and their control." Nat Rev Mol Cell Biol **4**(6): 435-45.

Wicking, C., I. Smyth and A. Bale (1999). "The hedgehog signalling pathway in tumorigenesis and development." Oncogene **18**(55): 7844-51.

Wiederhold, L., J. B. Leppard, P. Kedar, F. Karimi-Busheri, A. Rasouli-Nia, M. Weinfeld, A. E. Tomkinson, T. Izumi, R. Prasad, S. H. Wilson, et al. (2004). "AP endonuclease-independent DNA base excision repair in human cells." Mol Cell **15**(2): 209-20.

Williams, J. A., O. M. Guicherit, B. I. Zaharian, Y. Xu, L. Chai, H. Wichterle, C. Kon, C. Gatchalian, J. A. Porter, L. L. Rubin, et al. (2003). "Identification of a small molecule inhibitor of the hedgehog signaling pathway: effects on basal cell carcinoma-like lesions." Proc Natl Acad Sci U S A **100**(8): 4616-21.

Wolter, M., J. Reifenberger, C. Sommer, T. Ruzicka and G. Reifenberger (1997). "Mutations in the human homologue of the Drosophila segment polarity gene patched (PTCH) in sporadic basal cell carcinomas of the skin and primitive neuroectodermal tumors of the central nervous system." Cancer Res **57**(13): 2581-5.

Wood, R. D., M. Mitchell and T. Lindahl (2005). "Human DNA repair genes, 2005." Mutat Res **577**(1-2): 275-83.

Wulf, H. C., J. Sandby-Moller, T. Kobayasi and R. Gniadecki (2004). "Skin aging and natural photoprotection." Micron **35**(3): 185-91.

Yavin, E., A. K. Boal, E. D. Stemp, E. M. Boon, A. L. Livingston, V. L. O'Shea, S. S. David and J. K. Barton (2005). "Protein-DNA charge transport: redox activation of a DNA repair protein by guanine radical." Proc Natl Acad Sci U S A **102**(10): 3546-51.

Yoshioka, K., Y. Yoshioka and P. Hsieh (2006). "ATR kinase activation mediated by MutSalpha and MutLalpha in response to cytotoxic O6-methylguanine adducts." Mol Cell **22**(4): 501-10.

Yuan, C. Q., Y. N. Li and X. F. Zhang (2004). "Down-regulation of apoptosis-inducing factor protein by RNA interference inhibits UVA-induced cell death." Biochem Biophys Res Commun **317**(4): 1108-13.

Yung, W. K., R. E. Albright, J. Olson, R. Fredericks, K. Fink, M. D. Prados, M. Brada, A. Spence, R. J. Hohl, W. Shapiro, et al. (2000). "A phase II study of temozolomide vs. procarbazine in patients with glioblastoma multiforme at first relapse." Br J Cancer **83**(5): 588-93.

Zaphiropoulos, P. G., A. B. Unden, F. Rahnama, R. E. Hollingsworth and R. Toftgard (1999). "PTCH2, a novel human patched gene, undergoing alternative splicing and up-regulated in basal cell carcinomas." Cancer Res **59**(4): 787-92.

Zhong, J. L., A. Yiakouvaki, P. Holley, R. M. Tyrrell and C. Pourzand (2004). "Susceptibility of skin cells to UVA-induced necrotic cell death reflects the intracellular level of labile iron." J Invest Dermatol **123**(4): 771-80.

7 Appendix

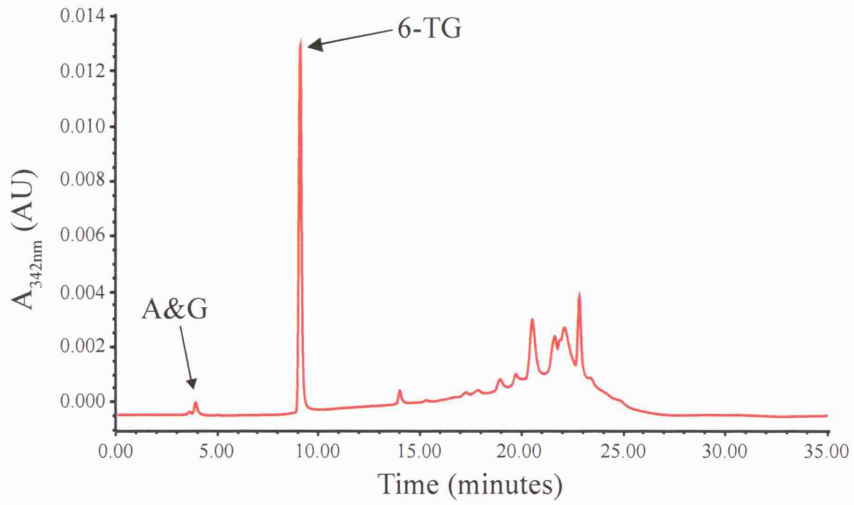

Fig 7.1 Resolution of 6-TG from Adenine and Guanine by RP-HPLC Coupled to A_{342nm} Detection. RP-HPLC coupled to A_{342nm} detection separates 6-TG from other purines in a DNA acid hydrolysate. A solution of acid hydrolysed DNA was spiked with 6-TG to give a final 6-TG concentration of 10μM. 100μl of the resulting solution was analysed by RP-HPLC with Abs_{342nm} detection. Adenine and guanine co-eluted at 4.0 minutes. 6-TG elutes at 9.0 minutes.

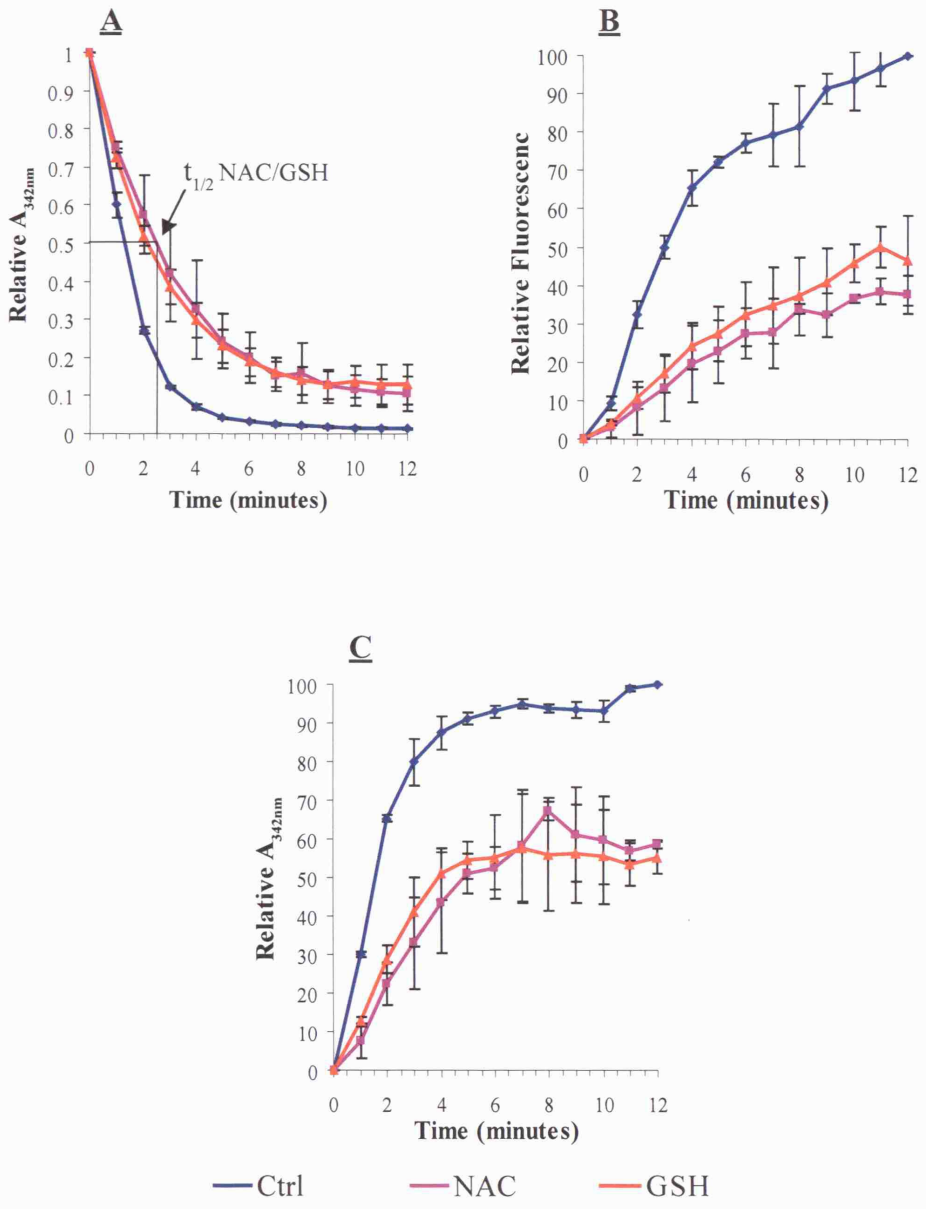

Fig 7.2 Anti-Oxidants Decrease the Rates of 6-TG/UVA Photoreactions. H_2O, NAC or GSH were added to a solution of 6-TG prior to UVA irradiation at a dose rate of 0.1kJ/m^2/s. During irradiation samples were analysed every 60 seconds by RP-HPLC coupled to A_{342nm}, A_{260nm} and fluorescence detection. **A** NAC and GSH increase the $t_{1/2}$ of 6-TG by approximately 60% . The rate of destruction was significantly decreased. Initial slope over first 2 minutes increased from -0.37min^{-1} to -0.21min^{-1} and -0.24min^{-1} with NAC and GSH, respectively. **B** & **C** Anti-oxidants decrase the rate of formation of G-6-SO_3 and G-S-G 4-fold (NAC) and 3-fold (GSH). Final levels of photoproducts were also lower than control samples (40% and 60% of control, respectively).

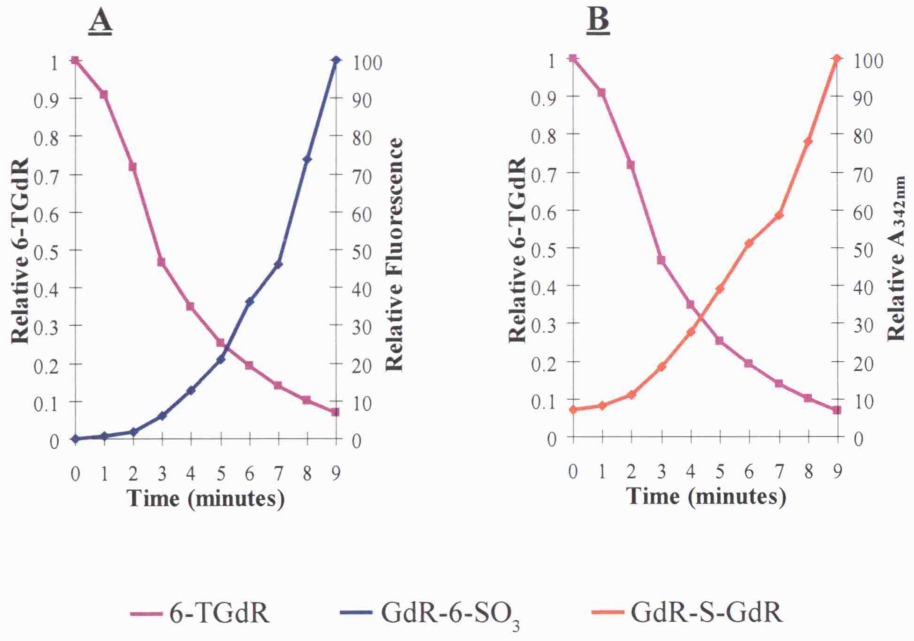

Fig 7.3 Kinetics of 6-TGdR/UVA Photoreactions. A solution of 6-TGdR was UVA irradiated at a dose rate of 0.1kJ/m^2/s. Samples were taken and analysed by RP-HPLC coupled to A_{342nm}, A_{260nm} and fluorescence detection. All relative absorbance and fluorescence measurements were calculated from peak areas. **A** 6-TGdR is destroyed and G-6-SO_3dR is formed after UVA irradiation. **B** GdR-S-GdR is also formed after UVA of 6-TGdR. Kinetics of 6-TGdR destruction and photoproduct formation are slower than for 6-TG base.

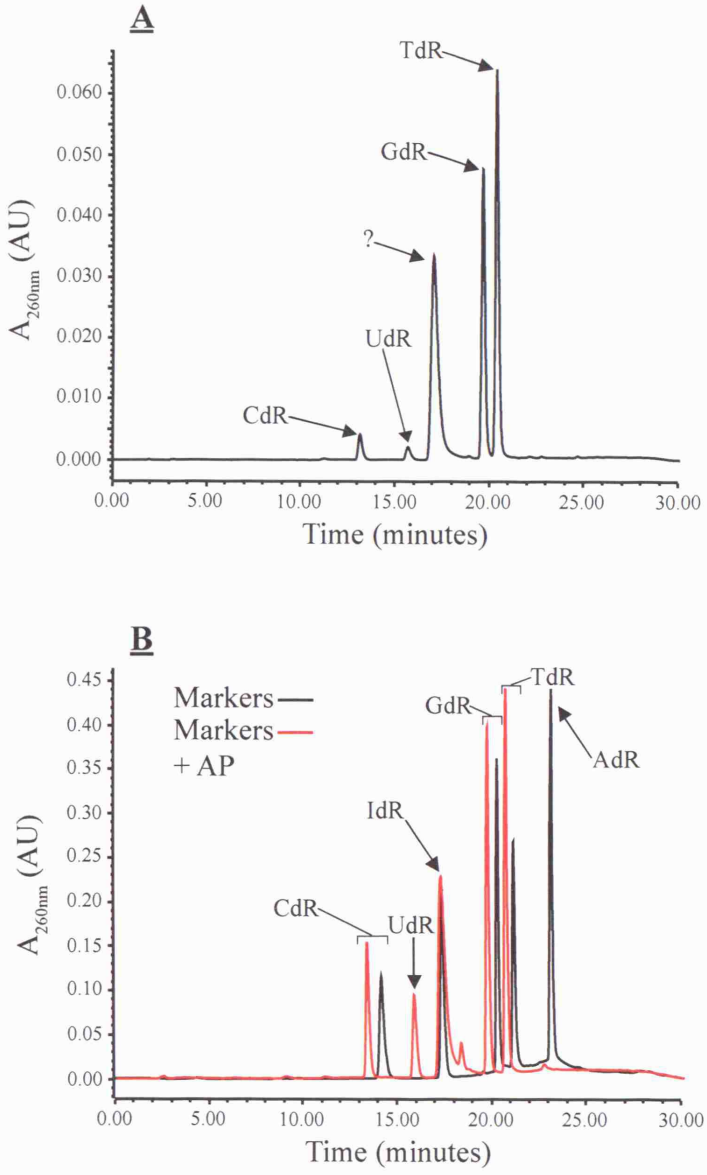

Fig 7.4 Digestion of Oligonucleotides and Conversion of Adenosine to Inosine. **A** Nucleotides can be separated by RP-HPLC after digestion of oligonucleotide. An 18mer oligonucleotide was digested to nucleoside level with Nuclease P1 and Acid Phosphatase (AP), and analysed by RP-HPLC coupled to A_{260nm} detection. Peaks matching CdR, UdR, GdR and TdR were all clearly visible. No peak for AdR was found. An unknown peak was observed (?). **B** Acid phosphatase contaminant is deaminating adenosine to inosine. Nucleoside markers (black) were treated with Acid Phosphatase as in A (red). The A_{260nm} AdR signal was virtually abolished, and a peak at the position of IdR was observed. The amount of IdR was identical to the expected amount of AdR.

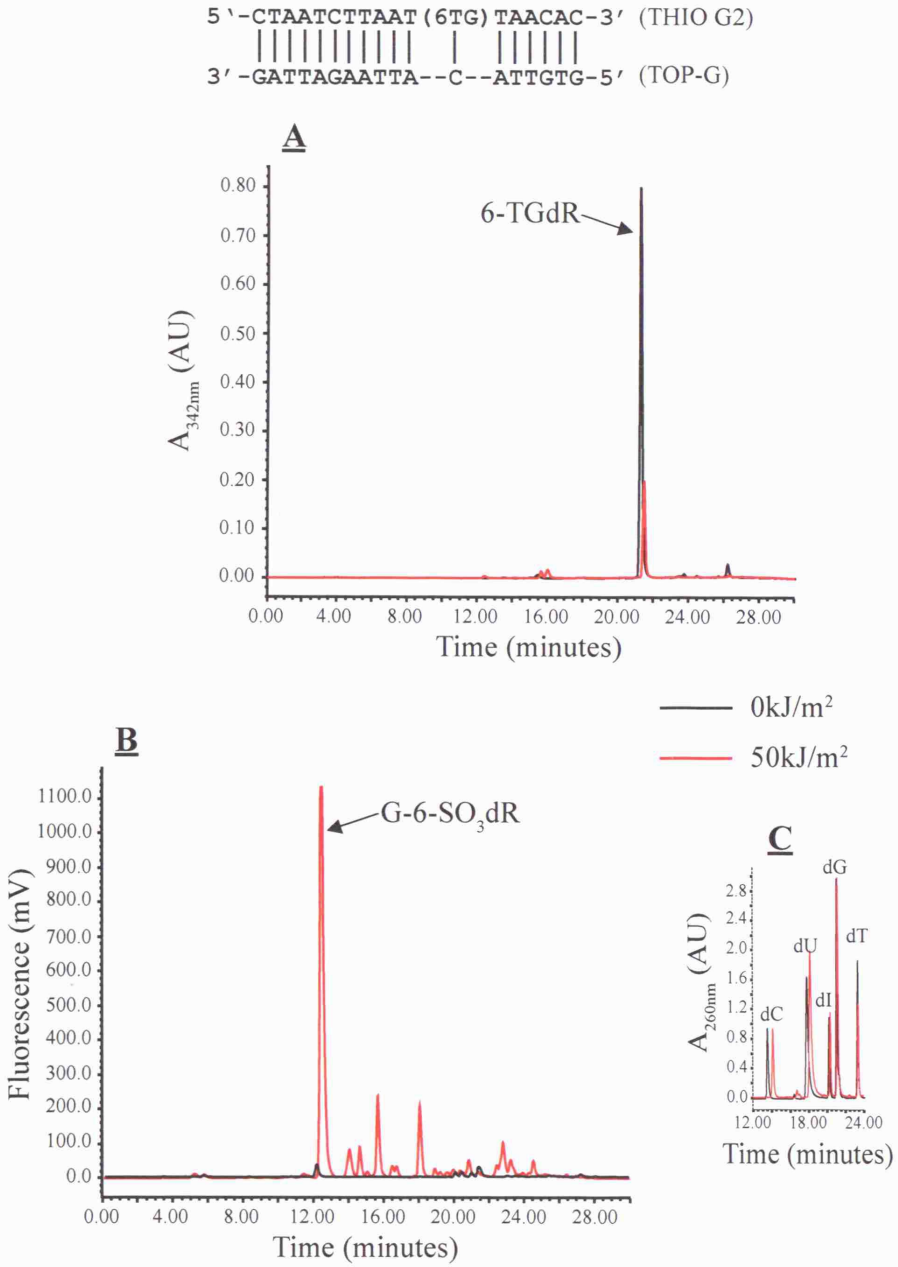

Fig 7.5 6-TG/UVA Photoreactions in dsDNA. A double stranded oligonucleotide (as shown above), was irradiated in solution with 50kJ/m^2 UVA, enzymatically digested to nucleosides and anlaysed by RP-HPLC coupled to A_{342nm}, A_{260nm} and fluorescence detection. **A** After UVA, there is a marked decrease in the A_{342nm} signal for 6-TGdR. After 50kJ/m^2 UVA, less than 20% 6-TGdR remains. **B** The decrease in 6-TGdR signal is accompanied by an increase in fluorescence signal at the elution position of G-6-SO_3dR. **C** UVA has no effect on the other components of the double stranded oligonucleotide.

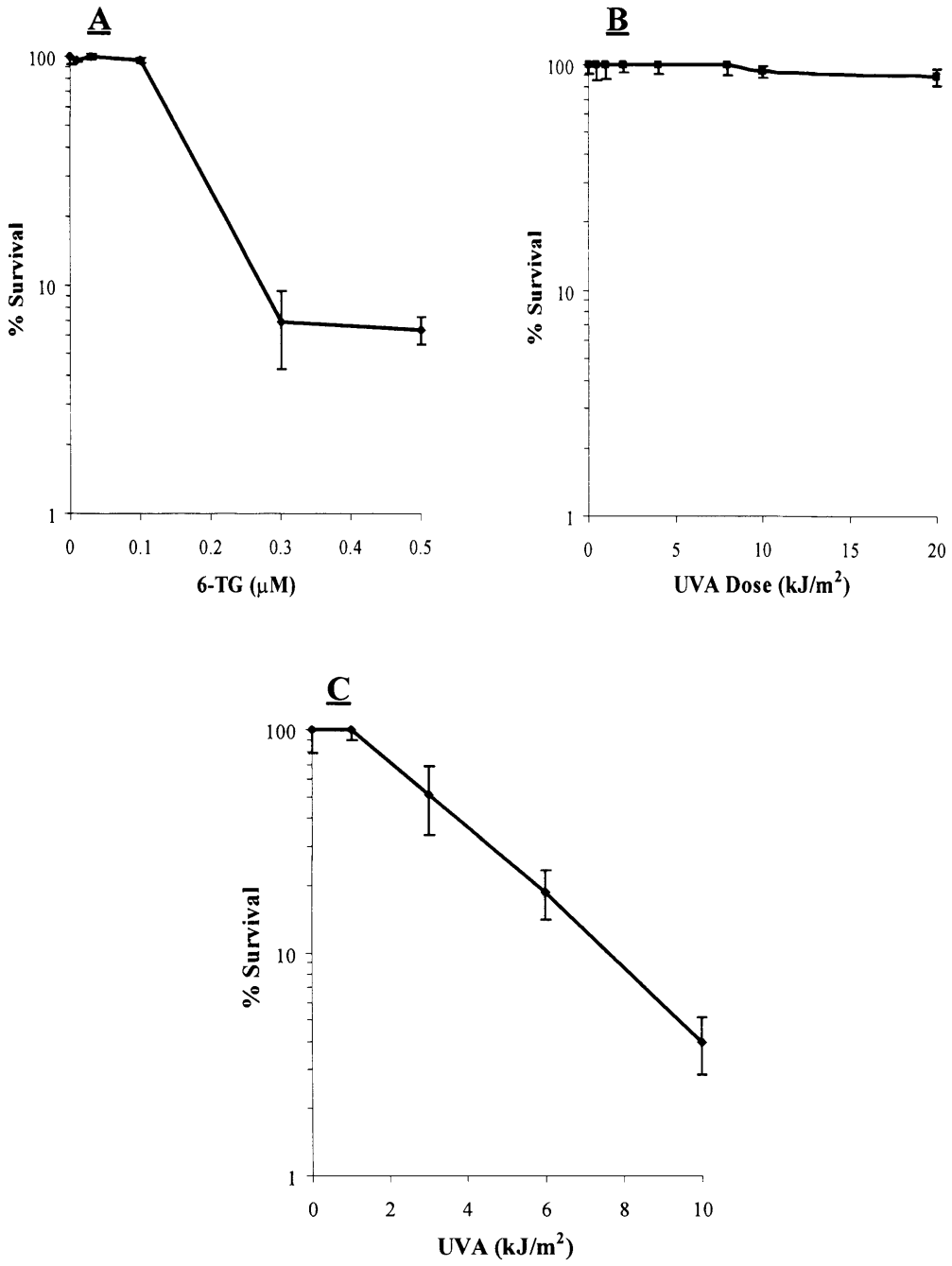

Fig 7.6 6-TG Sensitises CHO D422 to UVA. A Growth in 6-TG concentrations greater than 0.1μM are lethal. CHO D422 cells were grown for 10 days in the indicated concentrations of 6-TG. Survival was determined by clonogenic assay. B UVA doses up to 20kJ/m^2 showed no effect on survival. CHO D422 cells were irradiated with UVA at a dose rate of 0.1kJ/m^2/s. Cells were grown for 10 days post-UVA, and survival determined by clonogenic assay. C 6-TG Sensitises CHO D422 cells to UVA. CHO D422 cells were grown in 0.1μM 6-TG for 48 hours, and exposed to the indicated dose of UVA. Treatment with 6-TG resulted in a D_{37} of 4.0kJ/m^2 for UVA. Combined treatment showed no lethality at a UVA dose of 1.0kJ/m^2. Survival determined by clonogenic assay. Data shown is average of three experiments.

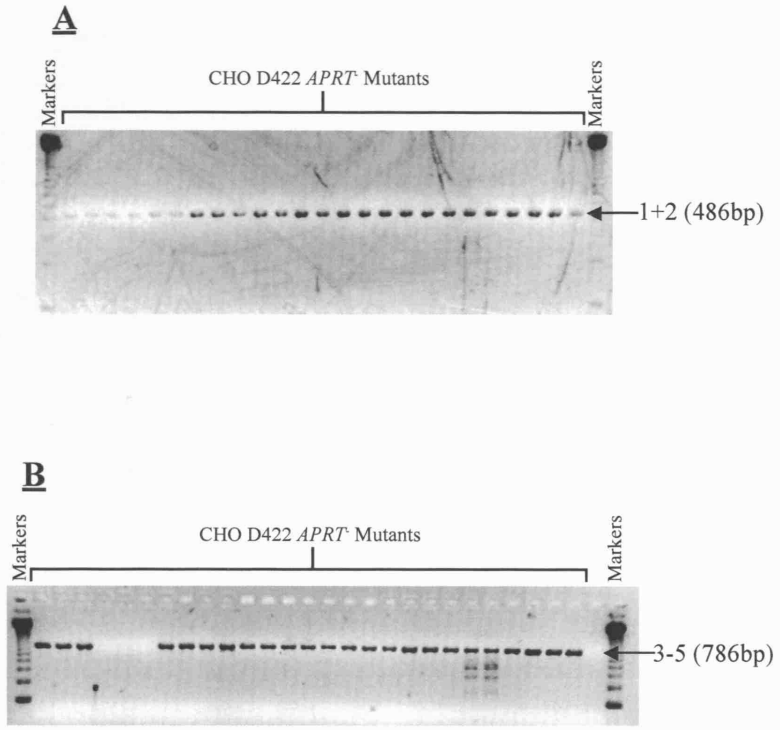

Fig 7.7 PCR Amplification of CHO D422 *APRT* Locus from 6-TG/UVA Induced *APRT*⁻ Mutants. CHO D442 cells were grown in the presence of 0.1μM 6-TG for 48 hours and exposed to 1.0kJ/m² UVA. Cultures were allowed to recover for 7 days, after which they were plated out in medium containing 4.0mM 8-azaadenine to select for *APRT*⁻ mutants. Individual mutant colonies were selected and expanded. Genomic DNA extracts were prepared from these mutant lines. The APRT locus was amplified by PCR in two fragments. Fragment A contained exons 1 and 2, and was 486 base pairs in length (**A**), while fragment B contained exons 3,4 and 5 and was 786 base pairs in length (**B**).

Mutant	Fragment	Position	Mutation	Sequence Context	Amino Acid Change
1	3 to 5	1743	G > A	TGG*G*CTG	G > D
2	1 + 2	394	A > G	GCT*A*TGG	M > V (Start codon)
3	1 + 2	647	C > T	CTT*C*CAT	S > F
4	3 to 5	1698	G > T	CCA*G*GGG	R > M
5	1 + 2	466 - 486	Deletion		
7	3 to 5	2157	C > G	TCA*C*CCC	Intronic (splice site)
8	3 to 5	2043	G > C	CTG*G*CCA	G > A
9	3 to 5	1698	G > T	CCA*G*GGG	R > M
10	3 to 5	2305	A > G	GTG*A*CTG	STOP > W
11	1 + 2	635	C > T	CCT*C*CTT	S > F
12	3 to 5	1698	G > T	CCA*G*GGG	R > M
14	1 + 2	614	C > G	CGC*C*CCT	P > R
15	1 + 2	703	A > T	TAC*A*TCG	I > F
16	1 + 2	703	A > T	TAC*A*TCG	I > F
17	3 to 5	2031	G > C	GTA*G*ATG	D > H
18	3 to 5	2031	G > C	GTA*G*ATG	D > H
19	1 + 2	468	Frameshift (-T)	CTG*T*TTA	
20	1 + 2	468	Frameshift (-T)	CTG*T*TTA	
21	1 + 2	447	T > C	GAC*T*TCC	F > L
22	1 + 2	703	A > T	TAC*A*TCG	I > F
23	3 to 5	1778	G > C	CCA*G*GCC	G > R
24	1 + 2	710	G > C	CAG*G*CGA	G > A
25	1 + 2	703	A > T	TAC*A*TCG	I > F
28	1 + 2	394	A > C	GCT*A*TGG	M > L (Start codon)
29	3 to 5	2219	T > C	GAG*T*GTG	C > R
30	1 + 2	620	T > C	TCC*T*GAA	L > P
31	1 + 2	647	C > T	CTT*C*CAT	S > F
32	3 to 5	2036	T > G	TGA*T*CTC	D > E
34	3 to 5	2003-2005	Deletion	CTT*A* ***GA***ACCT	Del of E
39	3 to 5	1743	G > C	TGG*G*CTG	G > A
40	3 to 5	2226	G > A	TGA*G*CCT	S > N
41	3 to 5	2187	T > G	AGC*T*GCT	L > R
42	3 to 5	1952	T > C	CTC*T*CAC	Intronic (splice site)
43	3 to 5	1757	C > G	ATC*C*GGA	R > G
44	1 + 2	708	A > C	CGC*A*GGC	A > A
45	1 + 2	611	C > T	TCT*C*GCC	S > L
46	3 to 5	2226	G > A	TGA*G*CCT	S > N
47	1 + 2	447	T > C	GAC*T*TCC	F > L
48	3 to 5	2289	T > G	CTC*T*CCT	L > R
49	1 + 2	399	G > T	GCG*G*AAT	G > STOP
50	1 + 2	640	C > T	TTC*C*GAG	A > STOP
52	3 to 5	2227	C > G	GAG*C*CTG	S > R
53	1 + 2	447	T > C	GAC*T*TCC	F > L
54	3 to 5	2023	T > G	TGG*T*TGT	V > G

Table 7.1 6-TG/UVA Mutation Spectrum at the CHO D422 *APRT* Locus

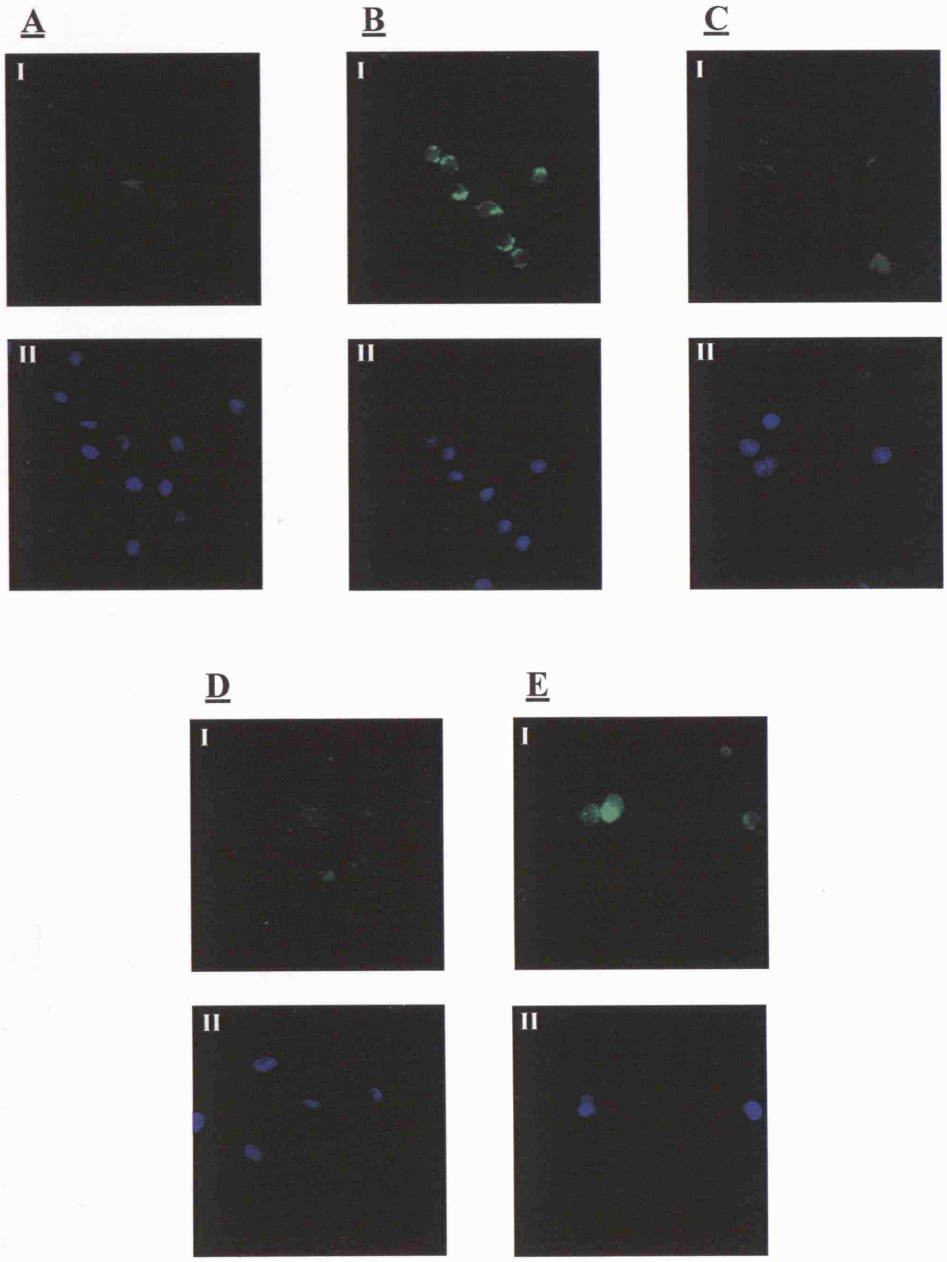

Fig 7.8 Visualisation of ROS in CHO D422. CHO D422 cells were grown in 0.1μM 6-TG for 48 hours, labelled with CM-H_2DCFDA, UVA irradiated with 1.0kJ/m^2, counterstained with DAPI and visualised by fluorescence microscopy. ROS is visualised by green fluorescence (**I**), while cell nuclei are visualised using blue fluorescence (**II**).**A** Untreated cells show a low level of background floures-cence. **B** Treatment with 0.03% H_2O_2 leads to green fluorsecnce. **C** and **D**, neither 0.1μM 6-TG nor 1.0kJ/m^2 UVA alone cause a significant increase in fluorescence signal. **E** 6-TG/UVA combined increases in green fluorescence.

Protein	Size (kDa)	Function
p21	17	CDK inhibitor
DNMT1	183	DNA methyltransferase
Fen1	43	Flap endonuclease
Polε	261	Polε catalytic subunit
Gadd45	18	Growth and DNA damage inducible
p50	**50**	**Polδ regulatory subunit**
UNG	35	Uracil DNA glycosylase
Polβ	38	BER DNA polymerase
MSH2/6	105/156	MMR
Myh	60	DNA glycosylase
RFC2	**39**	**Replication factor, PCNA clamp loader**
WSTF	171	Chromatin remodelling (binds ISWI))
MSH3	127	MMR
LIG1	102	DNA ligase
RFC5	**36**	**Replication factor, PCNA clamp loader**
RFC3	**38**	**Replication factor, PCNA clamp loader**
Exo1B	94	Exonuclease, 5' -> 3', dsDNA
APE2	57	AP endonuclease
DDX17	72	RNA dependent helicase
NONO	54	RNA processing
DNA-PKcs	469	DNA dependent protein kinase
PCNA	**33**	**DNA replication processivity factor**

Table 7.2 PCNA Interacting Proteins

Excluded by size (red), inducible factors (green), DNA repair factors (blue). Possible components of PCNA* (**black**).